DEVELOPMENT OF FLUXES FOR REFINING OF COPPER

A THESIS

submitted in fulfilment of the
requirements for the award of the degree
of
DOCTOR OF PHILOSOPHY
in
METALLURGICAL ENGINEERING

By

S. TANDON

DEPARTMENT OF METALLURGICAL ENGINEERING
UNIVERSITY OF ROORKEE
ROORKEE-247 667 (INDIA)

JULY, 1992

UNIVERSITY OF ROORKEE
ROORKEE

CANDIDATE'S DECLARATION

I hereby certify that the work which is being presented in the thesis entitled DEVELOPMENT OF FLUXES FOR REFINING OF COPPER in fulfilment of the requirement for the award of the Degree of Doctor of Philosophy, submitted in the Department of Metallurgical Engineering of the University is an authentic record of my own work carried out during a period from May,1989 to July,1992 under the supervision of Dr. R.D.Agrawal and Dr. M.L.Kapoor.

The matter embodied in this thesis has not been submitted by me for the award of any other degree of this or any other University.

Tandon

(S.TANDON)

This is to certify that the above statement made by the candidate is correct to the best of our knowledge.

Date : 22.8.92

Agrawal

(R.D.AGRAWAL)
PROFESSOR

Mlkapoor

(M.L.KAPOOR)
PROFESSOR AND HEAD

Department of Metallurgical Engineering
University of Roorkee
Roorkee - 247 667 (INDIA)

The Ph. D. viva-voce examination of Sri S.TANDON, Research Scholar, has been held on 04/12/92

Mlkapoor 4/12/92 Agrawal

Signature of Supervisor(s) Signature of H.O.D Signature of External Examiner

ACKNOWLEDGEMENTS

I wish to express my deep sense of gratitude and appreciation to my thesis supervisors Dr. R.D.Agrawal and Dr.M.L.Kapoor for their painstaking efforts, support and guidance during the course of present investigation. With out their timely help and constant encouragement, the present work could not have been possible.

My sincere and grateful thanks are also due to Professor M.L.Kapoor, present Head of the Deptt. and to Dr.Kailash Chandra, Director, USIC for providing the laboratory facilities to me during the course of the present investigation.

I would also like to record my appreciation for the assistance rendered by the staff of various laboratories of Metallurgical Engineering Department, namely, S/Sri S.B.Sharma, Rajendra Sharma, Vipin, Madhu Singh , Vinod Tyagi and others. Thanks are due to Sri M.C.Vaish, for his excellent draftsmanship, and Sri Ram Gopal, for his flawless type-writing.

I wish to express my thanks to the Department of Science and Technology and Council of Scientific and

Industrial Research, Govt. of India, for providing me financial help during the course of this investigation.

Last but not the least, I take this opportunity to express my deep sense of gratitude, to my family for showing tremendous patience and, to my friends for contributing directly or indirectly towards this achievement.

Dated : 22.8.92

(S.TANDON)

SYNOPSIS

Due to depletion of high grade copper ores, metallurgists are forced to use lower grade copper ores. This results in higher proportions of impurities being encountered during copper processing. Impurities such as As, Sb, Se, Te, Bi, Ni etc, besides getting carried over to copper refining stage and thereby affecting the process efficiency,are also occluded in copper produced thereby affecting its electrical and mechanical properties. The literature survey on copper refining shows that elements As, Sb, Bi, Ni, Se, Te, etc can be effectively removed from metal using soda bearing slags in a slag-metal reaction process. The use of sodium carbonate as a flux for removing the impurities has been significant recently. But use of sodium carbonate in pure form has posed many problems on industrial scale. A critical study of the published work has indicated that no systematic studies have been conducted on thermodynamic and mass transport aspects of soda-base slags and copper metal systems.

The present work has, therefore, been undertaken to establish the practical operating parameters for refining of copper using soda-base fluxes. The investigation has been confined to the removal of only Se and Te impurities from

copper using sodium- borate slags. The entire work has been reported in five chapters.

Chapter I has been devoted to the brief introduction on the problem and critical review of literature comprising thermodynamic and kinetic studies including slag viscosity measurements. Finally formulation of the problem has been taken up.

Chapter II deals with the thermodynamics of copper refining by flux and includes the theoretical analysis , experimental set-up and procedure used for the determination of selenium and tellurium equilibrium distribution coefficients for various Cu-Se and Cu-Te alloys, using sodium-borate slags of different compositions at 1473K . Effect of CaO and CaF_2 additions to sodium-borate slags on Se and Te distribution coefficients has also been studied. This chapter also includes the results obtained and their interpretations. It has been found that, i) with increase in slag basicity (i.e. wt% Na_2O/wt% B_2O_3 ratio), equilibrium distribution coefficient for both Se and Te increases, ii) addition of 50 wt% CaO to sodium -borate slag (wt% Na_2O/wt% B_2O_3 = 0.86) increases the distribution coefficient values by about 2 times for both Se and Te elements, iii) with addition of 20 wt% CaF_2 to the slag (30.9 wt% Na_2O, 35.8 wt% B_2O_3,33.3 wt% CaO), the distribution coefficient further increases by around 1.8 times for Se and 2.2 times for Te.

Chapter III has been devoted to the study of physico-chemical property i.e viscosity of various slag systems developed. It includes the theoretical aspects, experimental set- up and procedure used for measuring the viscosity of slag as a function of temperature and slag composition. It has been found from the results and their interpretations that, i) with increase in temperature, the viscosity decreases for all slag compositions, ii) with increase in Na_2O content (34.5wt%to 46.4wt%) in sodium-borate slag compositions developed for the present work, the viscosity decreases from 0.31 Pa-s to 0.29 Pa-s at 1473K, iii) with addition of CaO (10 wt% to 50 wt%) to sodium-borate slag (wt% Na_2O /wt% B_2O_3 = 0.86), its viscosity increases from 0.76 Pa-s to 1.12 Pa-s at 1473K and iv) with addition of CaF_2 (5wt% to 20wt%) to slag composition (30.9 wt% Na_2O, 35.8 wt%B_2O_3,33.3 wt%CaO), the viscosity decreases from 0.44 Pa-s to 0.38 Pa - s at 1473K.

Chapter IV deals with the kinetics of copper refining by soda-base flux and includes the theoretical aspects, experimental set-up and procedure used to study the Se and Te transfer as a function of gas flow rate in N_2 gas bubble agitated slag metal system at 1473K for Cu-Se and Cu-Te alloys using slag composition (25.7wt% Na_2O,29.8wt% B_2O_3, 27.8wt%CaO,16.7wt%CaF_2). Results obtained and their interpretations are also included in this chapter. It has

been observed that with increase in gas flow rate (5.0 to 17.0 cm^3/sec), the overall mass transfer coefficient increases from $2.04x10^{-3}$ to $3.06x10^{-3}$ cm/sec for Se while for Te it increases from $3.41x10^{-3}$ cm/sec to $5.02x10^{-3}$ cm/sec.

Chapter V includes conclusions while scope for future work is indicated separately.

LIST OF RESEARCH PAPERS FROM THESIS WORK

By

S.TANDON, R.D.AGRAWAL AND M.L.KAPOOR

1. 'Distribution Equilibria of Selenium between Liquid Copper and Na_2O - B_2O_3 slags'. Published in Mater. Trans., Japan Inst. of Metals, Vol. 32, No. 7, 1991.
2. 'Distribution Equilibria of Selenium between Liquid copper and Na_2O - B_2O_3- CaO slags'. Published in Mater. Trans., Japan Inst. of Metals, Vol.33, No. 1, 1992.
3. 'Selenium Distribution between Molten Copper and Na_2O-B_2O_3 slags'. Abstract published in Journal of Metals, Vol. 43, No. 11, 1991, p. C 62. TMS Annual Meeting, EPD congress, March 1-5, 1992, San Diego, California, p. 671.
4. 'Mass Transfer studies on Selenium and Tellurium between Gas-bubble agitated Molten Copper and Na_2O-B_2O_3 slags'. Revised manuscript sent to Mater. Trans., Japan Inst. of Metals. Final acceptance for publication is awaited.

NOMENCLATURE

A	interfacial area
B	slag basicity
$[C_b]_t$	molar concentration in bulk metal phase at time, t
$(C_b)_t$	molar concentration in bulk slag phase at time, t
$[C_b]_\infty$	molar concentration in bulk metal phase at infinite time
$(C_b)_\infty$	molar concentration in bulk slag phase at infinite time
$[C_i]_t$	interfacial molar concentration in metal phase at time,t
$(C_i)_t$	interfacial molar concentration in slag phase at time, t
D	diffusivity
E	emf (electro-motive force)
E_μ	activation energy
F	frequency of bubble formation.
G	gas flow rate
H	depth of orifice in liquid
J	rate of element transfer
K	equilibrium constant
L	distribution coefficient
N_{Mo}	Morton's number

$N_{Re,o}$	orifice Reynold's number
$N_{Re,b}$	bubble Reynold's number
N_{We}	Weber's number
P	pressure
S	rate of production of fresh surface per unit area
T	temperature
V_M	Volume of metal
V_b	bubble volume
a_i	activity of component,i
d_b	bubble diameter
d_{bvs}	Volume surface mean diameter of the bubble defined by eq. (4.35)
d_{be}	diameter of a sphere of volume equal to that of bubble under study
d_o	orifice diameter
g	acceleration due to gravity
g_c	conversion constant for eq. (4.38)
h_M	height of metal phase
h_S	height of slag phase
k_M	mass transfer coefficient in metal phase
k_S	mass transfer coefficient in slag phase
$\dot{n}$	total flux
η	Viscosity
η_o	constant (frequency factor) defined by eq. (3.2)
p	partial pressure

%	weight precent
d	diameter of particle diffusing for eq. (3.4)
t_R	residence time of bubble in the liquid
t_e	exposure time
u	rising velocity of bubble
u_t	terminal velocity of bubble
δ	thickness of the boundary film
μ_l	viscosity of liquid
ρ_M	density of metal phase
ρ_S	density of slag phase

LIST OF TABLES

LIST OF FIGURES

CONTENTS

CHAPTER - III VISCOSITY MEASUREMENT OF SLAGS

CHAPTER - IV KINETICS OF SLAG-METAL SYSTEM

CHAPTER - I

GENERAL

1.1 INTRODUCTION

With the depletion of high grade copper ores, metallurgists have been forced to use low and off-grade copper ores for copper production. Therefore large amount of impurities such as As, Sb, Bi, Ni, Se, Te etc. are encountered during copper production. These impurities, besides being carried over to electro refining stage thereby affecting the efficiency of the process, are also occluded in copper produced. These impurities lower the electrical and mechanical properties of copper. Figs.(1.1-1.2) show the loss of conductivity of tough pitch copper and oxygen free copper respectively with content of impurities while Table 1.1 gives the effect of individual impurity additions on softening temperature of pure copper [1]. Therefore, to keep the concentration of impurities in the copper as low as possible, it has become imperative to modify the existing process of copper extraction. The various unit processes of copper production include roasting, matte smelting, converting, anode furnace refining and electrolytic refining. The primary objective of roasting is to have

partial removal of sulphur or SO_2. The estimated distribution of elements during matte smelting is given in Table 1.2. These data serve only as a guide and the precise distribution of minor elements depends upon the smelting conditions and the type of process. The most important point derived from this table is that significant quantities of impurities harmful to copper enter the matte, specially Sb, As, Bi, Pb, Se and Te [2]. There is not much scope of modification in smelting operation. The representative analysis of converter charge and products and estimated distribution of impurity elements during converting are given in Tables (1.3-1.4) respectively. It is clear from these tables that though the main elements removed from matte during converting are Fe and S, many other impurities are also removed either as vapour or in the slag. The blister copper so produced has to be refined in anode furnace and subsequently by electrolytic process. Though there is some possibility of further removal of impurities like As and Sb during converting operation by adding suitable fluxes but impurities such as Se and Te will not be removed due to oxidising conditions. However, there is a greater flexibility of modification during anode furnace refining which is an essential step before electrolytic refining. Anode furnace refining can be divided into two stages : 1) oxidising period and 2) reducing period. By

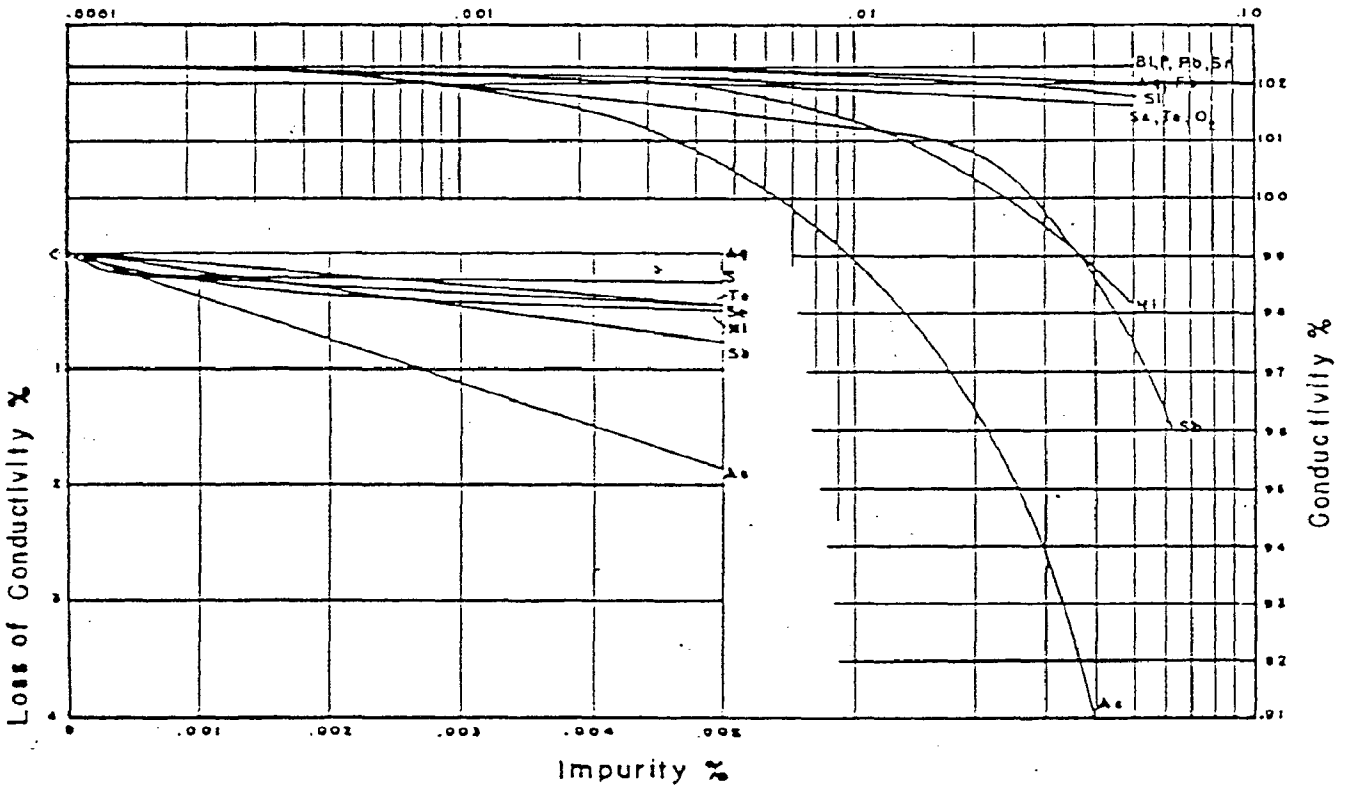

FIG. 1.1 DECREASE OF CONDUCTIVITY OF TOUGH-PITCH COPPER WITH CONTENT OF IMPURITIES [1].

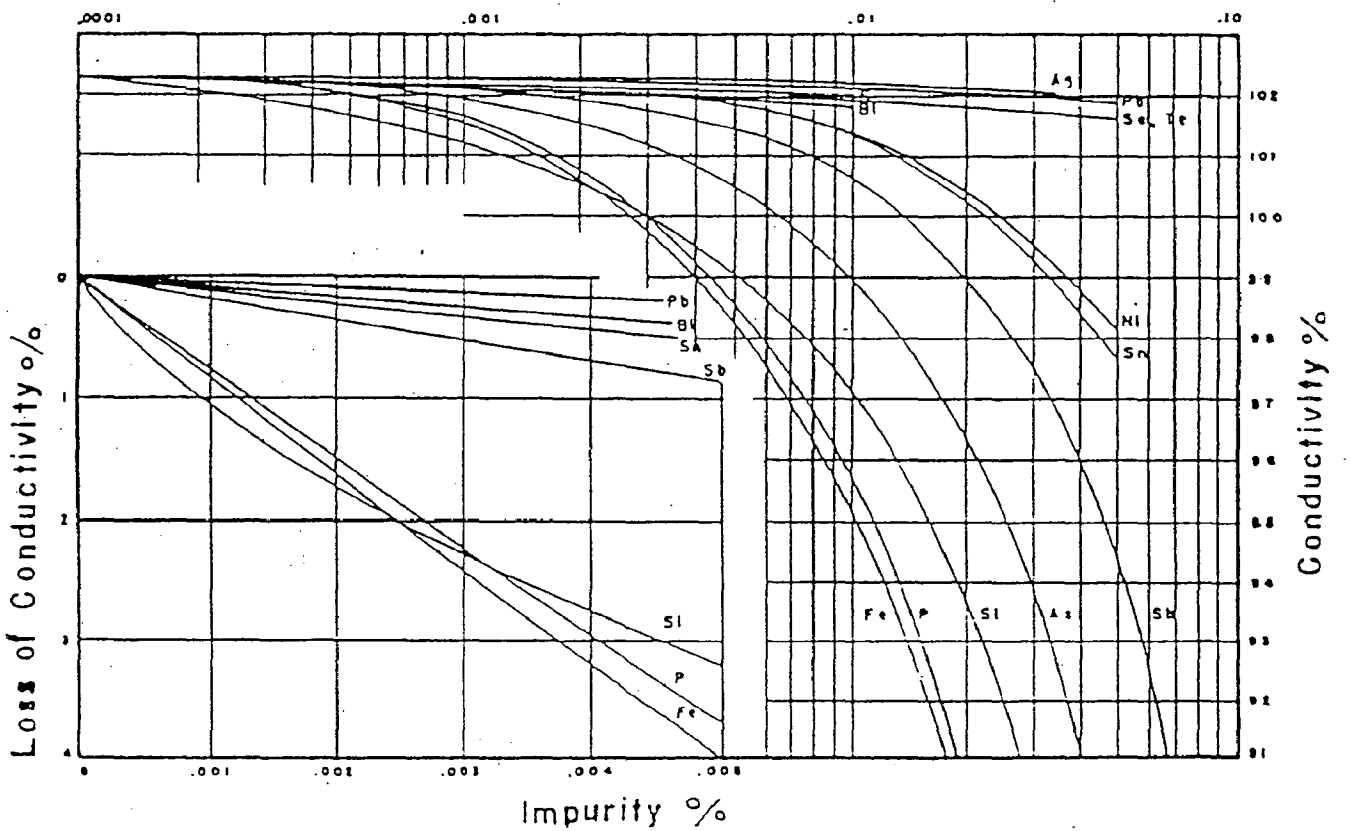

FIG. 1.2 DECREASE OF CONDUCTIVITY OF OXYGEN-FREE COPPER WITH CONTENT OF IMPURITIES [1].

TABLE - 1.1

SOFTENING TEMPERATURE (DEG.C) OF PURE COPPER CONTAINING INDIVIDUAL IMPURITY ADDITONS [1]

Quantity	0.002%		0.005%		0.01%		0.05%	
Impurity	T.P.[a]	O_2-free	T.P.	O_2-free	T.P.	O_2-free	T.P	O_2-free
O_2	140	140	140	140	140	140	140	140
Fe	140	146	140	153	140	155	148	167
Sb*	180	192	258	282	296	317	336	336
As	168	168	189	189	205	205	242	242
Ni	140	140	140	140	140	140	140	140
Pb*	146	250	146	270	146	274	146	286
Bi*	210	260	247	300	275	328	-	-
Ag	148	148	172	172	207	207	330	330
Sn	140	198	140	277	140	315	140	346
S**	181	181	183	183	183	183	-	-
Se**	222	222	234	234	240	240	250	250
Te**	212	212	228	228	238	238	250	250
P	140	258	140	284	140	300	-	-
Si	-	161	-	181	-	198	-	242
Co	-	145	-	152	-	161	-	161
Cr	-	152	-	190	-	260	-	320
Zn	-	148	-	151	-	152	-	156
Cd*	-	183	-	248	275	309	325	356

a Copper containing oxygen in the tough-pitch range.

* Tough-pitch values reflect partial oxide formation. Value equivalent to those given for oxygen-free copper can be obtained by heat treatment at temperatures in excess of 700°C (1290°F).

** Much higher values obtainable by heat treatment to increase solid solubility.

TABLE - 12

ESTIMATED DISTRIBUTION OF ELEMENTS DURING MATTE SMELTING [2]

Metal	Distribution		
	Matte	Slag	Volatilized[a]
Alkali and alkaline earth metals, aluminium, titanium	-	100	-
Ag, Au, platinum metals	99	1	-
Antimony	30	55	15
Arsenic	35	55	10
Bismuth	10	10	80
Cadmium	60	10	30
Cobalt	95	5	
Lead	30	10	60
Nickel	98	2	-
Selenium	40	-	60
Tellurium	40	-	60
Tin	10	50	40
Zinc	40	50	10

a Not including solids blown from the furnace (dust losses)

TABLE- 1.3

REPRESENTATIVE ANALYSIS OF CONVERTER CHARGES AND PRODUCTS [1,2]

SNo.	Constit-uents	In Matte (Wt%)	In Blister Copper (wt%)	In Preci-pitator dusts (wt%)	Converter slag
1.	Cu	35-65	98.5-99.5	5-15	2-15
2.	Fe	10-40	0.1	5-10	35-50
3.	S	20-25	0.02-0.1	10	-
4.	O	2-3	0.5 -0.8	-	-
5.	As	0-0.5	0 -0.3	0-1	-
6.	Sb	0-1	0 -0.3	0-1	-
7.	Bi	0-0.1	0-0.01	0-2	-
8.	Pb	0-5	0-0.1	0-30	-
9.	Zn	0-5	0.005	0-15	-
10.	Ag	0-0.1	0-0.1	0.05	-
11.	Se	-	0.04-0.30	-	-
12.	Te	-	0.01-0.04	-	-
13	SiO_2	-	-	-	20-30
14.	Fe_3O_4	-	-	-	15-25
15.	Al_2O_3	-	-	-	0-5
16.	CaO	-	-	-	0-10
17.	MgO	-	-	-	0-5

TABLE - 1.4

DISTRIBUTION (ESTIMATED) OF IMPURITY ELEMENTS DURING CONVERTING [2]

	Blister copper	Vapour[a]	Slag[b]
Ag	90	0	10
Au	90	0	10
Pt metals	90	0	10
As	15	75	10
Bi	5	95	0
Cd	0	80	20
Co	80	0	20
Fe	0	0	100
Ge	0	100	0
Hg	10	90	0
Ni	75	0	25
Pb	5	85	10
Sb	20	60	20
Se	60	10	30
Sn	10	65	25
Te	60	10	30
Zn	0	30	70

a Not including ejected droplets of matte and slag
b Including entrained matte.

developing suitable fluxes and using them in anode furnace, impurities like As, Sb, can be removed to a great extent during oxidising period while Se and Te can be removed during subsequent reducing period.

With this objective in mind, the present research work has been taken up to develop suitable flux composition (to be used in anode furnace) to remove these impurities in a form suitable for their subsequent recoveries in saleable compound forms.

The efficiency of removal of impurity elements from the metal phase depends on slag-metal thermodynamics and rates at which these equilibria can be achieved. Since the rate of reaction in slag-metal system at high temperature is essentially transport controlled and hence will be affected by slag viscosity. Several efforts have, therefore, been made in the past to study the thermodynamic and kinetic aspects of different slag-metal systems alongwith the viscosity measurements for various slag systems.

1.2 LITERATURE SURVEY

1.2.1 Thermodynamic Studies

In recent years several workers have studied the

thermodynamics of refining process using slag-metal reaction technique to remove various impurities from different metal baths such as Iron, Steel, Lead etc. using different slag systems. There have also been studies on removal of impurities from copper metal bath by using different fluxes. These studies have been briefly reviewed in the following sub-sections.

1.2.1.1 Different Metal-slag Systems

In case of sulphur removal from liquid iron, several attempts [3-9] were made to express numerically the distribution coefficient of sulphur as a function of slag basicity, though several different ways [10-16] were proposed to define 'basicity' of slag. Giedroye et al. [6] obtained following simple relationship for $CaO-MgO-Al_2O_3-SiO_2$ quaternary slag system,

$$B = \frac{(\%\ CaO) + (\%\ MgO)}{(\%\ SiO_2) + (\%\ Al_2O_3)}$$

and arrived at the following expression for distribution coefficient of sulphur,

$$\log\ (\%S)/a_s = 1.60\ B - 0.38$$

Suito et al. [17] observed a remarkable reduction

in desulphurisation and dephosphorisation in the presence of silicon as a result of consumption of flux Na_2CO_3 - Na_2SO_4 for the oxidation of Si present in iron. Shim and Ban-Ya [18] found that SiO_2 markedly decreased the distribution ratio of sulphur between liquid iron and Fe_tO - MgO, Fe_tO - SiO_2 - MgO, and Fe_tO - SiO_2 -CaO -MgO system slags saturated with MgO in the temperature range of 1550-1650^oC . Toporishchev et al. [19] observed that small initial values of FeO accelerate the initial desulphurisation process but retard the establishment of equilibrium. Equilibrium was established more rapidly by introducing strong deoxidising agents over a period of time. Additions of Al_2O_3 and CaF_2 contributed to considerable increase of the lime desulphurisation capacity because of liquification of the slag formed [20-22] . Several fundamental studies on external desulphurisation of hot metal using soda ash have been reported in literature [3,8,9,23]. The sulphur partition, particularly, between C-saturated iron and Na_2O-SiO_2 slags was studied [3,8,9,24]. Zhang and Toguri[25] studied the behaviour of FeO concentration and effect of temperature on equilibrium value of sulphur distribution. Based on the distribution equation , an expression developed for sulphur capacities of steel making slags agrees well with available experimental data. Tsao and Katayama [26] obtained the equilibrium data on sulphur distribution

between liquid iron and $CaO-MgO-Al_2O_3-SiO_2$ slag for ladle desulphurisation of liquid steel. Chan and Fruehen [27] estimated the sulphur partition ratio between carbon-saturated iron and Na_2O-SiO_2 slags and the sulphide capacity of these slags have been measured at 1200°C.

Several studies have been conducted to refine the liquid iron from phosphorous, manganese, Niobium etc. using several different types of slags. Niobium equilibrium distribution was studied between liquid iron and different slag systems such as MgO_{sat}- Fe_tO - SiO_2 - NbO_x - MnO, Na_2O $-SiO_2$ and slag containing Nb_2O_5 , SiO_2 and MnO [28-30] .

Several workers have investigated the manganese distribution between carbon saturated iron melts and various slag systems such as MgO_{sat} $-Fe_tO$. SiO_2 $-NbO_x$ $-MnO$, $CaO-CaF_2$ $-SiO_2$ $-MnO$ $-(BaO, Na_2O)$, lime or soda-based slags [30-32].

Tsukihashi et al. [29] measured the distribution of vanadium between carbon saturated iron and soda slag in the temperature range 1200° to 1350°C .

Lot of studies have been done for dephosphorisation of liquid iron using different slag systems such as Na_2O $-SiO_2$ $-PO_{2.5}$, CaO - FeO $-SiO_2$, CaO $-MgO$ - Fe_tO $-SiO_2$ $-Na_2O$, Na_2O $-SiO_2$ $-Fe_2O_3$, Na_2O $-MgO$ $-Fe_tO$ $-SiO_2$ $-(CaO, MnO, Al_2O_3)$, 2 CaO $-SiO_2$ -saturated Fe_tO $-P_2O_5$ $-CaO$ $-SiO_2$, MgO-sat. Fe_tO $-P_2O_5$ $-MgO$,

Fe_tO-P_2O_5-CaO -MgO , SiO_2-saturated Fe_tO -P_2O_5 -SiO_2 and CaO -MgO -Fe_tO -SiO_2 at 1550^oC and 1600^oC [33-38].

Rytkonen and Klarin [39] compared the distribution coefficient of main impurity elements Cu, Sb, As, Sn, Zn, Bi and Ag in lead for calcium ferrite slags and lead silicate slags and found that the distribution coefficients, (% Me in lead)/ (% Me in slag), were a lot smaller in calcium ferrite slags, leading one to expect that certain impurity elements form a slag component much more easily in calcium ferrite slags than in silicate slags. Studies have also been conducted to refine lead from impurities mainly Se, Te, As,Sn and Sb by using NaOH and $NaNO_3$ as the fluxing reagents [40].

1.2.1.2 Copper Metal-Slag Systems

In refining of copper through slag/metal reaction a number of distribution equilibria/thermodynamic studies have been done for different impurity elements.

Nagamori, Mackey and Tarassoff [41] have studied the distribution of As, Sb, Bi, Se and Te between molten copper and white metal and estimated the distribution coefficients at 1150^oC which were found to be independent of the Fe content of the matte up to 4% . Their results indicate that when copper coexist with white metal as in

continuous smelting and converting, As, Sb and Bi should concentrate in the copper, while Se and Te will segregate in the white metal which is continuously flushed by the converting air. Actual distribution coefficients (% X in Cu / % X in white metal)have been reported as a function of temprature. They have also studied the copper solubility in FeO -Fe_2O_3 -SiO_2 -Al_2O_3 slag and distribution equilibria of Pb, Bi, Sb, and As between slag and metallic copper and measured the distribution of Pb, Bi, Sb and As between Cu and slag by doping the metallic Cu [41]. The distribution coefficient was defined by (mole fraction X in metal)/(mole fraction in slag) assuming the FeO-$FeO_{1.5}$ - SiO_2 -$AlO_{1.5}$ -$CuO_{0.5}$ system slag. For lead it was found to be a function of the oxygen potential while PbO activity in the slag of 0.7 $\pm$ 0.01 was measured over the range of 1200^{o}C to 1300^{o}C . Dissolution of Bi, Sb and As in the slag was found to be independent of the oxygen potential , suggesting atomic rather than oxide dissolution. The observed distribution coefficient for Bi and Sb was 30 and for arsenic it was 300. The data are useful in analysing minor element behaviour in copper smelting processes.

Burylev, Tsemekhman and Feorova [42] estimated the activity of S, Se, and Te in molten copper and have analysed the equilibrium between the metallic phases , sulphides, selenides, and tellurides by means of an

isothermal holding method. They deduced the activities of the chalcogens in molten copper as function of temperature.

Ludmila Komorova [43] has made a thermodynamic analysis of the removal of Zn,Bi, Pb, As, Sb and Sn from crude copper by vaccum refining at 1200^{o}C. The results of experimental trials are tabulated and are claimed to be consistent with thermodynamic assumptions.

Jochen Bode, Johanues Gerlach and Franz Pawlek [44] have measured the activities for Al, As, Pb and Bi in liquid copper by estimating the partial vapour pressures above the melt, the vapour pressures of the pure metals being known. Earlier work was used to calculate the degree of atomic association of Pb, Bi, Sb and As in the vapour phase. The procedure is based on Wartenberg's entrainment method. The values are reported to remain unaffected by additions of Cu_2S and CuO. In vacuum purification trials, they have found that Pb can be removed from a Cu- 1% Pb alloy at 10^{-3} torr and at 1200^{o}C to .001 % in 45 minutes and Bi from Cu - 1% Bi alloy to .003 % under the same conditions. In this, the rate determining process is reported to be the diffusion of the impurity to the surface.

Czernecki et al. [45] have done experiments in the laboratory as well as in the industry aimed at refining Cu from arsenic in rotary anodic furnaces. As a refining addition, they used soda and lime in amounts depending on

the initial content of arsenic in Cu. This method of refining Cu from arsenic assures the production of anodic Cu containing < 0.08 % arsenic which is in accordance with requirements of the electrolytic refining [redacted] process.

Roine and Jalkanen [46] have used the transportation method to determine the activity coefficients of the minor impurity components As, Sb, Bi and Pb in homogeneous Cu matte (Cu-Fe-S) as functions of Cu/Fe mole fraction ratio and of the sulphur content of the matte at 1200^{o}C. All matte samples contained 0.2 wt. % As, Sb, Bi and Pb. The activity coefficients have been calculated on the basis of primary experimental data and available thermodynamic values of the gas components which exist over the mattes. The S-to metal ratio, which controls the activities of the main matte constitutents was found to be the most important factor influencing the activities. When the S-to metal ratio of the matte changed from S deficit to S excess, the activity coefficient of As is noted to vary from 0.52 to 38, Sb from 3.3 to 82, Bi from 75 to 3.4 and Pb from 25 to 0.079 in the matte. The activities of $AsS_{1.5}$, AsS, $SbS_{1.5}$, $BiS_{1.5}$ and PbS had negative deviations from the ideal behaviour.

Kojo, Taskinen and Lilius [47] determined the distribution equilibria of Sb, As, Cu, Se and Te in the system Cu-sodium carbonate as a function of oxygen activity

of the melt at 1200°C and have found that above $pO_2 = 10^{-7}$ bars, Sb and As exist in the slag predominantly as pentavalent, Se and Te as tetravalent, and Cu as monovalent cationic species. In more reducing conditions, Sb is converted to a trivalent state and Se and Te dissolve as divalent anionic species. The activity coefficient of the inpurity components in the slag has been calculated from the experimental distribution data using additional information from the literature. They have also discussed the efficiency of removing Sb and As by sodium carbonate in a reactor with a permanent or transitory slag contact .

Boichev et al. [48] have made the thermodynamic calculations of the equilibrium content of Antimony in copper in oxidation refining. On the basis of theoretical and experimental data they have presented a thermodynamic analysis of the equilibrium concentration of Sb in Cu under conditions of oxidation refining . At 1250°C the theoretical value of Sb is 0.31 wt % and this is supported by experiments carried out in a pure N_2 atmosphere. The saturation O content of Cu at 1250° is 2.47% and the corresponding equilibrium Sb content is 0.36 % . They have shown that it is impracticable to remove all the Sb in the Cu by oxidation alone. There is always a certain residual amount which varies with the temperature.

Following the previous report on phase equilibria

between Na_2CO_3-Na_2O -SiO_2 melts and liquid copper, Riveros et al. [49] have studied the same system at 1523K to investigate the optimum condition for removal of As and Sb from copper by use of soda flux. Experimental results have been explained in terms of oxygen potential and soda - ratio in slag. The isobars of the distribution ratio have been illustrated on the ternary diagram of (Na_2CO_3 + Na_2O) - SiO_2 -Cu_2O. They have found that (i) the increase in oxygen potential or in basicity of slag has resulted in high removalibity of these elements (ii) trivalent arsenic or antimony is common in the slag with low soda ratio but pentavalent becomes predominant as the basicity of slag or oxygen potential increases (iii) pentavalent state is more stable for arsenic than for antimony, and brings about drastic variation in the distribution ratio (iv) sodium carbonate melt under high oxygen potential represents high removability of arsenic and antimony with rather small dissolution of copper . They have also shown that basic sodium silicate slag has high removability of these detrimental elements, but copper content in slag is too high under high oxygen potential. High distribution ratio of arsenic and antimony is also observed for Cu_2O slag containing 10 to 20 % Na_2O.

Jalkanen et al. [50] suggested that thermodynamic factors play a decisive role in high temperature processes

of slagging and volatilisation and have given general equations of the gaseous and liquid phase reaction occuring in the process of impurity removal. The boundary condition have been defined by the stability ratio of Cu metal. The maximum O_2 partial pressure has been determined under standard conditions by the balance of the reaction

$$Cu_2S + O_2 = 2Cu + SO_2.$$

Theoretical and experimental studies of removal of impurities e.g. As, Sb, Sn, Pb, Bi, Zn, Mo, Cd, Co etc. have also been reported.

Sibanda and Baker [51] have conducted thermodynamic studies on dilute solutions of Bi in copper at 1100^{O}C . Canning Jr [52] has suggested a method for refining Cu which comprises treating an oxygenated molten copper bath with a flux which forms a skimmable slag containing iron oxide and silica in a weight ratio 0.4 -0.8.

Sakai et al. [53] studied the removal of elements (As,Sb) from molten Cu using a $CaO-Na_2SO_4$ flux and estimated the distribution coefficients of As and Sb between flux and molten copper at 1473K. They have found that (i) values of As distribution coefficient in a $CaO-Na_2SO_4$ flux were smaller than those in a Na_2CO_3 flux , but were sufficiently high to consider its use as a flux for removal

of arsenic (ii) the dissolved species of As in the flux is in the pentavalent state.

Kojo et al. [54] have investigated the distribution equilibria of Sb,As, Cu and Pb between Na silicate slag and molten oxygen-bearing copper at 1200^{o}C using a sampling technique. They have estimated the thermodynamic properties of the impurity species in the slag and have analysed sodium carbonate-silicate slags for its refining properties .

Sakai et al. [55] have carried out the thermodynamic studies for the removal of As, Sb, and Bi elements from copper in fire refining by alkaline carbonate fluxes such as Li_2CO_3,Na_2CO_3 and K_2CO_3 and found that Na_2CO_3 and K_2CO_3 fluxes were stable with molten copper during pO_2 = 10^{-4} - 10 Pa at 1473K and copper loss in fluxes was small. On the other hand , Cu_2O-LiO_2 slag appeared due to decomposition of Li_2CO_3 to Li_2O when Li_2CO_3 was added to the molten Cu. They have also estimated the distribution coefficients of As, Sb and Bi between alkaline carbonate fluxes and Cu melt at 1473K under different O_2 potentials. Nakamura et al. [56] also conducted the same thermodynamic studies for pO_2= 10^{-8} -10^{-5} atm and at different temperature range i.e. (1423K-1523K).

Takeda et al. [57,58] measured the distribution of Ag, Co, Zn, Ni, Sn, Pb, As, Sb and Bi between calcium

ferrite slag and metallic Cu at 1250°C under controlled $CO-CO_2$ atm. They also measured the distribution of Zn,Sn, Pb, As and Bi for iron silicate slag. Considering the relationship between the distribution coefficient and the oxygen potential, the minor elements were found to be present in the slag in following forms :- $CuO_{0.5}$, $AgO_{0.5}$, CoO, NiO,ZnO, SnO (SnO_2 in the range of high oxygen potential), PbO, $AsO_{1.5}$, $SbO_{1.5}$, $BiO_{1.5}$. They have concluded that the dissolution of As and Sb in ferrite slags is greater than in silicate slags and Pb and Zn are more soluble in silicate slags. They have also studied the influence of temperature and composition of slag and metal on the distribution of minor elements between Calcium ferrite slags and metallic copper. From the standpoint of molecular model for slags, they postulated that Henry's law is valid for $CuO_{0.5}$, $AgO_{0.5}$, $AsO_{1.5}$, $SbO_{1.5}$ and $BiO_{1.5}$ in slags.

Takeda and Yazawa [59] investigated the distribution equilibria between molten Cu and alumina-saturated Na_2O -Cu_2O or SiO_2 - Cu_2O slag at 1250°C for As and Sb and have shown that the distribution ratios of As and Sb are not affected by addition of SiO_2 to Cu_2O melt whereas Na_2O addition to the slag increases the distribution ratios. They have also observed that activity of $CuO_{0.5}$ shows negative deviation from ideal solution in

basic slag Na_2O -Cu_2O and positive deviation from ideal solution in alumina saturated SiO_2 -Cu_2O slag.

Eerola et al. [60] studied the thermodynamics of Cu and of minority elements in Ca ferrite slags by sampling technique in Cu refining conditions at 1250^oC and have determined the distribution coefficient between the slag and metal for As, Bi,Cu, Ni, Pb and Sb at O_2 concentration of 0.02-0.7 % in the alloy. The behaviour of the minor elements and the copper in the slag has also been analysed on the basis of the distribution results.

Taskinen [61] have determined the distribution coefficient of As, Bi, Cu, Pb and Sb between soda slags and oxygen-bearing blister coper at 1200^oC .

The distribution coefficient of As between slag and Cu and the activity of arsenic in silica saturated slag have been measured at temperature between 1473K and 1536K by Lynch and Schwartz [62]. They have analysed that As existed in a molecular form in simple acidic slags.

Goto et al. [63] measured the solubilities of Cu, As, Sb and Bi in slags against O_2 potentials and found out both oxidic and atomic types of dissolution except in the case of As. They have also discussed about the distribution coefficients of As, Sb and Bi between Cu and slag.

Kojo et al. [64] have determined the distribution

coefficients of As, Sb and Cu between slag and metal as a function of O_2 concentration of the alloy and calculated the activity coefficients of the dissolved species, treated as mono-atomic oxide on the basis of the measured distribution coefficients.

Yamauchi et al. [65] measured the distribution ratio of Sb between Na_2CO_3 -slag and molten copper at temperatures of 1423, 1473 and 1523K by using a sampling technique in a pure argon atmosphere against oxygen pressure of the alloy. On the basis of distribution results, they have suggested that the predominant dissolved species of Sb in Na_2CO_3-slag is pentavalent in the oxygen pressure range of 10^{-3} - 10^{-1} Pa. Further more they have estimated the effect of CO_2 pressure on the antimony distribution coefficient with the aid of activity data for Na_2O -CO_2 -Sb_2O_5 melt.

Very few slag systems have been tried so far for the removal of Se and Te impurity elements from copper .Kojo [66] has determined the distribution equilibria of Sb,As, Cu, Bi, Pb, Ni, Se, Te and Sn in the system Cu-Na_2CO_3 as a function of O_2 activity of the melt. As and Sb were fluxed as pentavalent cations; Sb was fluxed as a trivalent oxide at lower activities. Sn, Se and Te were removed as tetravalent cations under oxidising conditions. Bi existed as a trivalent species whereas lead and Ni formed bivalent

and Cu monovalent cationic species. He has also observed that under reducing condition below an O_2 partial pressure of about 10^{-8} bar, Se and Te in the slag form bivalent anionic species with the stoichiomteries of Na_2Se and Na_2Te . The distribution of Sn, Se and Te between alumina-containing fayalitic slags and metallic copper was measured by Nagamori and Mackey [67] at 1200 and 1300^oC under controlled $CO-CO_2$ atm. with oxygen partial pressure (pO_2) in the range $pO_2 = 10^{-6}$ to 10^{-11} atm. They observed that the solubility of Sn in slag increases linearly with increasing $pO_2^{1/2}$, whereas the solubility of Se in the slag decreases with increasing O_2 partial pressure upto $pO_2 = 4 \times 10^{-8}$ atm, but above this oxygen partial pressure it becomes practically constant. They have also estimated the distribution ratio (pct Se in slag/pct Se in Cu) to be 0.018 at 1200^oC and 0.036 at 1300^oC. The solubility of Te shows a similar variation with oxygen partial pressure and the ratio (pct Te in slag/pct Te in Cu) = 0.026 (at 1200^oC) and 0.032 (at 1300^oC) above $pO_2 = 10^{-8}$ atm.

Kojo et al. [68] have studied the thermodynamics of removal of Se and Te from liquid copper by sodium carbonate slags and measured the distribution equilibria at 1473K by sampling technique as a function of the oxygen partial pressure of the system in pure CO_2 (gas; 1 bar). Their results showed that from thermodynamic point of view,

both Se and Te can be removed from copper effectively in reducing conditions by sodium carbonate slags, whereas their slag-metal distribution coefficients, even at small minority element concentrations, <0.01 pct, in liquid copper,are high, reaching a value of $L^{s/c}_{Se,Te} \approx 1000$ at $pO_2 = 10^{-15}$ bar (atm).

1.2.2 Kinetic Studies

1.2.2.1 Different Metal-slag Systems

Several studies have been conducted on the mass transfer of impurities between gas bubble agitated slag/metal systems. Patel et al. [69] studied the transfer of chromium between molten iron and FeO bearing slag at 1600^{o}C in the presence of gas bubbles and have observed that the bubbles noticeably increased the mass transfer. A mathematical model was developed by Kaddah and Szekely [70] for desulphurisation kinetics in argon stirred laddles. They have concluded that the fluid-flow phenomena and turbulence are key parameters in desulphurisation kinetics. Effect of slag composition was studied [20,71-76] and it was observed that rate of mass transfer increases with an increase in slag basicity. The temperature dependence of S transfer from metal to slag has been studied [17,72,75,77]

and it was found that the desulphurisation reaction got suppressed considerably with increasing temperature. Low sulphur steel could be obtained by mag-coke process using an inert gas at low cost [78-82] and mag-process was found better than carbide treatment. Schulz [83] analysing operational results from a number of steel plants concluded that higher degrees of desulphurisation can be obtained using immersed lances or stirrers, irrespective of the temperature, composition, and, initial sulphur content of pig iron. Bahout [84] studied external desulphurisation of hot metal pig iron by pneumatic injection of soda ash and concluded that deep injection of soda ash considerably improves the desulphurisation efficiency as compared to classical techniques. In steel making, different techniques for blowing gas into the liquid metal were used [85-90] and the mass transfer rate of S, P, Mn, C and oxygen between slag and molten steel was found to improve through gas bubble stirring.

Soifer et al. [91] have studied the influence of basicity on the kinetics of Mn removal from pig iron with ferrous slag under laboratory and plant conditions, and obtained low kinetic efficiency for slag basicity of 0.6-1.3. However, on addition of CaF_2 to slag, Mn oxidation rates increased.

1.2.2.2 Copper metal- slag systems

Several workers have carried out kinetic studies on the removal of elements from copper using different slag systems. Sakai et al. [53] have measured the removal rates of As and Sb from molten copper using $CaO-Na_2SO_4$ flux at different temperatures and oxygen potentials. Sakai et al. and Nakamura et al. [55,56] have investigated the removal rates of elements As, Sb, Bi from Cu in fire refining by alkaline carbonate fluxes such as Li_2CO_3, Na_2CO_3 and K_2CO_3 at two different temperature ranges of 1323-1423K and 1423-1523K for two oxygen potential ranges of $pO_2 = 10^{-4}-10$ atm and $pO_2 = 10^{-8}-10^{-5}$ atm respectively and found that removal rates of As and Sb were higher than that of Bi. Nakamura et al. [92] also studied the kinetic aspect of removing As, Sb, Bi, from molten copper using Na_2CO_3 flux at 1150-1250^{o}C under different O_2 potential and found that As, Sb elimination reaction rate increased with increasing O_2 content.

Hirasawa et al. [93] investigated the fundamental aspects of the role of gas injection stirring in slag- metal reactions using a molten slag- Cu system and have examined the application of dimensionless correlation equation to practical ladle refining processes. Hirasawa et al. [94,95] have developed several models on the role of gas injection

stirring and metal-side mass transfer in molten slag-Cu reactions of Si oxidation by FeO at 1250^{o}C and found that the dimensionless correlations equations obtained are appplicable to data on ladle desulphurisation. They have also investigated the relations between apparent metal side mass transfer coefficient, and gas injection stirring conditions, i.e. gas flow rate, metal depth, crucible diameter and slag depth.

Several kinetic studies [96-99] have been done on the mechanism of Si oxidation reaction between a molten LiO_2- SiO_2-Al_2O_3-FeO slag and Cu-Si alloy at different temperatures. The mechanism of the reaction in the reaction zone of metal-slag reactions under the conditions of rate controlling Si transport in the metal phase has been examined. It was concluded that the reaction zone is not always located at the slag-metal interface at high temperature. Mass transfer coefficient was determined under different experimental conditions such as bath stirring,metal depth, slag depth, and crucible diameter.

Tadeusz and Themelis [100] investigated the removal of Sb from Cu by injecting Soda ash at 1473K and have found that the reaction was controlled by diffusion of Sb in metal phase. On the basis of experimental work, the over all volumetric mass transfer coefficient (cm^3/s) at 1473K was expressed in terms of two subprocesses as follows

$$(k_dA)_{ov} = (k_dA)_{pc} + (k_dA)_{tc} = 1.25\ Q_g^{0.29} + 0.28\ (HQ_f)$$

where Q_g is injection gas flow rate (litre/min)

H is depth of injection (cm)

Q_f is the rate of flux injection (gm/sec)

pc and tc are permanent and transitory contacts

1.2.3 Viscosity Measurements

1.2.3.1 Different Slag Systems

Numerous investigations to determine slag viscosities have been undertaken. Kato and Minowa [101] studied and discussed viscosity and density relationship in ternary $CaO-SiO_2-Al_2O_3$ system and quarternary $CaO-SiO_2-Al_2O_3$ system containing other oxides, fluorides and chlorides.

Takumoto and Kim [102] measured the viscosity of experimental slags containing Na_2O, Al_2O_3 and TiO_2 obtained in laboratory smelting of copper-sulphide ores using the Rising-Ball method and found that Na_2O decreased both the slag loss and viscosity while Al_2O_3 and TiO_2 decreased the slag loss but increased the viscosity.

Gimmerfarb [103] measured the viscosity of quarternary $CaO-SiO_2-FeO-Al_2O_3$ while Semik et al. [104]

studied viscosity and fusibility of highly basic fluoride containing slags with $(CaO+MgO)/SiO_2$ ratios of 1.5-2.0 and containing 0.5-2 % Fluorine.

Korpachev et al.[105] estimated the viscosity of open-hearth slags at various stages in the furnace at 1450-1650^{o}C by measuring the angle of torsion of a thread during the rotation of a spindle in the slag and found that on heating by 100-150^{o}C above the liquidus temperature, the value of viscosity being 3-0.5 N/sec.m^{2}, shows a little change with time.

Davis and Wright [106] measured the viscosity of CaF_2 -CaO-Al_2O_3 system between temperatures below the liquidus temperature Te to 1550^{o}C with reference to CaF_2-based fluxes used in electro-slag refining and have observed no significant relationship between η and Te.

Venyukov et al. [107] studied viscosity of FeO-Fe_2O_3-SiO_2 and FeO-Fe_2O_3-CaO-SiO_2 slags used in conversion of copper mattes in oxidising atmospheres. They have found that temperature-dependence of viscosity obeyed an experimental law, with an activation energy of 9-13 kcal/mole. Both volume and surface viscosities play role in converting process. Dissolution of FeS in slag may reduce their viscosity by as much as 25%.

Klemeshov et al. [108] determined the melting point and viscosity of several O.H. slags in relation to

their composition and observed that primary slags tended to have the lowest liquidus temperature range (1200-1280^{o}C). Hadfield and Charette [109] studied viscosities and structures of eleven compositions of industrial high titania slags obtained from industrial electric arc smelting furnaces and containing 3.3-15% FeO and 80-67% TiO_2. They have concluded that melts rich in TiO_2 easily crystallise, are structurally different from polymerised silicate melts and that the main factor affecting their fluidity is the presence of solid particles in the melt.

Efimov et al. [110] also studied viscosities of synthetic slags used in the casting of carbon-and alloy steels at temperatures in the range of 950-1500^{o}C using a vibration type viscometer and have observed that viscosity genrally reduced on reduction of SiO_2 and Al_2O_3 content and on increasing the proportions of Na_2O or CaF_2 in the slag.

Tokumoto et al.[111] analysed the effect of viscosity on copper loss in slags containing Al_2O_3,MgO and ZnO by measuring viscosity and copper contents of slags and found that the viscosity increased in the increasing order of Al_2O_3,MgO and ZnO contents while the extent of copper loss was in the reverse order.

Toguri et al. [112] measured the viscosity of molten FeO-Fe_2O_3-SiO_2 system using a rotational cylinder technique, in the composition range of interest to copper

smelting with SiO_2 contents varying from 20-35 wt % at 1200-1350^{o} and found that viscosity of slag is generally decreased with increasing temperature and decrease in silica content.

Sikora et al. [113] measured viscosity, conductivity and diffusion coefficient of synthetic slags of SiO_2-CaF_2-Na_2O system and presented relationships between these parameters for the slags studied.

Dobovisek et al. [114] determined the visocisty of electric reduction furnace slags producing iron and containing 9-15% MgO and 13-15% Al_2O_3 between 1390-1520^{o}C and found no significant differences between the values of viscosity of white-and grey-iron slags despite the higher MgO contents of the latter.

Bodnar et al. [115] studied viscosity by a rotary method at 1300^{o}C of FeO-SiO_2 slag systems for SiO_2 varying between 20-30 wt % and Fe_2O_3 from 5-22% . They have found that Fe_2O_3 content upto 17 wt% increased viscosity of such slags, above this concentration , rise was more rapid. Viscosity decreased for SiO_2 content greater than 30% and at FeO/SiO_2 =1.67.

Pomelnikova et al. [116] measured the viscosity of Na-B-Silicate melts with additions of B_2O_3,SiO_2,BaO, Na_3AlF_6, KF, Fe_2O_3 and Cr_2O_3 using vibrational method. Additions of B_2O_3,BaO,Na_3AlF_6 and KF reduced viscosity ,

obviously related to their effects on the structure of melts.

Shiraishi et al. [117] measured viscosity using a rotating cylinder method for $FeO-SiO_2$ system with special emphasis on fayalitic melts. Their results revealed small but sharp humps on viscosity vs. composition curves near the fayalite (Fe_2SiO_4) composition.

Nowakowski [118] investigated the viscosity of synthetic slags from $CaO-SiO_2-Al_2O_3$ equilibrium system , containing between 0.6 and 15.6 % Cu_2O, at temperature between 1450 and 1670K and found that temperature and Cu_2O content significantly affect slag viscosity.

Akberdin et al. [119] have plotted the viscosity diagrams for melts $CaO-SiO_2-Al_2O_3$ at temperature 1473-1923K. They investigated the ranges of composition and temperatures and observed that B_2O_3 reduced the viscosity of slags and increased their stability .

Seki and Oeters [120] measured the viscosity of $CaO-FeO-Fe_2O_3-SiO_2$ slags at 1600^{o}C under air and CO_2 atm. for CaO/SiO_2 ratios of 0.66,1.00 and 1.5 and observed that increase in iron oxide content decreases viscosity. They also found out that for Fe_2O_3 /(FeO+CaO) = 0.5, viscosity changes due to change in atomic sturcutre of the slag.

Williams et al. [121] examined $CaO-FeO-SiO_2-MgO$ slags for viscosity measurements in the temperature range

1120-1470^{O}C using a rotary viscometric technique applied in a vertical tube furnace and compared it with the limited existing known data.

1.2.3.2 Na_2O-B_2O_3 Slag Systems

There have been studies done on viscosity measurements for sodium-borate slag systems for different temperatures and slag compositions. Kazuhiro et al. [122] estimated the absorption coefficient of ultrasonic waves for Na_2O-B_2O_3 slags in the temperature range 1000K as it depends on viscosity and temperature. They found that a melt with higher content of B_2O_3 has larger absorption coefficient because of high viscosity. Volarovich and Tolstoi [123] have measured the viscosity of binary system $Na_2B_4O_7$-B_2O_2 in the molten state.

Shartsis et al. [124] conducted the viscosity measurements of Na_2O-B_2O_3 slag system for a temperature range of 600-1000^{O}C and found that viscosity isotherms in the range 700-800^{O}C show minima in the low alkali region followed by maxima as the alkali concentration was increased.

1.3 FORMULATION OF THE PROBLEM

Generally, the ingradients of a flux can be

oxides, chlorides, fluorides or other suitable slag forming compounds. From the available data on free energy of formation of oxides, chlorides and fluorides as shown in the Table 1.5 [68,125-127], the free energies of formation of oxides of Nickel, Bismuth and Arsenic are more negative as compared to that for the formation of Cu_2O. This difference is less for corresponding chlorides and the difference appears to be more in case of fluorides which indicates the preferential use of oxides over chlorides or fluorides as flux. Table 1.6 [128] shows the values of cation-anion interaction parameters for various oxides, chlorides and fluorides. The difference in cation-anion interaction parameter is higher for oxides than for chlorides or fluorides. Hence it can be said that from this point of view also, oxides will be more effective than chlorides or fluorides as fluxes. On the basis of available data as shown in Table 1.5, it can be concluded that there is a possibility of removal of Ni, Bi and As from molten copper by oxidation. However, the free energies of formation of tellurium oxide and selenium oxide are less negative than that of copper. Hence these can not be removed by oxidation. Further, on the basis of free energies of formation of chloride and fluorides of Cu, Se and Te as shown in the Table 1.5, it is expected that both these elements, i.e. Se and Te can not be removed as oxides,

TABLE- 15

FREE ENERGY CHANGE OF FORMATION OF COMPOUNDS [68,125-127]

Compounds	ΔG^{o}_{298K}, KJ/mole	ΔG^{o}_{1473K}, KJ/mole
$CuCl_2$	-175.56	-58.52
CuF_2	-	-173.80
Cu_2O	-144.58	-61.69
Se_2Cl_2	- 76.07	-
$SeCl_4$	-108.26	-
SeF_6	-1015.74	-
SeO_2	-	9.32
Na_2Se	-	-88.95
$TeCl_4$	-240.76	-
TeF_4	-773.3	-
TeF_6	-1220.56	-
TeO_2	-269.61	-49.86
Na_2Te	-	-73.02
Na_2O	-	-221.54
K_2O	-	-163.02
NiO	-	-108.26
$NiCl_2$		-54.76
NiF_2	-	-227.77
As_2O_3	-	-133.76
$AsCl_3$	-	-72.48
AsF_3	-	-535.04
Bi_2O_3	-	-110.02
$BiCl_3$	-	- 66.71

TABLE- 1.6

CATION - ANION INTERACTION PARAMETERS [128]

Cation	Cl^- (1.81)	F^- (1.36)	O^{2-} (1.40)
Cu^+	0.361	0.431	0.847
Bi^{3+}	1.172	1.422	2.790
Bi^{5+}	1.961	2.381	3.861
As^{5+}	2.193	2.732	4.310
Sb^{3+}	1.224	1.500	2.409
Sb^{5+}	2.057	2.525	4.048
Na^+	0.362	0.433	0.851
K^+	0.318	0.372	0.823
Mg^{2+}	0.813	0.955	1.951
Ca^{2+}	0.714	0.851	1.673
P^{5+}	-	-	5.745

chlorides or fluorides whereas the values of free energy of formation of telluride and selenide of alkali metal being more negative than that of oxide of Se,Te and Cu reveal the possibility of these elements being removed as tellurides and Selenides. Previous studies [61,64,68] on removal of As, Sb, Se and Te show that Na_2CO_3 is a suitable flux to be used in the anode furnace. But its use as such on industrial scale poses following problems :

1. The activity of sodium oxide will be a function of partial pressure of a gaseous species, namely , CO_2 which can not serve as a controllable parameter for the process.
2. Sodium oxide formed from its carbonate shall be very corrosive and will, therefore, reduce considerably the life of the furnace refractories.
3. In case traces of sulphur are present in the metal, it will lead to the formation of sodium sulphide which, in turn, will lead to pollution problems.

To overcome these difficulties, and to dilute the highly reactive Na_2O, a carrier oxide should be used alongwith this principle component of the flux. As the working temperature in the present study is around 1473K, B_2O_3 seems to be an attractive ingradient in view of the fact that the liquidus temperature of the flux system Na_2O-B_2O_3 is well below this temperature. Further it can offer following advantages :

1. By adjusting the relative amounts of Na_2O and B_2O_3 , it will be possible to work over a range of flux composition out of which the most suitable could be selected.
2. Na_2O-B_2O_3 fluxes will be capable of dissolving some sulphur as sulphides and thus avoid its escape into the atmosphere as Na_2S.

In view of the above facts, therefore, for the present investigation, (Na_2CO_3)Na_2O-B_2O_3 slag system has been chosen to study the transfer of impurities from liquid copper to the slag. The effects of CaO and CaF_2 additions to Na_2O-B_2O_3 slag system on equilibrium distribution coefficients will also be investigated . Apart from studying the slag- metal thermodynamic equilibria, it is equally important to examine the rate at which the slag-metal reaction proceeds. This study forms the subject matter of kinetics. The rate of reaction in high temperature slag-metal system is generally transport controlled and hence will be affected by the slag viscosity which governs the flow characteristic of slag during separation from metal. Therefore, the viscosity of slags developed will also be studied. Finally,how far the rate of transfer of impurity is influenced by diffusion in the metal and in the slag phases shall be determined by overall mass transfer coefficient of the impurity elements.

The present investigation is confined to the removal of Se and Te impurities from copper in anode furnace. During fire refining in the anode furnace, impurities such as As, Sb,Bi,Fe and S are removed during oxidising period and then reducing conditions are maintained by introducing hydrocarbons to bring down the level of dissolved oxygen in copper from 0.6 % to 0.05% . A sodium-borate flux of suitable composition can be introduced in the anode furnace during the reduction stage to selectively recover Se and Te impurities as by product in form of selenide and telluride to slag phase.

For thermodynamic and kinetic studies, experimental set ups will be fabricated locally and effect of different process variable will be investigated. In case of thermodynamic studies on slag-metal equilibria, effects of different process variables such as slag composition, temperature of reaction and initial concentration of impurity element in copper will be investigated. Effects of CaO and CaF_2 additions to different sodium-borate slags on distribution coefficient will be studied to develop a suitable optimum slag composition for removal of impurities. For kinetic studies, optimum slag composition developed under thermodynamic investigations , will be mixed with molten copper of particular initial concentration of impurity element and stirred by bubbling dry and purified N_2

gas. Effects of different gas flow rates on rate of removal of impurity from copper will be investigated. For viscosity measurements of slags of different compositions at different temperatures, Haake's 'Rotovisco RV20' viscometer, which is designed to measure the viscosity of melts upto $1600^{o}C$, will be used.

Samples of slag and metal will be analysed for their Se and Te contents for different experimental runs. From the experimental data so obtained, distribution coefficient, rate of selenium and tellurium removal and mass transfer coefficient will be computed. The activation energy for different slag systems will be estimated for a temperature range (1273-1573K) from the viscosity data obtained experimentally.

CHAPTER-II

THERMODYNAMICS OF SLAG-METAL SYSTEM

2.1 GENERAL

Development of fluxes for refining of metal is based on two important branches of physical chemistry of slag-metal reactions, namely, thermodynamics and kinetics. Thermodynamics enables us to arrive at the necessary chemical conditions which must be satisfied by the slag phase formed as a result of the reaction between the flux and the components of the metallic phase. The ingradients of a flux can, in general,be oxides, chlorides, fluorides and other suitable slag forming compounds. With the available data as shown in Table 1.5 it is clear that the free energies of formation of selenium oxide and tellurium oxide are less negative than that of copper oxide. Hence these can not be removed by oxidation. Similarly, on the basis of free energies of formation of chlorides and fluorides of Cu, Se and Te as shown in the Table 1.5, it is expected that both these elements i.e. Se and Te can not be removed effectively as chlorides or fluorides. The values of free energy of formation of telluride and selenide of alkali

metal as given in the same Table 1.5, are more negative than that of oxides of Se, Te and Cu. This reveals the possibility of these elements being removed as tellurides and selenides of alkali metals.

Further, selenium and tellurium are known to show slight positive deviation from ideal behaviour in molten copper. The value of Henry's law constant is known to be between 1.01 and 1.001 [129]. This will also facilitate Se and Te removal as selenide and telluride.

2.2 THEORETICAL ANALYSIS

A thermodynamic analysis of distribution equilibria for Se and Te between slag and molten copper bath can be explained by the following reaction :

$$[Me] + m/2\ (Na_2O) = (Na_mMe) + m/4\ O_{2(g)} \quad \ldots\ (2.1)$$

where 'Me' represents minority metal/element Se and Te . The extent of removal of Se or Te from the metal bath to the slag containing Na_2O will depend on the prevailing oxygen partial pressure of the system and free energy of formation of compounds involving the base metal and the minority metal.

At equilibrium for reaction (2.1), the equilibrium constant,

$$K_{1,eq} = \frac{a_{(Na_mMe)} \cdot P_{O_2}^{m/4}}{a_{(Na_2O)}^{m/2} \cdot a_{[Me]}} \quad \ldots(2.2)$$

suggests that lower oxygen partial pressure and higher activity of Na_2O favours the formation of sodium metallide thereby lowering the minority metal 'Me' content in molten copper. Further, lower oxygen potential will avoid copper loss to the slag and bring about effective removal of Se and Te from copper to the slag phase as sodium selenide and telluride respectively .

The oxygen partial pressure of the system will be controlled by following reaction,

$$C + 1/2\ O_2 = CO \quad \ldots(2.3)$$

for which the equilibrium constant $K_{2,eq} = \frac{P_{CO}}{a_C \cdot P_{O_2}^{1/2}}$ ...(2.4)

As the furnace atmosphere contains CO and N_2, maximum value of P_{CO} can not be more than 1 atm i.e.101.08 KPa. Therefore, assuming P_{COmax} = 1 atm and a_C= 1, we get

$$K_{2,eq} = (P_{O_2})^{-1/2} \quad \ldots(2.5)$$

Since for CO formation, ΔG^{O}_{1473K} =-240.59 KJ/mole,

therefore, p_{O_2}= 8.6 x 10^{-18} atm (i.e.8.6x10^{-13}Pa) which corresponds to emf E =-732 mV at 1473K for the cell :

Ni,NiO|ZrO_2 + CaO| metal/slag.

Due to corrsoive nature of slag, only once the emf of the cell could be measured during the equilibria studies and it came out to be E =-760 mV which yields oxygen partial pressure , p_{O_2}= 3.5 x 10^{-18} atm (3.5x10^{-13}Pa) of the system. This value almost corresponds with the one obtained theoretically after assuming $p_{CO_{max}}$= 1 atm.

2.3 EXPERIMENTAL

The thermodynamics of removing selenium and tellurium from liquid copper by slag was approached by their distribution equilibria measurements. Since the refining behaviour of a slag phase with respect to the liquid metal is a function of temperature and of the compositions of the metal and slag phases,slags of different compositions were equilibrated with various (Cu-Se) and (Cu-Te) alloys at a pre-selected temperature. The equilibrium distribution coefficients were determined by sampling technique.

2.3.1 Experimental set-up

Fig.2.1 shows the schematic block-diagram of experimental set-up used in the present investigation. The essential components of this set-up, designed and fabricated locally, include, a gas purification train and slag-metal equilibration unit for thermodynamic studies of element transfer from metal to slag at equilibrium. Details of different units are briefly presented below.

2.3.1.1 Gas purification train

High purity nitrogen gas procured from M/s Modi Gas and Chemicals Ltd., Modi Nagar, was further purified by removal of associated moisture vapour and oxygen using a simple purification train shown schematically in Fig.2.2. Nitrogen gas from the cylinder was first bubbled through alkaline pyrogallol solution and concentrated sulphuric acid and then passed over phosphorous pentaoxide powder. Ten pyroglass bubblers connected in series with the first, fourth, seventh and tenth bubblers kept empty to avoid mixing of different reagents used. The second and third bubblers containing alkaline pyrogallol solution, remove oxygen while bubblers containing concentrated sulphuric

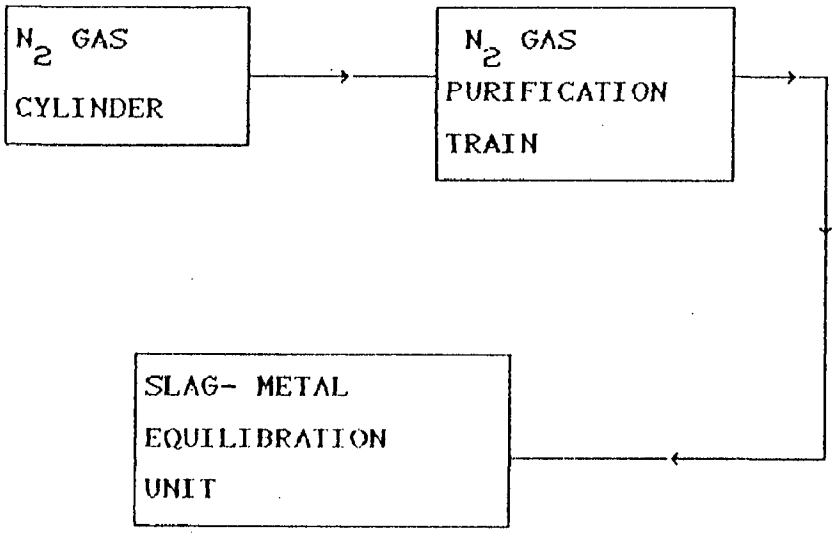

FIG. 2.1 SCHEMATIC BLOCK-DIAGRAM OF EXPERIMENTAL SET-UP FOR THERMODYNAMIC STUDIES.

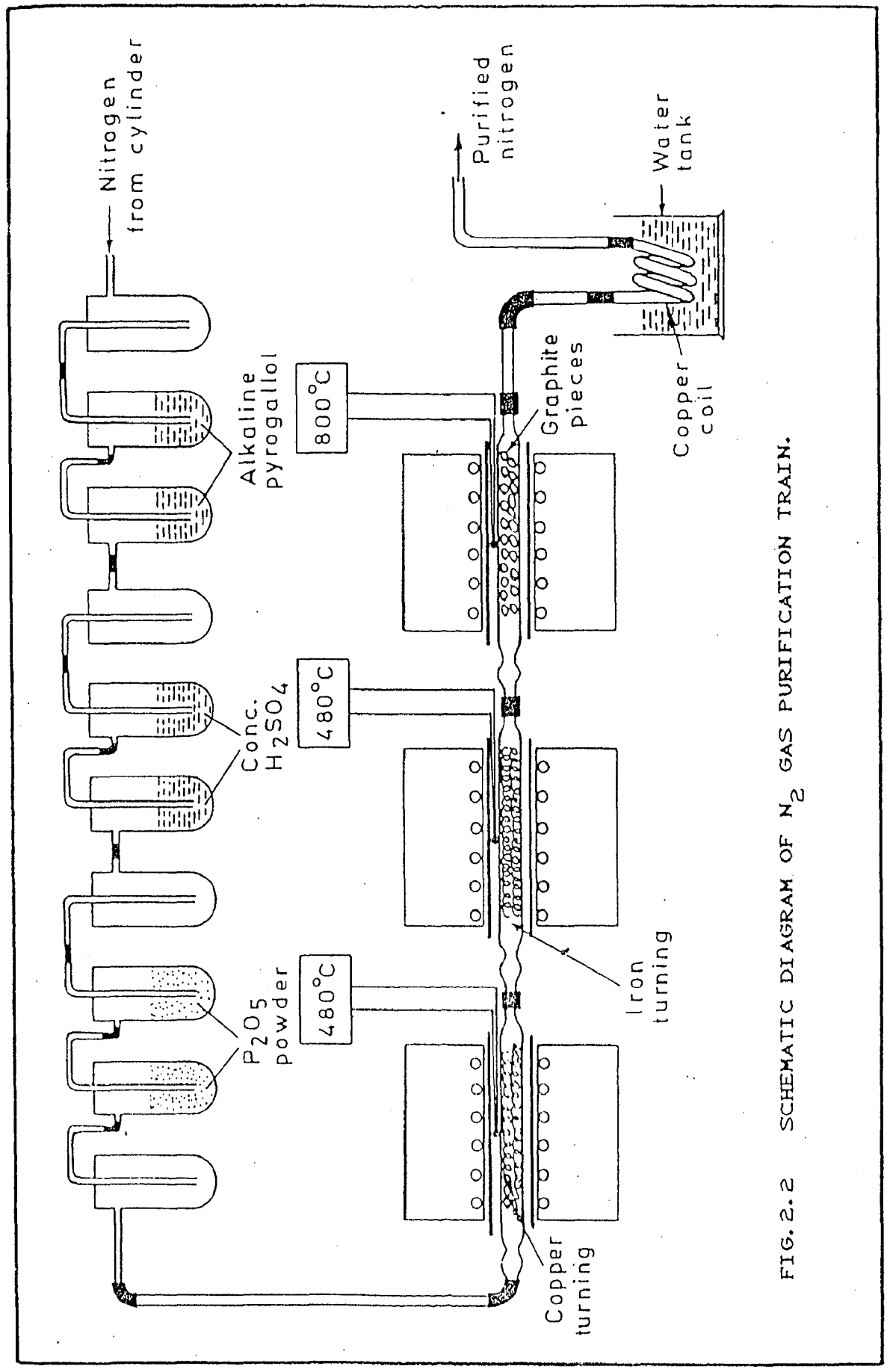

FIG. 2.2 SCHEMATIC DIAGRAM OF N_2 GAS PURIFICATION TRAIN.

acid and powdered phosphorous pentaoxide remove moisture from nitrogen gas. The bubbled gas was then passed over copper turnings, iron turnings and graphite pieces of 1-2 mm size kept in three different tubular furnaces maintained respectively at 480,480 and 800^{o}C to ensure oxygen and moisture removal. Finally, the purified gas was passed through a copper coil immersed in a water tank for cooling before passing the purified gas into slag-metal equilibration unit.

2.3.1.2 Slag-metal equilibration unit

Fig.2.3 shows the essential components of the experimental unit. It includes,

(a) **Furnace assembly :** A horizontal globar furnace with both ends open and employing silicon carbide rods as heating element to develop a temperature upto 1400^{o}C , was used for melting the charge. High alumina tube of 65 mm OD and 55 mm ID was horizontally placed between the four silicon carbide rods. Temperature of the furnace was controlled within $\pm$ 2^{o}C .Pt/Pt-13% Rh thermocouple was used to measure the temperature.

(b) **Graphite reaction boat:** Boats designed as shown in Fig.2.4 were fabricated from spent graphite electrodes

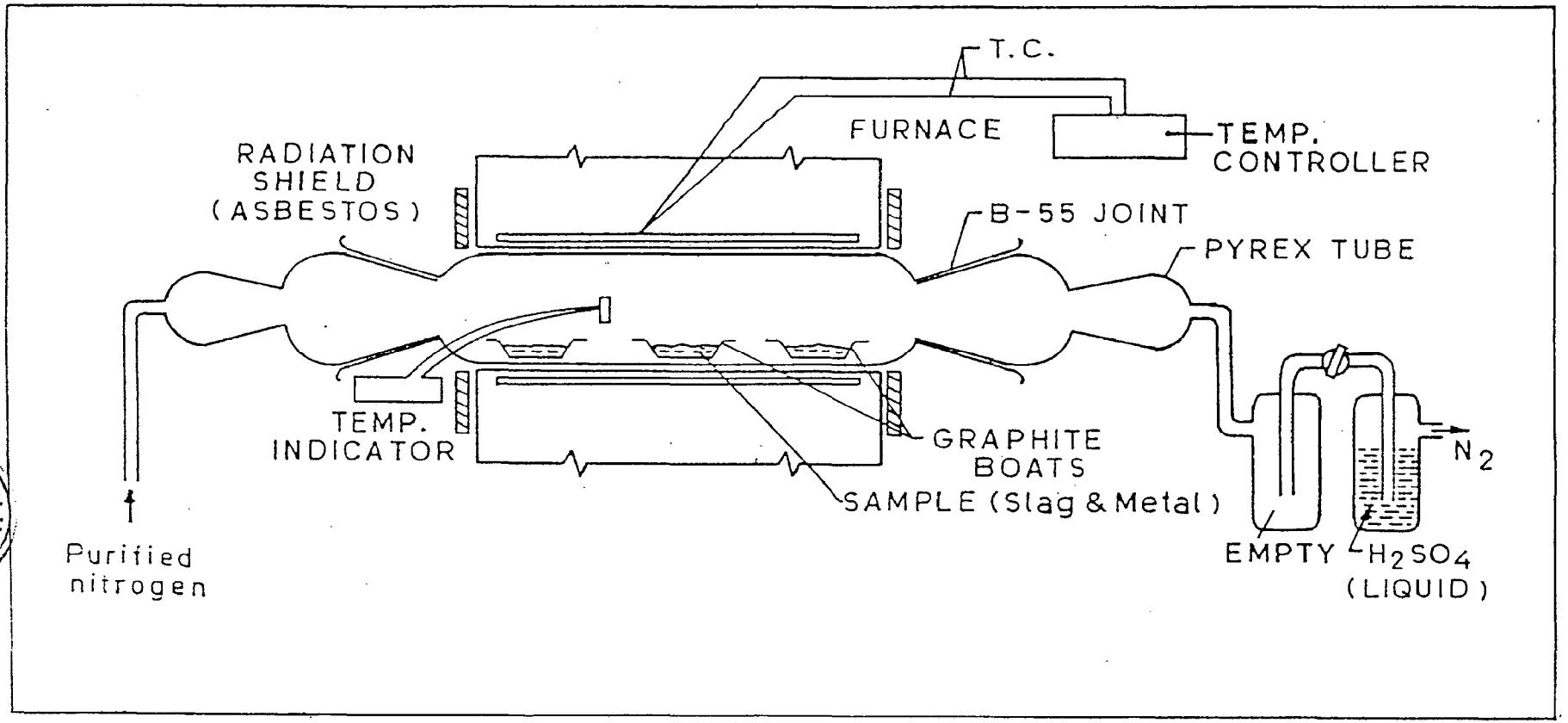

FIG. 2.3 SLAG-METAL EQUILIBRATION UNIT.

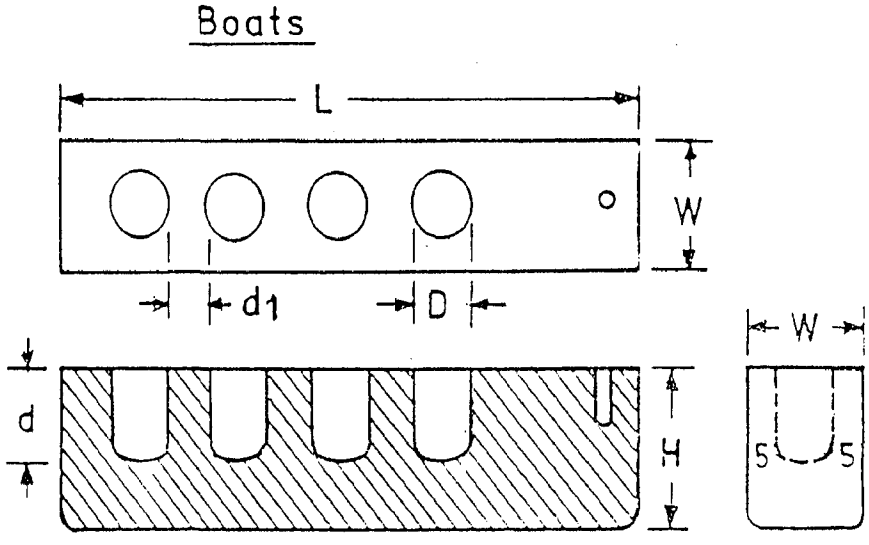

H = 25 to 30 mm , D = 10 to 15 mm , d = 15 to 20 mm

W = 20 to 25 mm , d_1 = 10 mm , L = 120 – 150 mm

FIG. 2.4 REACTION BOAT SKETCH.

obtained from mini-steel plant. The boats were placed in the hot zone for experimental runs containing samples of metal and slag for equilibration.

2.3.2 Preparation of slag

Chemical systems of different basicities were prepared by mixing sodium carbonate and borax (both of anal.r. grade) in desired proportions and calcining the mixture in the furnace for long time (3-4 days) at 1023K followed by crushing, grinding, thorough mixing and recalcination of the mixtures for 2 days at the same temperaure. For preparation of Na_2O-B_2O_3-CaO slag systems with different CaO proportions, sodium borate slag (wt% Na_2O/wt% B_2O_3 = 0.864) was first prepared in a similar manner as mentioned before and then CaO (anal.r.grade) in desired proportions was mixed with this sodium borate slag. The different mixtures were melted at 1223K and kept for long time (1-2 days) at this temperature. The mixtures were once again crushed and put in the furnace at 1273K for several hours (25-30 hours) to ensure proper mixing. For preparation of Na_2O-B_2O_3-CaO-CaF_2 slag systems with different CaF_2 proportions, first of all, slag composition (30.9 wt% Na_2O, 35.8 wt% B_2O_3, 33.3 wt% CaO) was prepared

using same method as mentioned earlier and then CaF_2 (anal.r.grade) in desired proportions were mixed thoroughly with this slag system. The different mixtures were melted at 1123K and kept for long time (28-30 hours) at this temperature. The mixtures were again crushed and put in the furnace again at the same temperature for enough time (10-12 hours) to ensure proper mixing.

2.3.3 Preparation of Copper alloys

For selenium distribution equilibria studies, (Cu-12.9 wt% Se) master alloy was prepared by adding copper (99.99 wt% pure) in selenium (99.99 wt% pure) and melting it in graphite boats under purified nitroen atmosphere. The alloys of desired compositions (0.316 wt% to 0.446 wt% Se in copper) were obtained by adding copper to the master alloy and analysing them on Inductively Coupled Plasma Sepectrometry (I.C.P.S.) for exact composition. For tellurium distribution equilibria studies, (Cu-4.0 wt% Te) master alloy was prepared by adding copper (99.99 wt% pure) in tellurium (99.99 wt% pure) and melting it in graphite boats under purified nitrogen atmosphere. The alloys of desired composition (1.597 wt% Te to 3.923 wt% Te in copper) were obtained by adding copper to the master alloy and

anlaysing them on Inductively Coupled Plasma Spectrometry for exact compositions.

2.3.4 Procedure :

Experiments were conducted on slag-metal equilibria using different slag compositions containing Na_2O,B_2O_3,CaO and CaF_2 and copper alloys containing elements Se and Te in different concentrations. As these studies were to be conducted under reducing atmosphere, specially designed graphite boats were used. These boats were fabricated from spent electrodes of a mini-steel plant. Equilibration studies were carried out by melting slag and metal samples in the graphite boat at 1473K for 16-18 hours under continuous flow of purified N_2 gas to determine the selenium and tellurium distribution coefficients between metal and slag. The amount of metal/alloy phase varied in the range 0.5 to 1.0 gm and that of slag in the range 0.2 to 0.4 gm in different experiments. The slag and metal samples were chemically analysed on Inductively Coupled Plasma Spectrometry (I.C.P.S.) to estimate the amount of Se and Te transferred from metal to slag. The oxygen partial pressure of the system was determined by an oxygen sensoring device i.e. high temperature oxygen concentration cell using calcia

stabilised zirconia as solid electrolyte. The emf of the cell, represented by the scheme :

$$(I)\ Ni, NiO | ZrO_2 + CaO |\ Metal/slag\ (II),$$

could be measured at 1473K only once due to corrosive nature of the slag. Its value was noted to be E =-760 mV (-0.76V). The oxygen partial pressure was then calculated as 3.5×10^{-18} atm (3.5×10^{-13} Pa) using equation $p^{II}_{O_2} / p^{I}_{O_2} = \exp\left(\frac{4FE}{RT}\right)$

$$\text{Where } p^{I}_{O_2} = \exp\left(\frac{2 \times \Delta G^{o}_{NiO}}{RT}\right)$$

$$T = 1473K\ ,\ E = -0.76\ V$$

and ΔG^{o}_{NiO} = - 23760 Cal. at 1473K.

= - 99.32 KJ

2.4 RESULTS AND DISCUSSIONS

Thermodynamics of the refining behaviour of a slag phase with respect to the liquid metal is a function of temperature and of the compositions of the metal and slag phases [130] and therefore, the equilibrium distribution coefficient of impurity element would be one of the parameters which determine the efficiency of the process. In

the present investigation, effect of basicity of sodium borate slag and effect of CaO and CaF_2 additions to sodium borate slag on equilibrium distribution coefficient have been studied.

The calculated values of equilibrium distribution coefficient 'L' of Se and Te between slag and metal, defined as $L_{Se} = \frac{(\%Se)}{[\%Se]}$ and $L_{Te} = \frac{(\%Te)}{[\%Te]}$ for different slag basicities (i.e. wt% Na_2O/wt%B_2O_2) at 1473K are given in the Tables (2.1-2.2) and plotted as ln L vs. slag basicity for different alloy compositions in Figs.(2.5-2.6) for Se and Te respectively. It is noted from Fig.2.5 that the selenium distribution equilibria follows a linear relationship in the composition range of present study. Regression Analysis of the data leads to the relationship $\ln \frac{(\%Se)}{[\%Se]} = 4B-2.76$. Similarly Fig.2.6 shows that the tellurium distribution equilibria follows a quantitative relationship $\ln \frac{(\%Te)}{[\%Te]} = 2.8B - 0.08$. (%Se) and (%Te) represent the amounts of Se and Te by weight in slag respectively while [%Se] and [%Te] represent the respective amounts by weight in metal phase. 'B' denotes the slag basicity. It is further noted from the Fig.2.5 that selenium distribution coefficient increases from 0.4 to 2.9 as slag basicity increases from 0.527 to 0.864 for Cu-0.446 wt% Se alloy while tellurium distribution coefficient increases

TABLE- 2.1

SELENIUM DISTRIBUTION FOR Na_2O-B_2O_3 SLAGS AT 1473K

%Initial Conc. of Se in Cu	% Na_2CO_3 in Borax	Slag Basicity	(%Se)	[%Se]	ln $\frac{(\%Se)}{[\%Se]}$
		(% Values by weight)			
0.316	10	0.527	0.141	0.298	-0.745
0.316	20	0.612	0.166	0.247	-0.400
0.316	30	0.696	0.215	0.229	-0.060
0.316	40	0.780	0.335	0.184	0.598
0.316	50	0.864	0.382	0.209	0.606
0.353	10	0.527	0.213	0.265-	-0.220
0.353	20	0.612	0.272	0.261	0.040
0.353	30	0.696	0.193	0.258	-0.290
0.353	40	0.780	0.373	0.249	0.404
0.353	50	0.864	0.712	0.327	0.778
0.442	10	0.527	0.294	0.399	-0.304
0.442	20	0.612	0.296	0.392	-0.280
0.442	30	0.696	0.400	0.300	0.289
0.442	40	0.780	0.279	0.292	-0.044
0.442	50	0.864	0.561	0.198	1.041
0.446	10	0.527	0.138	0.364	-0.969
0.446	20	0.612	0.169	0.322	-0.640
0.446	30	0.696	0.293	0.287	0.020
0.446	40	0.780	0.291	0.269	0.078
0.446	50	0.864	0.391	0.134	1.070

TABLE- 2.2

TELLURIUM DISTRIBUTION FOR $Na_2O-B_2O_3$ SLAGS AT 1473K

%Initial Conc. of Te in Cu	% Na_2CO_3 in Borax	Slag Basicity	(%Te)	[%Te]	ln $\frac{(\%Te)}{[\%Te]}$
		(% Values by weight)			
1.597	10	0.527	4.524	1.321	1.231
1.597	20	0.612	18.956	3.456	1.702
1.597	30	0.696	15.161	3.101	1.587
1.597	40	0.780	9.262	0.847	2.392
1.597	50	0.864	9.153	1.064	2.152
2.005	10	0.527	7.647	1.259	1.804
2.005	20	0.612	9.014	1.171	2.041
2.005	30	0.696	10.301	1.129	2.211
2.005	40	0.780	7.588	0.799	2.251
2.005	50	0.864	13.620	1.371	2.296
2.639	10	0.527	11.992	2.708	1.488
2.639	20	0.612	12.298	2.687	1.521
2.639	30	0.696	11.156	2.638	1.442
2.639	40	0.780	12.352	1.665	2.004
2.639	50	0.864	1.186	0.097	2.504
3.923	10	0.527	10.626	3.616	1.078
3.923	20	0.612	11.371	3.347	1.223
3.923	30	0.696	22.573	3.167	1.964
3.923	40	0.780	12.366	2.149	1.750
3.923	50	0.864	43.509	3.071	2.651

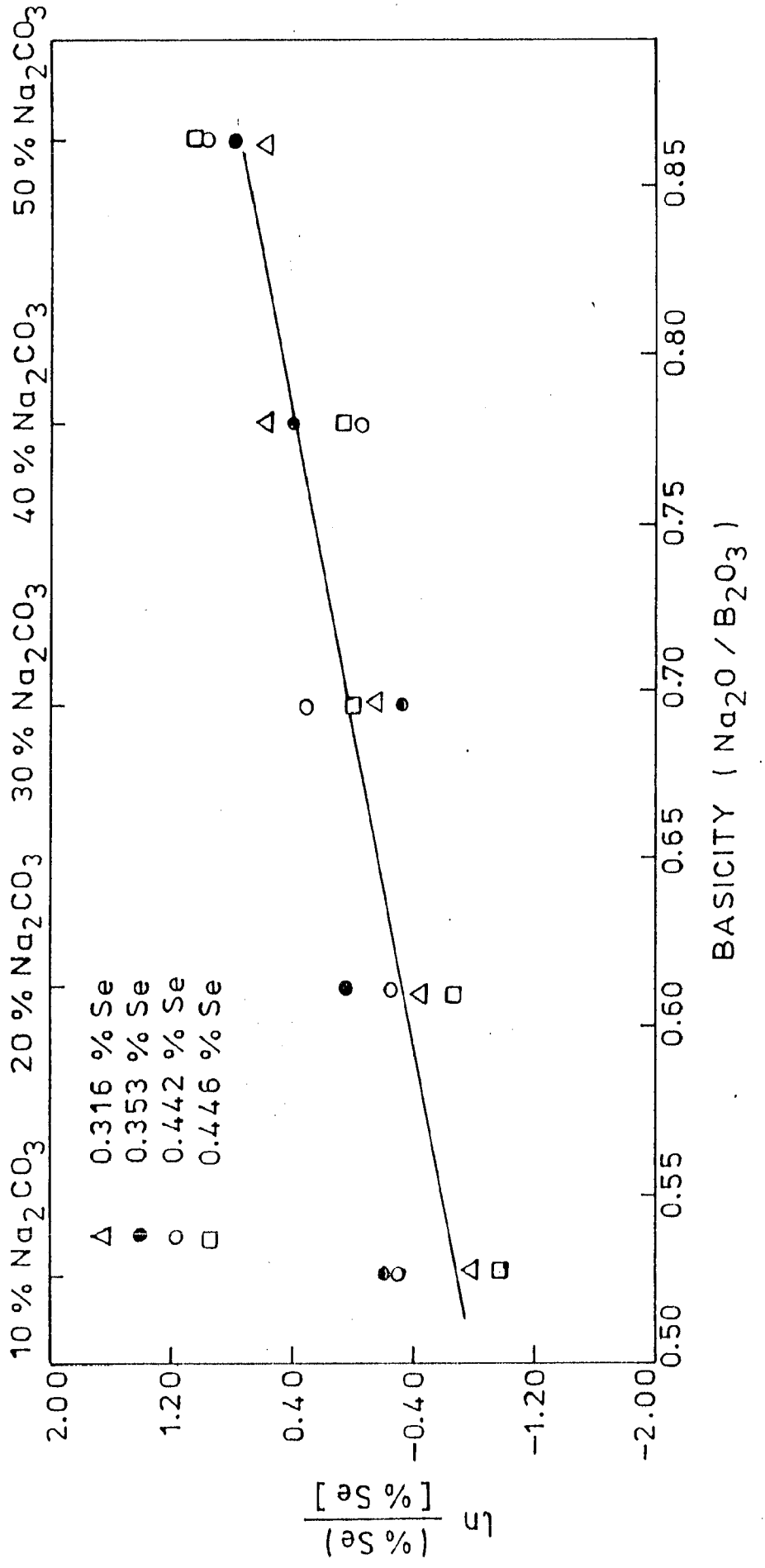

FIG. 2.5 SELENIUM DISTRIBUTION BETWEEN SLAG AND METAL Vs. SLAG BASICITY.

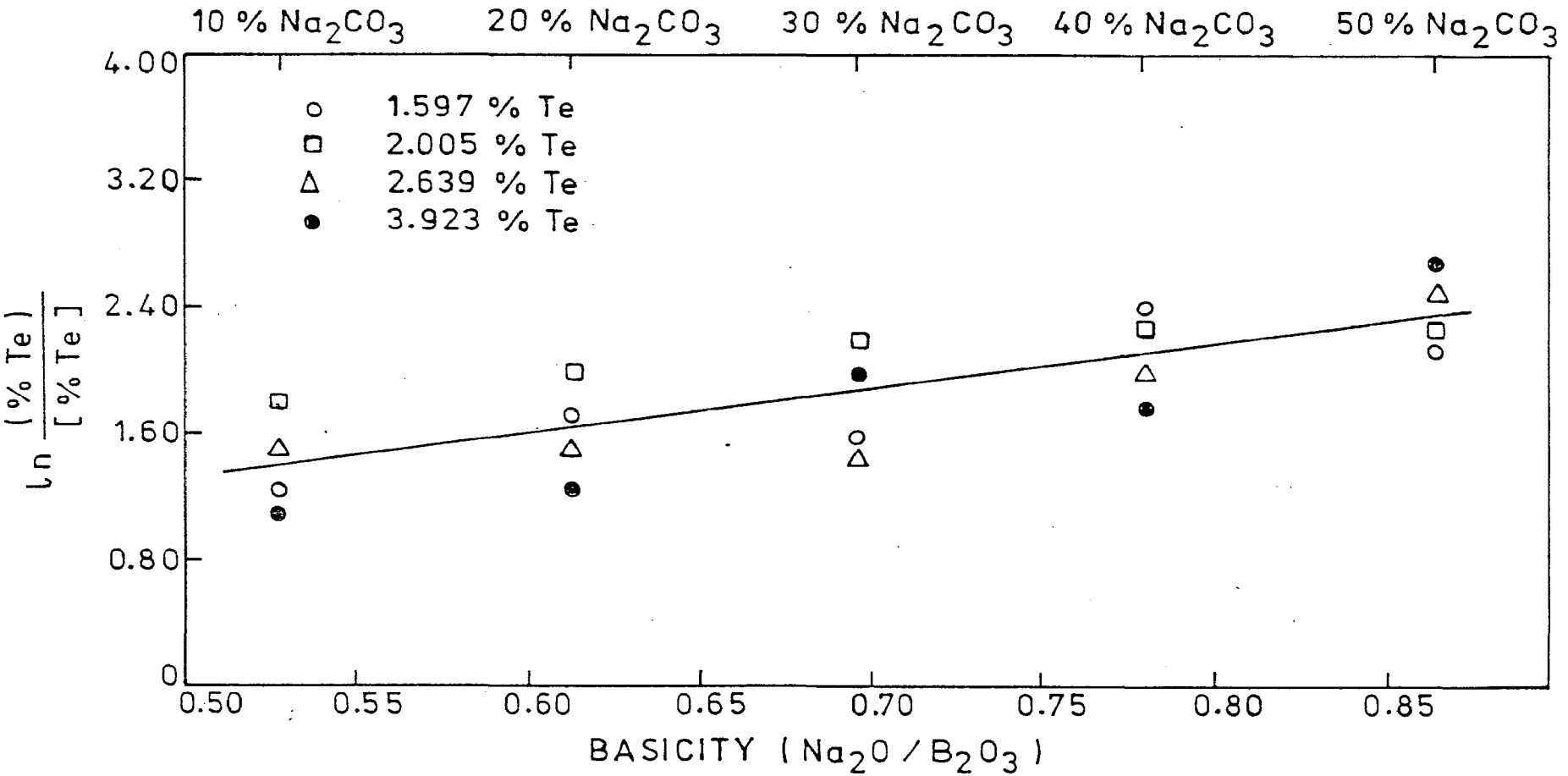

FIG. 2.6 TELLURIUM DISTRIBUTION BETWEEN SLAG AND METAL Vs. SLAG BASICITY.

from 2.9 to 14.2 for Cu-3.923wt%Te alloy with the same increase in the slag basicity as shown in Fig.2.6.

The improvement in Se and Te transfer,from metal to slag under reducing conditions with the increase in sodium ion content in the slag, can be attributed to the predominant presence of Na-Se and Na-Te compounds under the prevailing oxygen partial pressure ($p_{O_2} \simeq 3.5 \times 10^{-18}$ atm). Kojo et al.[68] have confirmed the formation of Na_2Se and Na_2Te in the slag under reducing conditions and formation of tetravalent selenium and tellurium species in sodium carbonate flux under oxidising conditions.

It has also been observed from the results plotted in Figs.(2.5-2.6) that the maximum values of equilibrium distribution of Se and Te achieved for Cu-0.446 wt% Se and Cu-3.923 wt% Te alloys respectively with slag (wt% Na_2O/wt% B_2O_3 = 0.864) system are low (L_{Se} = 3 and L_{Te} = 14) from industrial application point of view and will require the use of higher proportion of slag (i.e.35% slag by weight of metal). Therefore, in the further investigation, effect of CaO additions (10-50 wt%) on slag-metal distribution of Se and Te were studied at the same temperature (i.e.1473K) using sodium borate slag (wt% Na_2O/wt%B_2O_3= 0.86) with the objective of improving the distribution coefficient. The results are given in Tables (2.3-2.4) for Se and Te

TABLE- 2.3

SELENIUM DISTRIBUTION FOR Na_2O-B_2O_3-CaO SLAGS AT 1473K.

Sl. No.	Slag Composition	Initial Se % in Cu	(%Se)	[%Se]	$\frac{(\%Se)}{[\%Se]}$	$\ln \frac{(\%Se)}{[\%Se]}$
			(% Values by weight)			
1.	(46.4% Na_2O	0.316	0.382	0.209	1.833	0.606
2.	+53.6%B_2O_3)	0.353	0.712	0.327	2.177	0.778
3.		0.442	0.561	0.198	2.832	1.041
4.		0.446	0.391	0.134	2.915	1.070
5.	(42.1% Na_2O	0.316	0.432	0.188	2.295	0.831
6.	+ 48.8%B_2O_3	0.353	0.333	0.141	2.363	0.860
7.	+ 9.1% CaO)	0.442	0.992	0.281	3.528	1.261
8.		0.446	0.969	0.266	3.644	1.293
9.	(35.6% Na_2O	0.316	0.384	0.128	3.004	1.101
10.	+41.3% B_2O_3	0.353	0.582	0.162	3.596	1.282
11.	+23.1% CaO)	0.442	1.228	0.263	4.669	1.541
12.		0.446	1.196	0.241	4.963	1.602
13.	(33.1% Na_2O	0.316	0.484	0.146	3.320	1.201
14.	+38.3% B_2O_3	0.353	0.555	0.137	4.055	1.402
15.	+28.6% CaO)	0.442	1.238	0.240	5.160	1.641
16.		0.446	1.200	0.223	5.382	1.683
17.	(30.9% Na_2O	0.316	0.423	0.120	3.525	1.261
18.	+35.8% B_2O_3	0.353	0.582	0.135	4.315	1.462
19.	+33.3% CaO)	0.442	1.291	0.226	5.714	1.743
20.		0.446	1.256	0.211	5.954	1.784

TABLE- 2.4

TELLURIUM DISTRIBUTION FOR Na_2O-B_2O_3-CaO SLAGS AT 1473K.

Sl. No.	Slag Composition	Initial Te % in Cu	(%Te)	[%Te]	$\frac{(\%Te)}{[\%Te]}$	$\ln \frac{(\%Te)}{[\%Te]}$
			(% Values by weight)			
1.	(46.4% Na_2O	1.597	9.153	1.064	8.602	2.152
2.	+53.6%B_2O_3)	2.005	13.619	1.371	9.934	2.296
3.		2.639	1.186	0.097	12.231	2.504
4.		3.923	43.509	3.071	14.168	2.651
5.	(42.1% Na_2O	1.597	4.578	0.449	10.196	2.322
6.	+48.8% B_2O_3	2.005	4.208	0.340	12.378	2.516
7.	+9.1% CaO)	2.639	12.358	0.881	13.901	2.632
8.		3.923	21.692	1.251	17.331	2.853
9.	(35.6% Na_2O	1.597	5.349	0.427	12.528	2.628
10.	+41.3% B_2O_3	2.005	4.378	0.263	16.643	2.812
11.	+23.1% CaO)	2.639	15.517	0.785	19.767	2.984
12.		3.923	18.108	0.806	22.466	3.112
13.	(33.1% Na_2O	1.597	5.970	0.389	15.348	2.731
14.	+38.3% B_2O_3	2.005	4.679	0.258	18.138	2.898
15.	+28.6% CaO)	2.639	19.736	0.787	25.078	3.222
16.		3.923	16.779	0.606	27.688	3.322
17.	(30.9% Na_2O	1.597	6.548	0.361	18.138	2.898
18.	+35.8% B_2O_3	2.005	6.139	0.247	24.854	3.213
19.	+33.3% CaO)	2.639	16.010	0.587	27.275	3.306
20.		3.923	18.752	0.634	29.577	3.387

respectively and plotted in Figs. (2.7-2.10). The variation of selenium distribution coefficient with initial wt% Se in copper for different wt% CaO in slag has been plotted in Fig.2.7 while Fig.2.8 shows the effect of CaO on equilibrium distribution of Se between slag and metal for different Cu-Se alloys. It has been observed from Fig.2.7 that the values of selenium distribution coefficients for Cu-0.446 wt% Se alloy are 5.9 for slag composition (30.9 wt% Na_2O, 35.8 wt% B_2O_3,33.3 wt%CaO) and 3 for slag composition (46.4 wt% Na_2O, 53.6 wt% B_2O_3,0 % CaO) i.e. for the same wt% Na_2O/wt% B_2O_3 ratio but without lime. This clearly shows an improvement in Se transfer from metal to slag by about 2 times on addition of 50 wt% CaO to sodium-borate slag (wt% Na_2O/wt% B_2O_3=0.86). Similarly the variation of tellurium distribution coefficient with initial wt% Te in copper for different wt% CaO in slag has been plotted in Fig.2.9 while Fig.2.10 shows the effect of CaO on equilibrium distribution of Te between slag and metal for different Cu-Te alloys. It has been observed from Fig.2.9 that the values of tellurium distribution coefficients for Cu-3.923 wt% Te alloy are 29.6 for slag composition (30.9 wt% Na_2O, 35.8 wt% B_2O_3, 33.3 wt% CaO) and 14.2 for slag composition (46.4 wt% Na_2O, 53.6 wt% B_2O_3,0 wt% CaO) i.e. for the same wt% Na_2O/wt% B_2O_3 ratio but without lime. This shows an improvement in Te

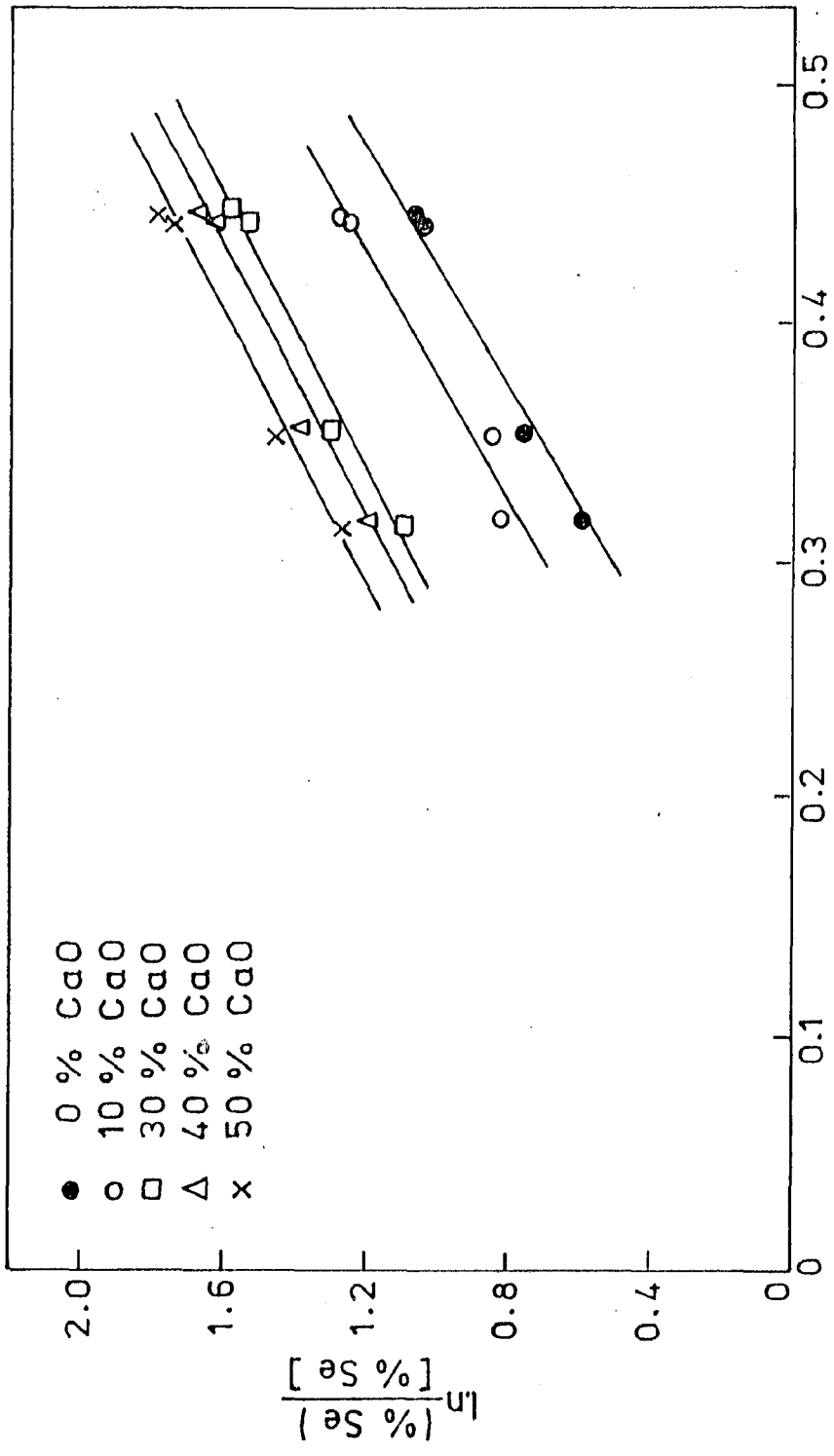

FIG. 2.7 SELENIUM DISTRIBUTION BETWEEN SLAG AND METAL Vs. INITIAL % Se IN COPPER FOR % CaO IN SLAG.

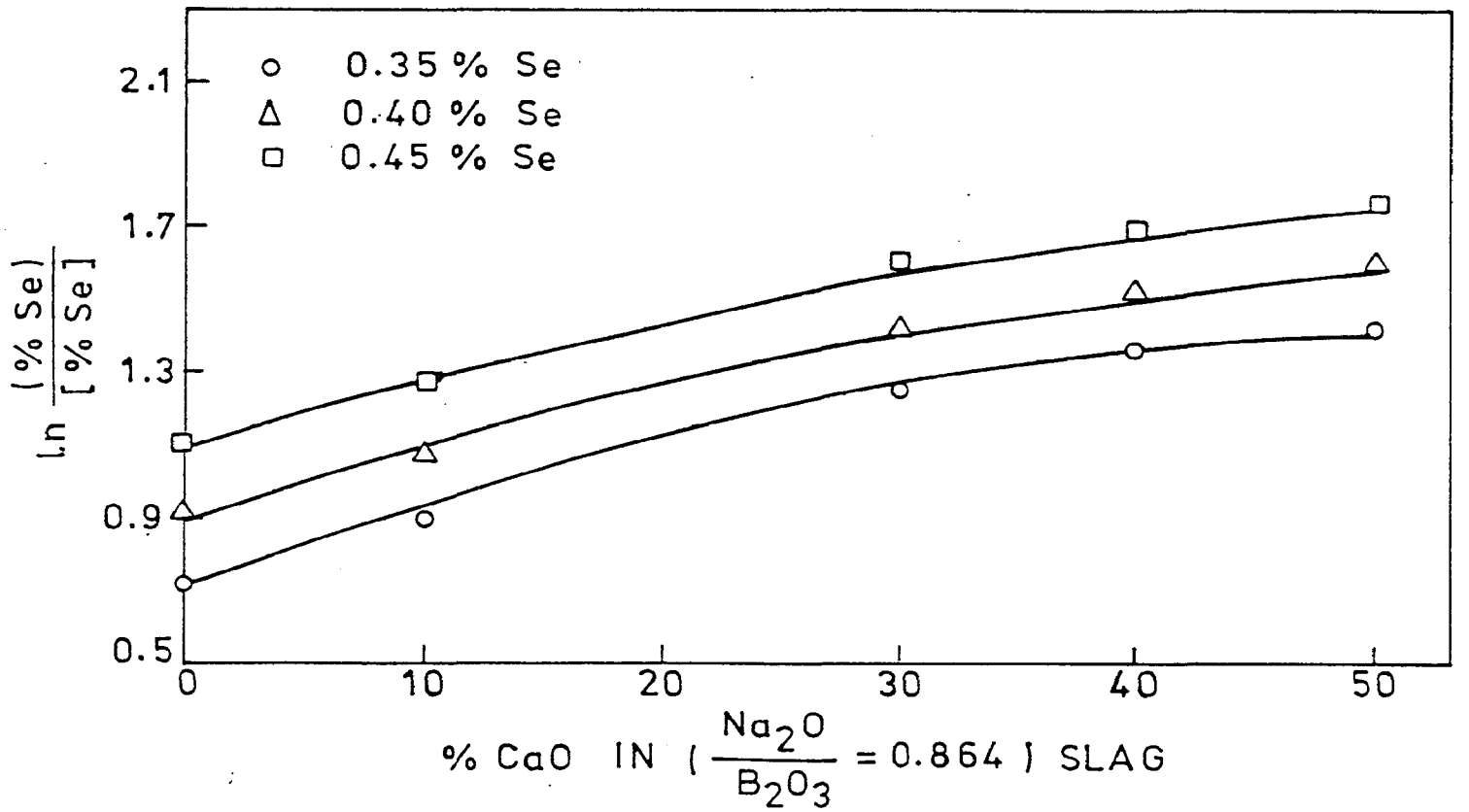

FIG. 2.8 SELENIUM DISTRIBUTION BETWEEN SLAG AND METAL Vs. % CaO IN SLAG.

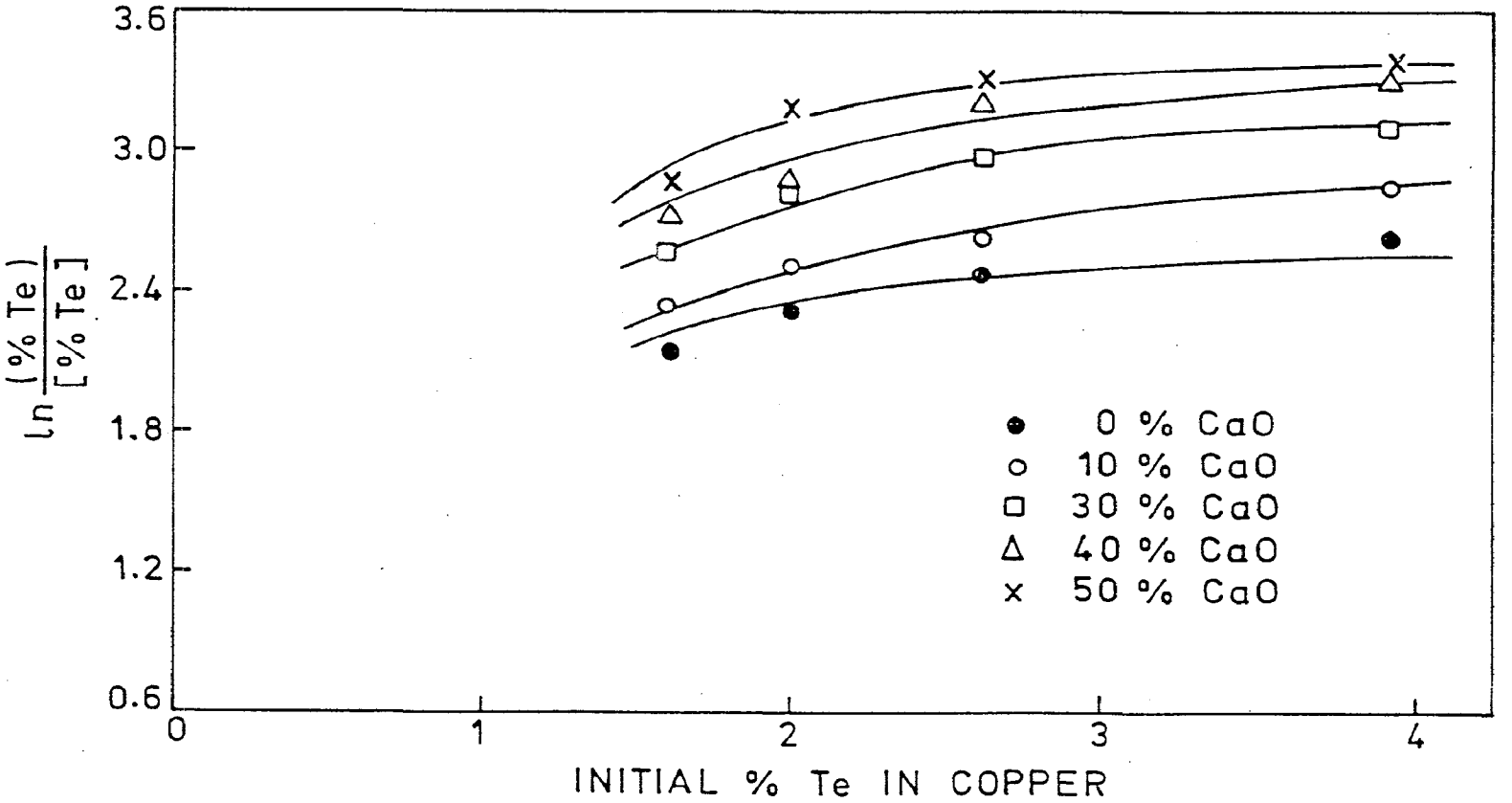

FIG. 2.9 TELLURIUM DISTRIBUTION BETWEEN SLAG AND METAL Vs. INITIAL % Te IN COPPER FOR % CaO IN SLAG.

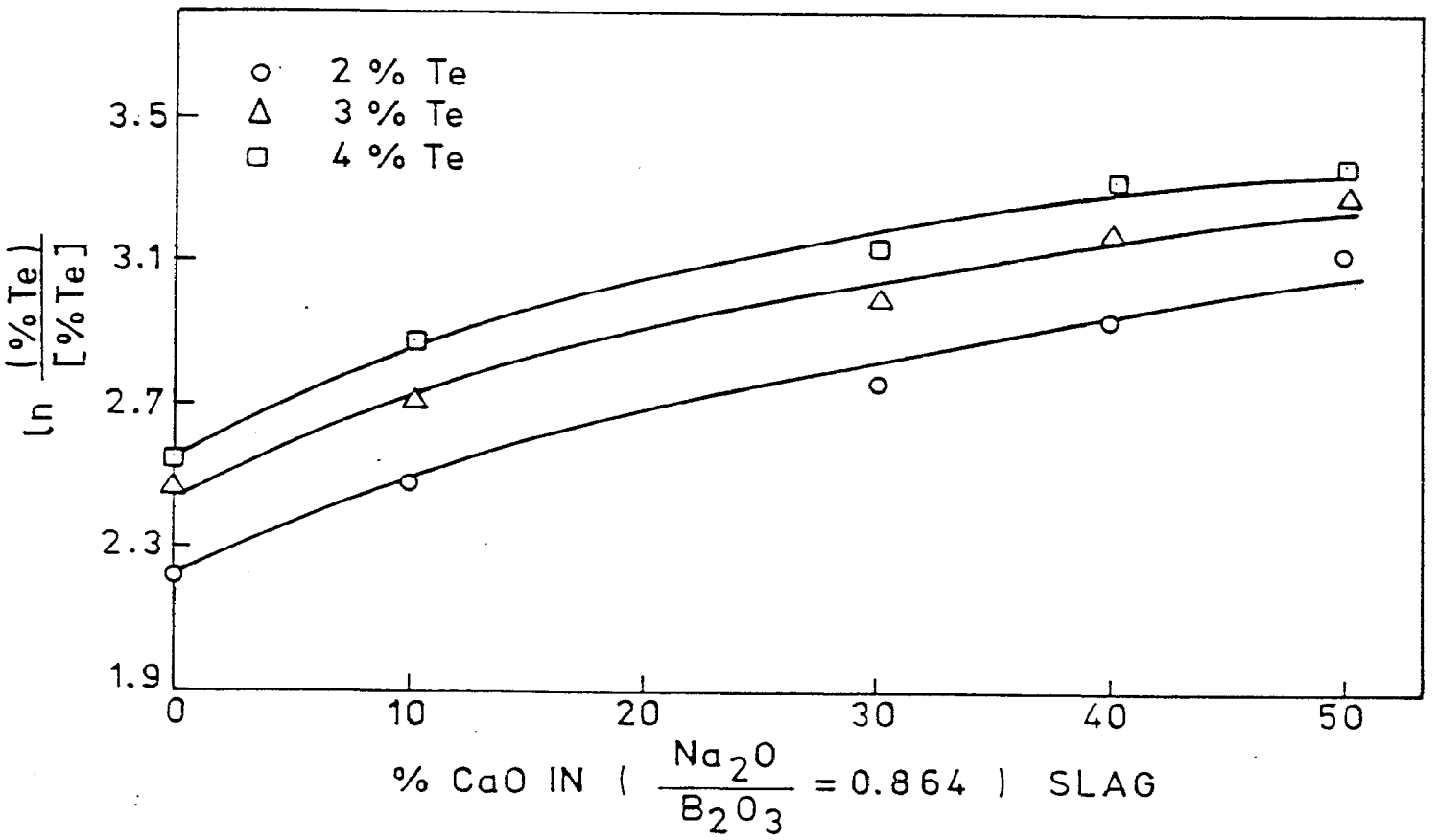

FIG. 2.10 TELLURIUM DISTRIBUTION BETWEEN SLAG AND METAL Vs % CaO IN SLAG.

transfer from metal to slag by more than 2 times on addition of 50 wt% CaO to sodium-borate (wt% Na_2O/ wt% B_2O_3).

The considerable improvement in both Se and Te transfer from metal to slag on adding CaO to the sodium-borate slag can be attributed to the increase in slag basicity.

In an effort to lower the viscosity of the slag, which increased considerably due to CaO additions, and thus make its industrial application effective, CaF_2 additions (5-20 wt%) were made to the above slag (i.e. 30.9 wt% Na_2O, 35.8 wt% B_2O_3, 33.3 wt% CaO). These slags were then equilibrated with Cu-Se and Cu-Te alloys to see its effect on distribution coefficients of Se and Te. The results of the equilibria studies for Se and Te are given in Tables (2.5-2.6) and plotted in Figs.(2.11-2.14). Fig. 2.11 shows the Se distribution coefficient variation with change in initial Se content in copper for different wt% CaF_2 in slag while effect of CaF_2 on Se distribution equilibria for various Cu-Se alloys has been shown in Fig.2.12. It is noted from Fig. 2.11 that the maximum Se distribution coefficient is 10.6 for Cu-0.446 wt% Se alloy and (25.7 wt% Na_2O, 29.8 wt% B_2O_3,27.8wt% CaO, 16.7 wt% CaF_2) slag system. This value is around 1.8 times the value of distribution

TABLE- 2.5

SELENIUM DISTRIBUTION FOR Na_2O-B_2O_3-CaO- CaF_2 SLAGS AT 1473K.

Sl. No.	Slag Composition	Initial Se % in Cu	(%Se)	[%Se]	$\frac{(\%Se)}{[\%Se]}$	$\ln \frac{(\%Se)}{[\%Se]}$
			(% Values by weight)			
1.	(30.9% Na_2O	0.316	0.423	0.120	3.525	1.261
2.	+35.8%B_2O_3	0.353	0.582	0.135	4.314	1.462
3.	+33.3% CaO)	0.442	1.291	0.226	5.714	1.743
4.		0.446	1.256	0.211	5.953	1.784
5.	(29.4% Na_2O	0.316	0.536	0.129	3.811	1.338
6.	+34.1% B_2O_3	0.353	0.495	0.130	4.162	1.426
7.	+31.7% CaO	0.442	1.331	0.198	6.766	1.912
8.	+4.8% CaF_2)	0.446	1.521	0.201	7.568	2.024
9.	(28.1% Na_2O	0.316	0.506	0.115	4.401	1.482
10.	+32.5% B_2O_3	0.353	0.613	0.126	4.869	1.583
11.	+30.3% CaO	0.442	1.538	0.192	8.012	2.081
12.	+9.1% CaF_2)	0.446	1.672	0.196	8.533	2.144
13.	(26.9% Na_2O	0.316	0.565	0.116	4.874	1.584
14.	+31.1% B_2O_3	0.353	0.805	0.124	6.494	1.871
15.	+28.9% CaO	0.442	1.722	0.188	9.161	2.215
16.	+13.1%CaF_2)	0.446	1.708	0.192	8.899	2.186
17.	(25.7% Na_2O	0.316	0.673	0.109	6.178	1.821
18.	+29.8% B_2O_3	0.353	0.893	0.118	7.568	2.024
19.	+27.8% CaO	0.442	1.825	0.181	10.084	2.311
20.	+16.7%CaF_2)	0.446	1.935	0.182	10.633	2.311

TABLE- 2.6

TELLURIUM DISTRIBUTION FOR Na_2O-B_2O_3-CaO-CaF_2 SLAGS AT 1473K.

Sl. No.	Slag Composition	Initial Te % in Cu	(%Te)	[%Te]	$\frac{(\%Te)}{[\%Te]}$	$\ln \frac{(\%Te)}{[\%Te]}$
			(% Values by weight)			
1.	(30.9% Na_2O	1.597	6.548	0.361	18.138	2.898
2.	+35.8%B_2O_3	2.005	6.139	0.247	24.854	3.213
3.	+33.3% CaO)	2.639	16.010	0.587	27.275	3.306
4.		3.923	18.752	0.636	29.577	3.387
5.	(29.4% Na_2O	1.597	8.465	0.352	24.051	3.18
6.	+34.1% B_2O_3	2.005	11.201	0.401	27.942	3.33
7.	+31.7% CaO	2.639	13.572	0.431	31.504	3.45
8.	+4.8% CaF_2)	3.923	19.542	0.602	32.462	3.48
9.	(28.1% Na_2O	1.597	8.797	0.348	25.279	3.23
10.	+32.5% B_2O_3	2.005	11.234	0.369	30.447	3.416
11.	+30.3% CaO	2.639	15.117	0.421	35.909	3.581
12.	+9.1% CaF_2)	3.923	27.017	0.591	45.331	3.814
13.	(26.9% Na_2O	1.597	9.43	0.341	27.66	3.32
14.	+31.1% B_2O_3	2.005	13.29	0.342	38.86	3.66
15.	+28.9% CaO	2.639	22.14	0.418	52.98	3.97
16.	+13.1%CaF_2)	3.923	32.09	0.582	55.15	4.01
17.	(25.7% Na_2O	1.597	12.421	0.326	38.09	3.64
18.	+29.8% B_2O_3	2.005	12.051	0.298	40.44	3.70
19.	+27.8% CaO	2.639	17.214	0.409	42.09	3.74
20.	+16.7%CaF_2)	3.923	35.751	0.558	64.07	4.16

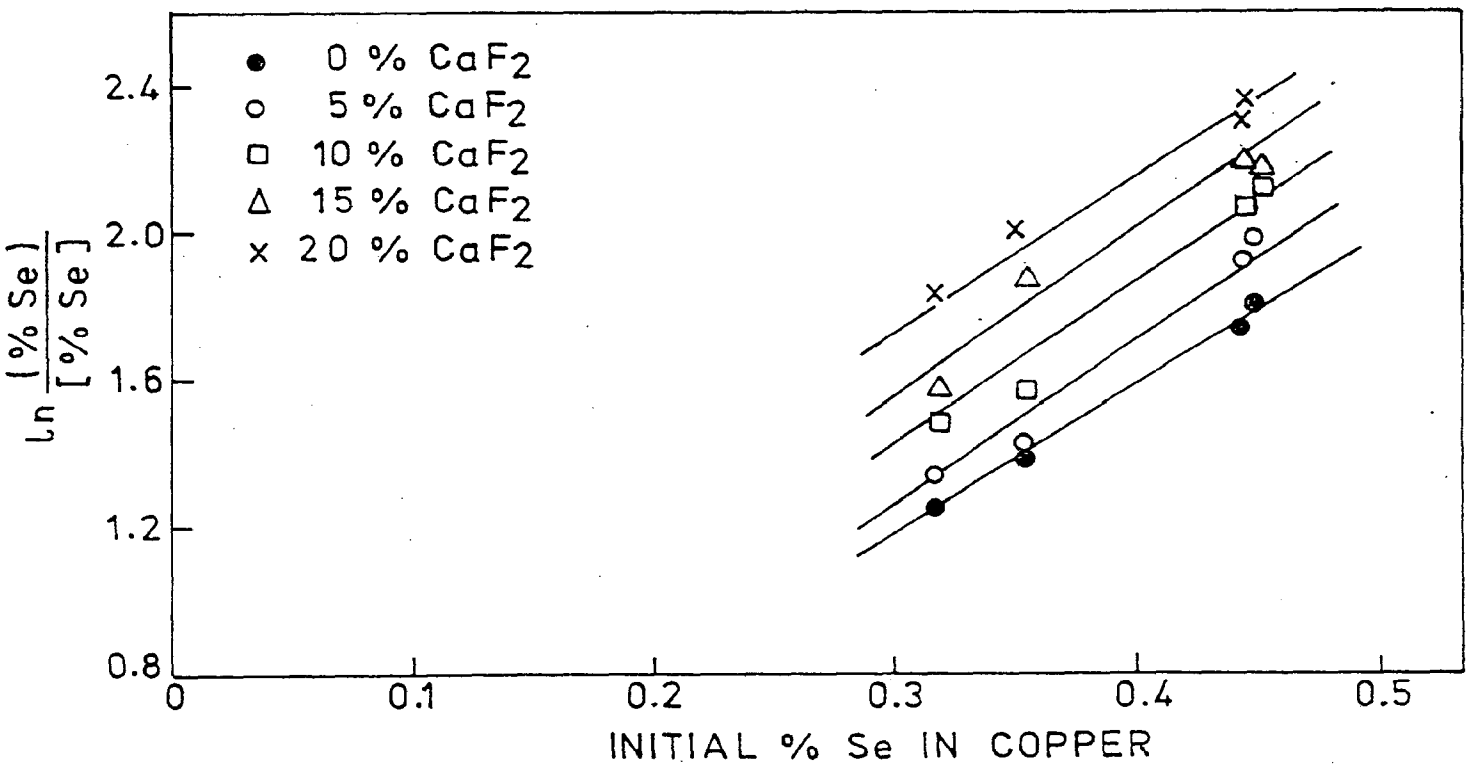

FIG. 2.11 SELENIUM DISTRIBUTION BETWEEN SLAG AND METAL Vs. INITIAL % Se IN COPPER FOR % CaF_2 IN SLAG.

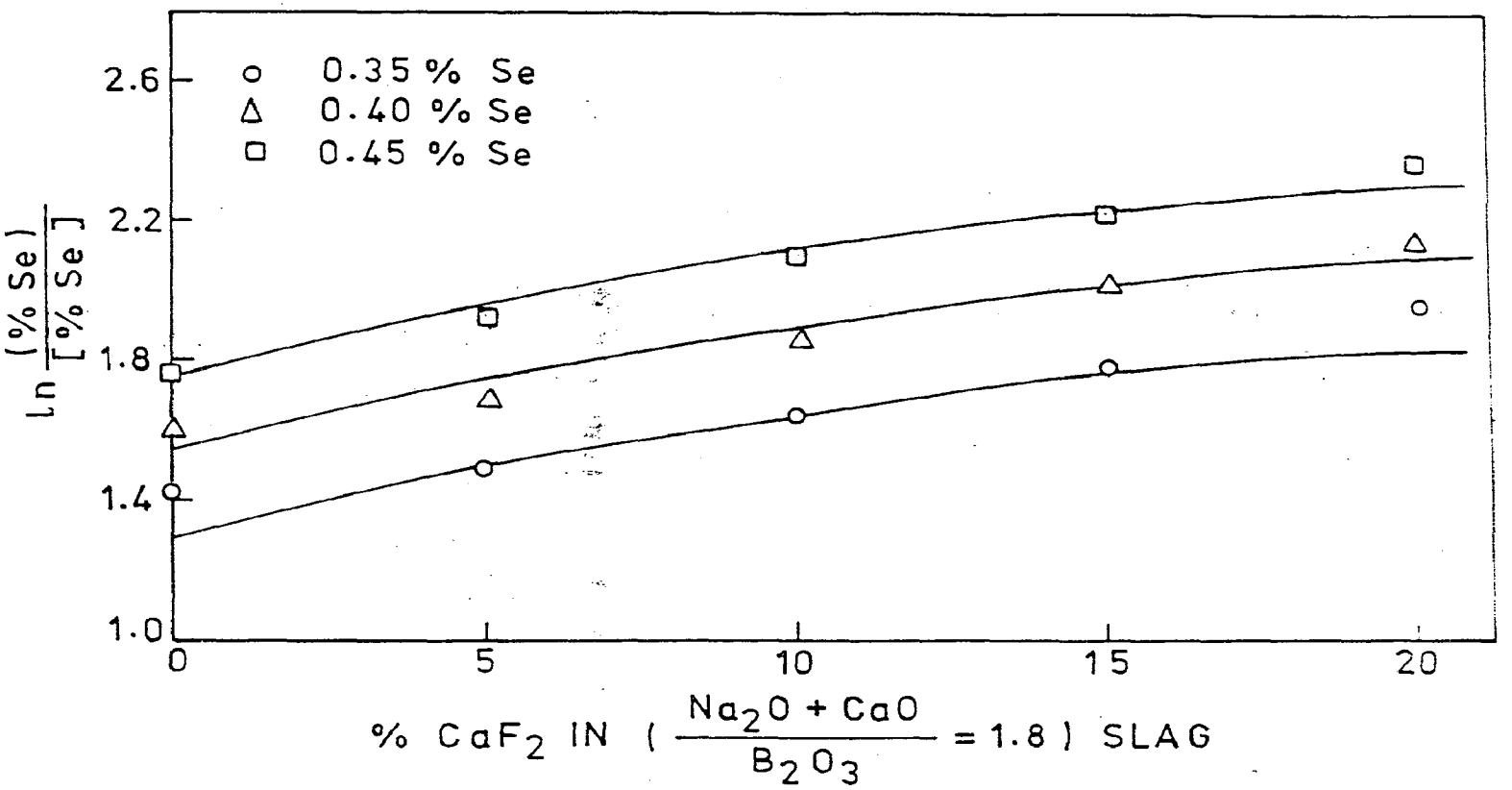

FIG. 2.12 SELENIUM DISTRIBUTION BETWEEN SLAG AND METAL Vs. % CaF_2 IN SLAG.

coefficient obtained for the same Cu-Se alloy using slag without CaF_2 addition i.e. for slag composition (30.9 wt% Na_2O,35.8 wt% B_2O_3, 33.3 wt% CaO). In case of equilibria studies for Te, Fig.2.13 shows the change in Te distribution coefficient with initial Te content in copper for different wt% CaF_2 in slag while effect of CaF_2 on Te distribution equilibria for various Cu-Te alloys has been shown in Fig.2.14. It is noted from Fig.2.13 that the maximum Te distribution coefficient is 64.1 for Cu-3.923 wt% Te alloy and (25.7 wt% Na_2O, 29.8 wt% B_2O_3, 27.8 wt% CaO, 16.7 wt% CaF_2) slag system. This value is around 2.2 times the value of distribution coefficient obtained for the same Cu-Te alloy using slag without CaF_2 addition i.e. for slag composition (30.9 wt% Na_2O, 35.8 wt% B_2O_3, 33.3 wt% CaO).

Although CaF_2 mainly improves the kinetics of the slag-metal reaction by decreasing the viscosity of the slag, it increases the distribution coefficient as well due to the fact that enhanced O^{2-} release on CaF_2 addition improves the slag basicity. It is also noted from Figs. (2.7, 2.9, 2.11, 2.13) that Se and Te distribution coefficient values increased with increase in initial concentrations of Se and Te in copper respectively for all slag compositions in general.

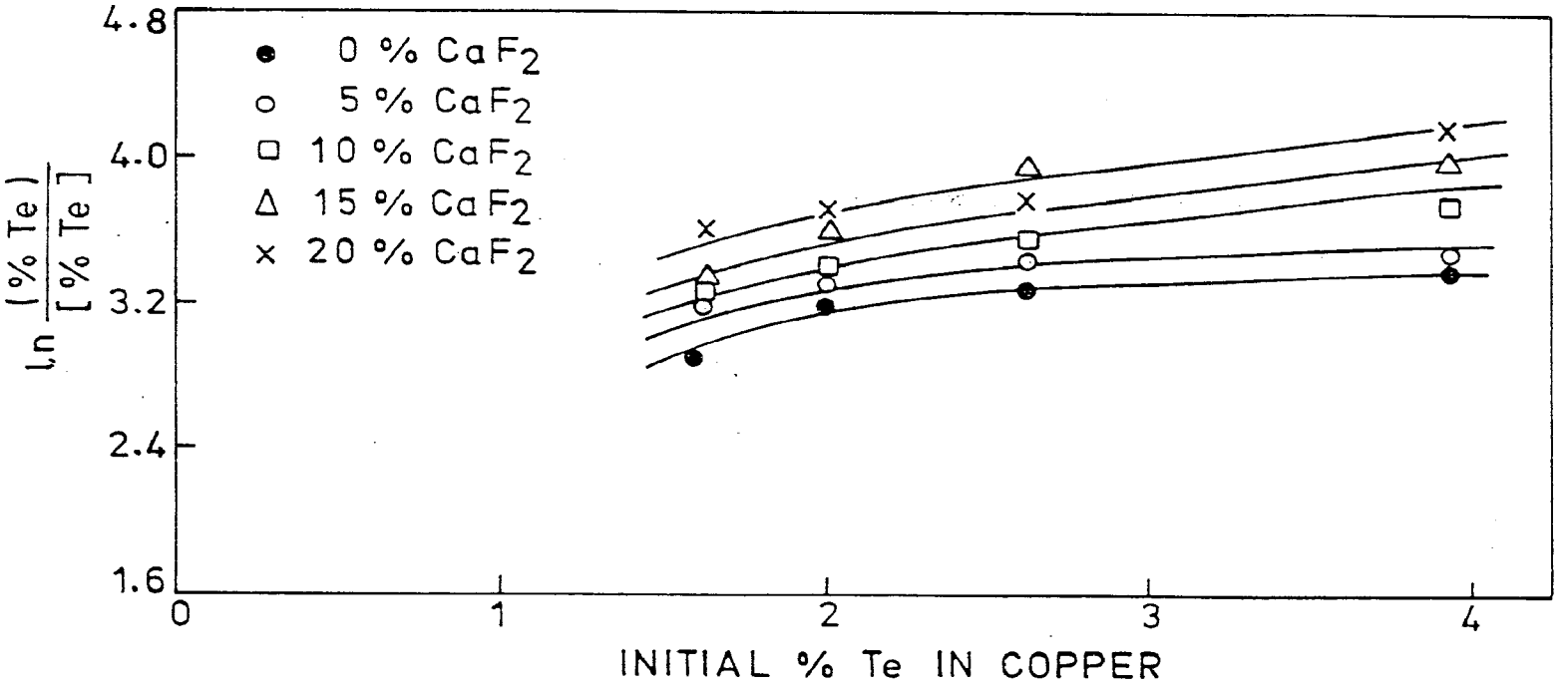

FIG. 2.13 TELLURIUM DISTRIBUTION BETWEEN SLAG AND METAL Vs. INITIAL % Te IN COPPER FOR % CaF_2 IN SLAG.

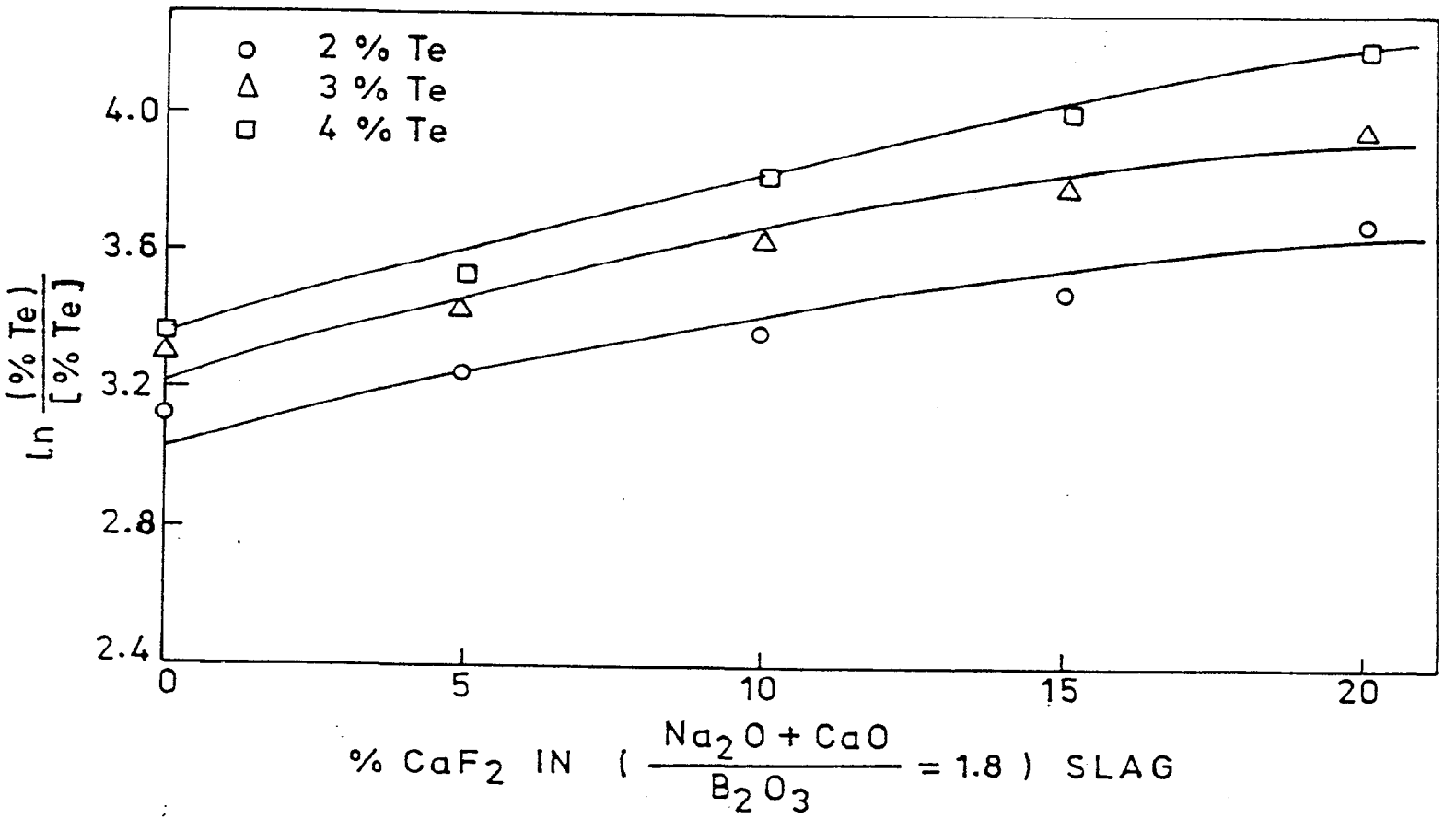

FIG. 2.14 TELLURIUM DISTRIBUTION BETWEEN SLAG AND METAL Vs. % CaF_2 IN SLAG.

From the above results and discussions, it is, therefore, inferred that in the composition range and temperature of the present study, selenium and tellurium distribution coefficients increase with increase in the $Na_2O - B_2O_3$ slag basicity. By adding CaO and CaF_2 to the above slag system, the distribution coefficients for both Se and Te further increase. Also, the initial concentration of selenium or tellurium in copper affects the distribution coefficient for all slag compositions used.

CHAPTER - III

VISCOSITY MEASUREMENT OF SLAGS

3.1 GENERAL

Pyrometallurgical unit processes of reduction - or matte-smelting, converting and fire-refining involve two types of melts, one 'metallic phase' consisting of all elements in reduced state and the other 'slag' consisting of, generally, unreduced oxides and occasionally halides, derived from the furnace charge. Of the various physical properties of such melts viz. fusibility, melting point, liquidus-solidus temperature range, viscosity, surface tension, conductivity, diffusivity etc., viscosity plays a significant role in efficient and economic control of such operations in production of high-purity metals.

Kinetics of slag-metal reactions, essentially controlled by mass-transfer step in such heterogeneous systems, involves viscous resistance and diffusion rates in such melts which in turn are affected appreciably by the gas-absorption and bubble, froth or foam-formation in the two interacting phases especially in processes involving lancing of air or oxygen. 'Metal-losses' resulting due to entrapped-granules in slag are also dependent largely on

'Slag-viscosity'. Chemical attack or scorification of refractories by slags is yet another phenomenon involving viscosity. Recently developed 'electro-slag' or 'electro-flux' remelting/refining processes also involve setting of metal droplets through a mass of molten-slag/flux and properties such as viscosity, electrical conductivity and chemical reactivity of such slags/fluxes essentially control their utility for any specific application.

The common slag systems involving oxides as simple oxides, silicates, phosphates, borates, aluminates, ferrites or their combinations in complex mixtures involve either covalent, ionic or both types of bonds. Properties being manifestation of structure, a scientific study of different properties of such slags thus involves study of structure of such melts for interpretation of experimental data on such physical properties. Extensive research has therefore been conducted in the recent past on such oxide, silicate, phosphate, borate and aluminate slags and their binary and other complex mixtures as also on synthetic carbide slags used in the ESR process and halide melts for evaluation of their basic physical and thermodynamic properties, effects of additions, temperature and pressure on these as also for the structure-property correlation of such melts.

There has been a greater demand for Soda base fluxes in copper refining in recent times and hence the

present investigation on viscosity of sodium-borate slag forms a part of the systematic research work on thermodynamic and transport properties of the fluxes for refining of copper.

3.2 THEORETICAL ANALYSIS

Viscosity is a measure of the internal resistance of one plane of a fluid to slip over an adjacent plane under an applied shearing stress causing flow of the fluid.

Mathematically,

$$\eta = \frac{F}{A\ (dv/dx)} \qquad \ldots(3.1)$$

where η is called the coefficient of viscosity, F is the shearing force due to internal resistance of a plane of area A moving with a relative velocity 'v' on another plane of same area and separated from it by a distance x. Thus dv/dx represents the velocity gradient within the fluid.

The property, η, also called, 'dynamic viscosity', is thus a characteristic constant for any fluid depending upon its compositions and structure. It decreases with a rise in temperature but increases with an increase in pressure. Unit of viscosity in CGS system is Poise $(\text{dyne-sec}^{-1}/\text{cm})^2$. Fluids following above relationship are called Newtonian fluids.

Kinematic viscosity υ, is defined as the ratio of dynamic viscosity η to density ρ of the fluid and has unit 'Stokes' and is the value measured directly by many viscometers.

Viscosity η is a strong function of temperature [130,131] and is expressed by an expression similar to Arrhenius expression for activated processes, viz.

$$\eta = \eta_o . \exp\ (E_\mu / RT) \qquad \ldots(3.2)$$

where η_o is a constant (frequency factor) and E_μ the activation energy of viscous flow at constant pressure, R is the universal gas constant and T the absolute temperature.

To take into account the variation of density of fluids due to a change in temperature, Andrade [132] proposed following expression for the inter-relationship between viscosity and temperature,

$$\eta . v^{1/3} = \beta . \exp\ (C/v.T) \qquad \ldots(3.3)$$

where β and C are constants for the particular fluid and v its specific volume.

Diffusion and viscosity are inter-related [132] by Stokes-Einstein relationship,

$$D = k.T/6\pi\ \eta.\sigma \qquad \ldots(3.4)$$

where D is the diffusion coefficient expressed as a function of temperature and activation energy for diffusion E_D by a relation similar to eq.(3.2) above, k is Boltzmann's constant and σ the diameter of the particle diffusing.

3.3 METHODS USED

Different methods [132-137] used for measurement of viscosity of melts are classified in following four groups.

(a) Capillary Viscometers

Based on Poiseulle's equation for viscous flow of fluid in capillaries, these viscometers are either of 'vertical' or 'horizontal' capillary type and have simple design and construction . Measurements also being easier, these have been extensively used for study of liquid metals and fused salts upto 1250^{o}C. Both 'Absolute' and 'Relative' viscosities compared to certain standard liquid can be measured. Vertical capillary viscometers adopted more commonly, use gravitational force as driving force and electrical contacts for measurement of volume of fluid and flow rate, and, in fact measure 'Kinematic viscosity'. Jena glass, supermax glass, fused silica or platinum capillaries

have been used for study of metals and corundum, alumina etc. for salts and silicate melts.

Major limitations of the method, especially for high temperature work, include material-compatibility, necessity of electrical contacts for accurate measurements of volume and rate of flow of fluids, blockage of capillary due to entrapped impurities or suspended particles and 'calibration errors'. Corrections must be made for the 'kinetic energy' and 'thermal expansion of apparatus' at elevated temperatures and an accurate knowledge of density of melt at the temperature of study.

(b) Falling Sphere Technique or Stokes method

Based on Stokes relationship, with suitable corrections viz. Ladenberg correction, for the free fall of fine spheres in stationary fluids, these viscometers use two techniques-viz. 'free falling sphere' and the 'restrained sphere' technique. Fine balls of normally platinum, platinum-rhodium alloy, nickel, molybdenum or tantalum of different diameters and sillimanite, alumina or corundum capillaries or capsules have been used. Resistance or induction heating is used in furnace to attain long-uniform temperature zones. Accurate measurement (and control) of temperature, density of sphere and fluid at temperature of

study and height of fall of sphere are needed for calculation of viscosity.

'Counter-balanced' or 'restrained' sphere technique uses bobs suspended from one arm of a balance and their upward or downward movement in the melt is produced by varying weights placed on the pan attached to the other arm of the balance

(c) Oscillating Viscometers

These use geometrical bodies such as discs, sphere, cups, cylinders etc, oscillating in a crucible or spherical container and are more useful for liquids of lower viscosities at higher temperature especially liquid metals and alloys. In these, the viscosity of the fluid under study is calculated from the measurement of damping effect of the fluid upon the oscillating pendulum as the normal mode of oscillation is damped by the viscous drag of the contained fluid. The apparatus needs calibration for damping effect against fluids of known viscosities and can measure both 'absolute' or relative viscosities.

In general high temperature studies involve problems of (i) accurate measurement and control of temperature, (ii) maintenance of uniform temperature zones of adequate lengths required by the processes, (iii)

selection of suitable material of construction-inert to melt to minimize corrosion and of easy fabricability, to exact and reproducible dimensions,selection of apparatus and method for any specific application depends upon (i) sample size (depending upon cost and availability, and, fabricability and cost of container), (ii) ease of data acquisition, (iii) whether 'absolute' or 'relative' viscosity measurement necessary (iv) precision in measurement, and, (v) risk of sample contamination due to exposure to environment. Electromagnetic rotating viscometers are more suitable for high-viscosity melts whereas oscillating viscometers for lower viscosity metallic melts. Vertical capillary viscometers have advantage of simplicity and have been exclusively used upto $1000^{o}C$ for study of salts.

(d) Rotational Viscometers or Method of Concentric Cylinders

[132]

Developed by Margules for room temperature work and modified by Searle and Coutte [133] and later by several other workers for use at high temperatures for study or molten glasses, slags and salts, these viscometers have two type of variation. (i) rotation of inner cylinder of bob within a stationary outer cylindrical crucible, and. (ii) rotation of outer crucible with inner cylinder or bob stationary.

Viscosity of the liquid contained between the two cylinders is evaluated by measurement of the torque developed in terms of measurement of angle or deflection/displacement of the inner cylinder or bob. Molybdenum resistance furnaces and Mo, Mo-W or Pt-Pt/Rh alloys and even ceramic materials as cylinder materials have been used for walk upto 1800^{o}C. Simple geometrical shapes, measurements of angle of deflection or rotational speed external to the furnace and study at different temperatures with same sample without need of refilling are characteristic features of the process. Limitations of the technique however include necessity of inert atmosphere to prevent evaporation, oxidation or contamination of the melt under study, suspended impurities influence movement of bob or cylinder, alignment problems and difficulties in attaining uniform rotation due to deterioration of bearings resulting from heating. 'End-corrections' and 'corrections due to expansion on heating' must be applied for accurate results. Other sources of error include 'inaccuracy in temperature measurement' and 'on-set of turbulence' in the fluid.

Bockris and Lowe[136] improved apparatus used for study of liquid silicates by making use of an electro-magnetic force to counter-balance the viscous torque permitting use of accurate null-point method. Thus

measurements in a wide range from 0.05 to $\tilde{}$ 10^3P with single suspension could be made possible. Bockris, Mackenzie and Kitchener[137] modified the apparatus further and made use of graphite tube resistance furnace and a smaller inner cylinder to measure the viscosity of liquid silica ($\tilde{}$ 10^5P) in a tungsten crucible at temperatures upto 2200°C. Lowe and Mackenzie type electromagnetic viscometer could also be used upto 2200°C and over a viscosity range of 0.05-10^5P.

3.4 EXPERIMENTAL

3.4.1 Viscometer Unit

The rotating viscometer 'Rotovisco RV20' with high temperature measuring system ME 1700 for measuring the viscosity of melts upto temperature of 1700°C (Preferable temperature range : 800°C to 1600°C) has been used. Figs.(3.1-3.3) show the geometries of cylinderical cup, rotor, and sectional cut of the viscometer unit. A platinum 30% rhodium/platinum 6% rhodium type B (Pt Rh 18) thermocouple has been used to measure the slag temperature.

The viscometer unit incorporates (i) Heating unit with high temperature furnace in vertical design, servo-motor controlled charging of substances and gas cover for investigations under protective gas (ii) Rotovisco basic

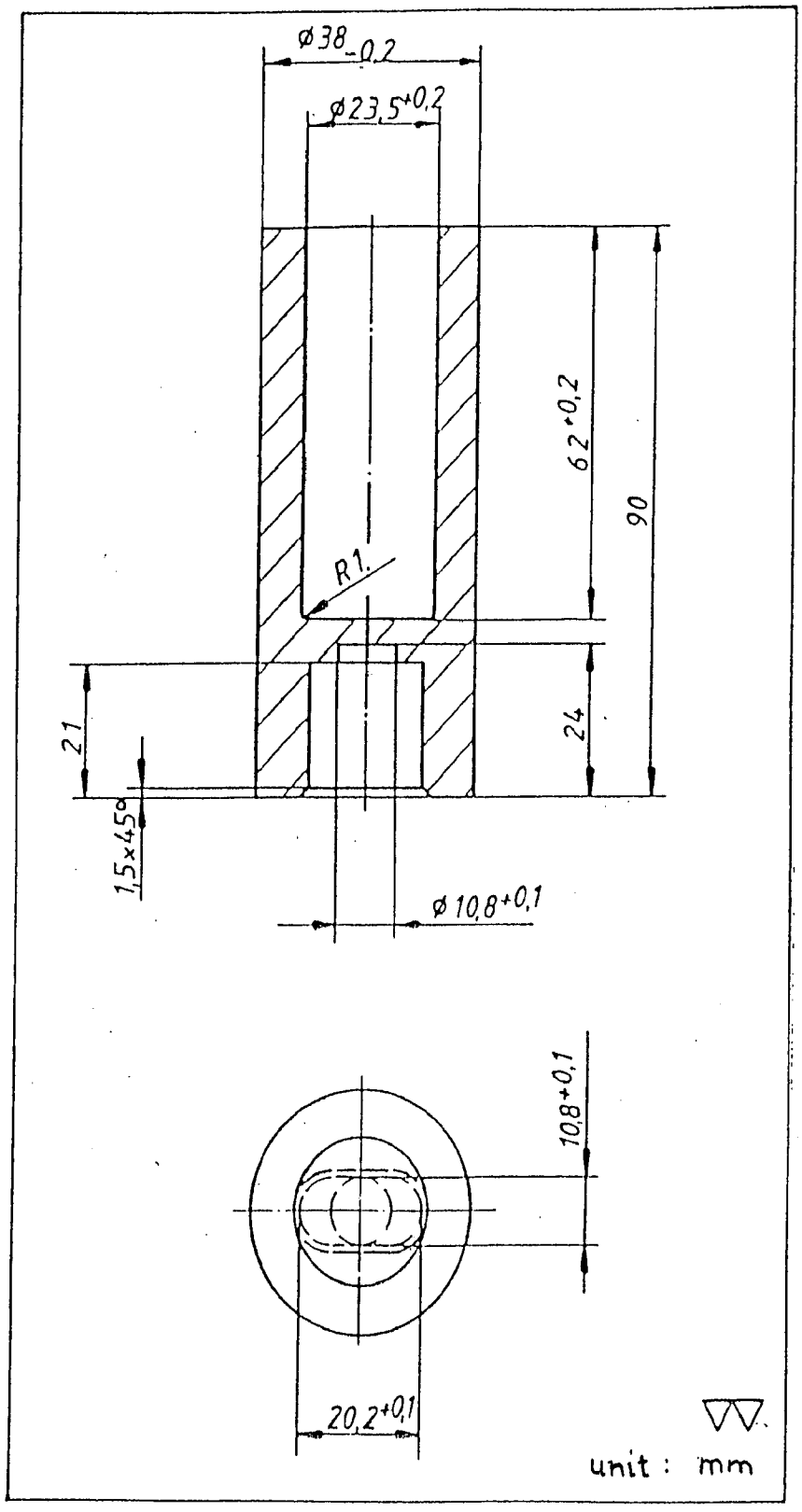

FIG. 3.1 SKETCH OF THE CUP FOR VISCOSITY MEASUREMENT.

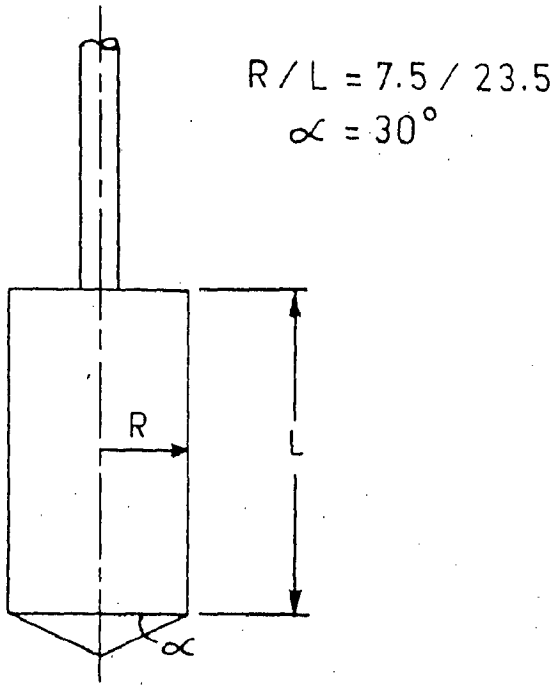

FIG. 3.2 SKETCH OF THE ROTOR FOR VISCOSITY MEASUREMENT

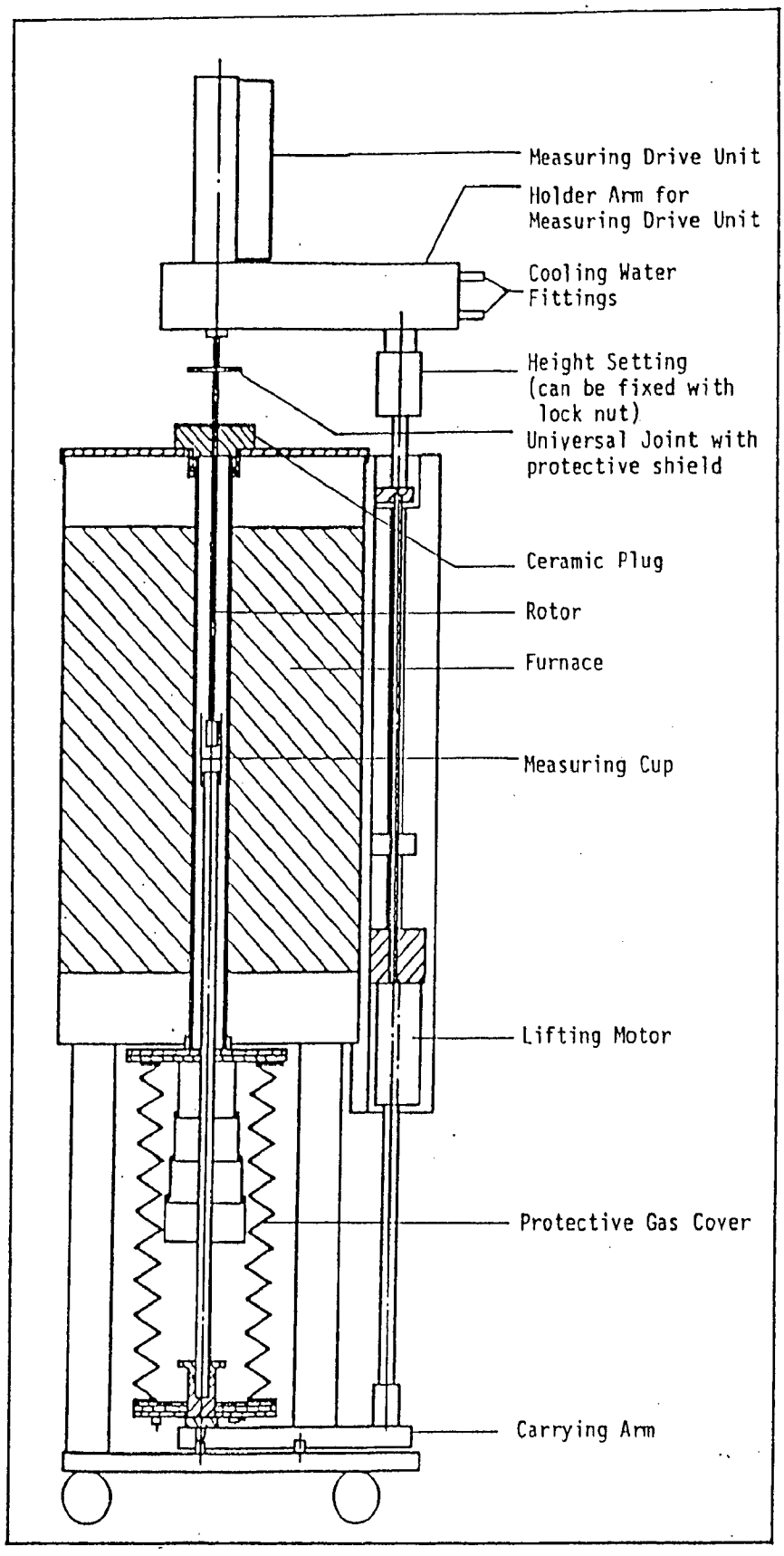

FIG. 3.3 SECTIONAL CUT OF THE VISCOMETER UNIT.

unit with drive unit and torque sensor (iii) control unit with programmable temperature controller (iv) The rotor and measuring cup of temperature resistant Graphite material.

3.4.1.1 Principle

This instrument is based on searle type rotational viscometer which involves the rotation of inner cylinder or bob/stirrer within a stationary outer cylinderical crucible. The rotating inner cylinder forces the liquid in the annular gap to flow. The resistance of the liquid being sheared between the stationary and rotating boundaries results in a viscosity related torque working on the inner cylinder which counteracts the torque provided by the drive motor. A torque sensing element, normally a spring that twists as the result of the torque, is placed between drive motor and the shaft of the inner cylinder. The twist of the torque spring is a direct measure of the viscosity of the sample tested.

This particular instrument has a especially designed sensor system (rotor and cup) which is used for viscosity measurements of the slag upto a temperature of $1500^{O}C$. The calculation factors 'A' and 'M'of the sensor system are used to determine the shear rate and shear stress and the viscosity of Newtonian liquid is calculated from the equation :

$$\text{(Viscosity)}\ \eta = \frac{\tau}{D} = \frac{A.\ \%\ \tau}{M.\ \%\ D}\quad \frac{[Pa]}{[1/s]} \qquad \ldots(3.5)$$

Where % τ and % D are the indicated shear stress and preset shear rate respectively. 'A' denotes the shear stress factor which depends on the characteristic geometry of the rotor and the constant of the torsion bar alongwith the electrical specification of both the basic unit and the measuring system. The proportionality factor 'M' recognises the characteristic geometry of the sensor system. It is defined as the shear rate per speed unit. The values of 'A' and 'M' factors have been computed to be 43.3 and 1.75 respectively [138].

3.4.2 Preparation of Slags

Chemical systems of different basicities were prepared by mixing sodium carbonate and borax (both of anal.r.grade) in required proportions and calcining the mixtures in the furnace for long time (3-4 days) at (1023K) followed by crushing, grinding, thorough mixing and recalcination of the mixtures for 2 days at the same temperature. For preparation of Na_2O-B_2O_3-CaO slag systems with different CaO proportions ,sodium borate slag (wt% Na_2O/wt% B_2O_3 = 0.864) was first prepared in a similar manner as mentioned above and then CaO (anal.r.grade) in

desired proportions was mixed with this sodium borate slag. The different mixtures were melted at 1223K and kept for long time (1-2 days) at this temperature. The mixtures were once again crushed and put in the furnace at 1273K for several hours (25-30 hours), to ensure proper mixing. For preparation of Na_2O-B_2O_3-CaO-CaF_2 slag systems with different CaF_2 proportions, first of all Na_2O-B_2O_3-CaO slag composition (30.9 wt% Na_2O, 35.8 wt% B_2O_3, 33.3 wt% CaO) was prepared using same method as mentioned earlier and then CaF_2 (anal.r.grade) in required proportions were mixed thoroughly with this slag system. The different mixtures were melted at 1123K and kept for long time (28-30 hours) at this temperature. The mixtures were again crushed and put in the furnace again at the same temperature for (10-12 hours) to ensure proper mixing.

3.4.3 Procedure

Viscosity measurements were taken for each slag prepared in the temperature range 1273-1573K on 'RV 20 Rotovisco'viscometer. The amount of slag used for experimental runs adjusted so that the rotor/stirrer remained in the molten slag.

For a particular temperature, the viscosity of slag was calculated on the basis of shear stress 'τ' and shear rate 'D' values measured during the experiment.

3.5 RESULTS AND DISCUSSIONS

The viscosity of liquid slag systems is an important physical property especially for the quantitative description of impulse, heat, mass transfer and for understanding of the atomic structure of slags [139]. The rate of reaction in slag-metal system is transport controlled and will hence be affected by slag viscosity. In the present investigation, viscosity of different chemical systems containing Na_2O, B_2O_3, CaO and CaF_2 have been measured in the temperature range 1273 - 1573K and effect of CaO and CaF_2 additions on activation energy of the slag has been estimated.

The viscosity values for different slag basicities (wt% Na_2O/wt% B_2O_3 = 0.527 to 0.864) at different temperatures (1273 to 1573K) are given in the Table 3.1. It is noted that with increase in slag basicity from 0.53 to 0.86, the viscosity of slag decreases from 0.39 Pa-s to 0.33 Pa-s at 1273K while at temperature 1573K, the value decreases from 0.28 Pa-s to 0.26 Pa-s for the increase in slag basicity in the same composition range. The relation between ln (viscosity η) and reciprocal of absolute temperature as shown in Fig.3.4 indicates that with the increase in temperature, viscosity decreases and it follows an Arrhenius-type relationship. The average value of activation

TABLE - 3.1

VISCOSITY OF Na_2O-B_2O_3 SLAGS AT DIFFERENT TEMPERATURES

Sl. No.	Wt.% Na_2CO_3 in Borax	Slag basicity	Temperature (K)	Viscosity η (Pa-s)	ln η
1.	10	0.527	1273	0.386	-0.951
2.	10	0.527	1373	0.341	-1.075
3.	10	0.527	1473	0.316	-1.152
4.	10	0.527	1573	0.284	-1.258
5.	20	0.612	1273	0.380	-0.965
6.	20	0.612	1373	0.335	-1.092
7.	20	0.612	1473	0.308	-1.176
8.	20	0.612	1573	0.281	-1.270
9.	30	0.696	1273	0.355	-1.035
10.	30	0.696	1373	0.328	-1.115
11.	30	0.696	1473	0.295	-1.220
12.	30	0.696	1573	0.277	-1.281
13.	40	0.780	1273	0.341	-1.075
14.	40	0.780	1373	0.316	-1.151
15.	40	0.780	1473	0.286	-1.250
16.	40	0.780	1573	0.266	-1.322
17.	50	0.864	1273	0.332	-1.102
18.	50	0.864	1373	0.301	-1.201
19.	50	0.864	1473	0.279	-1.275
20.	50	0.864	1573	0.260	-1.345

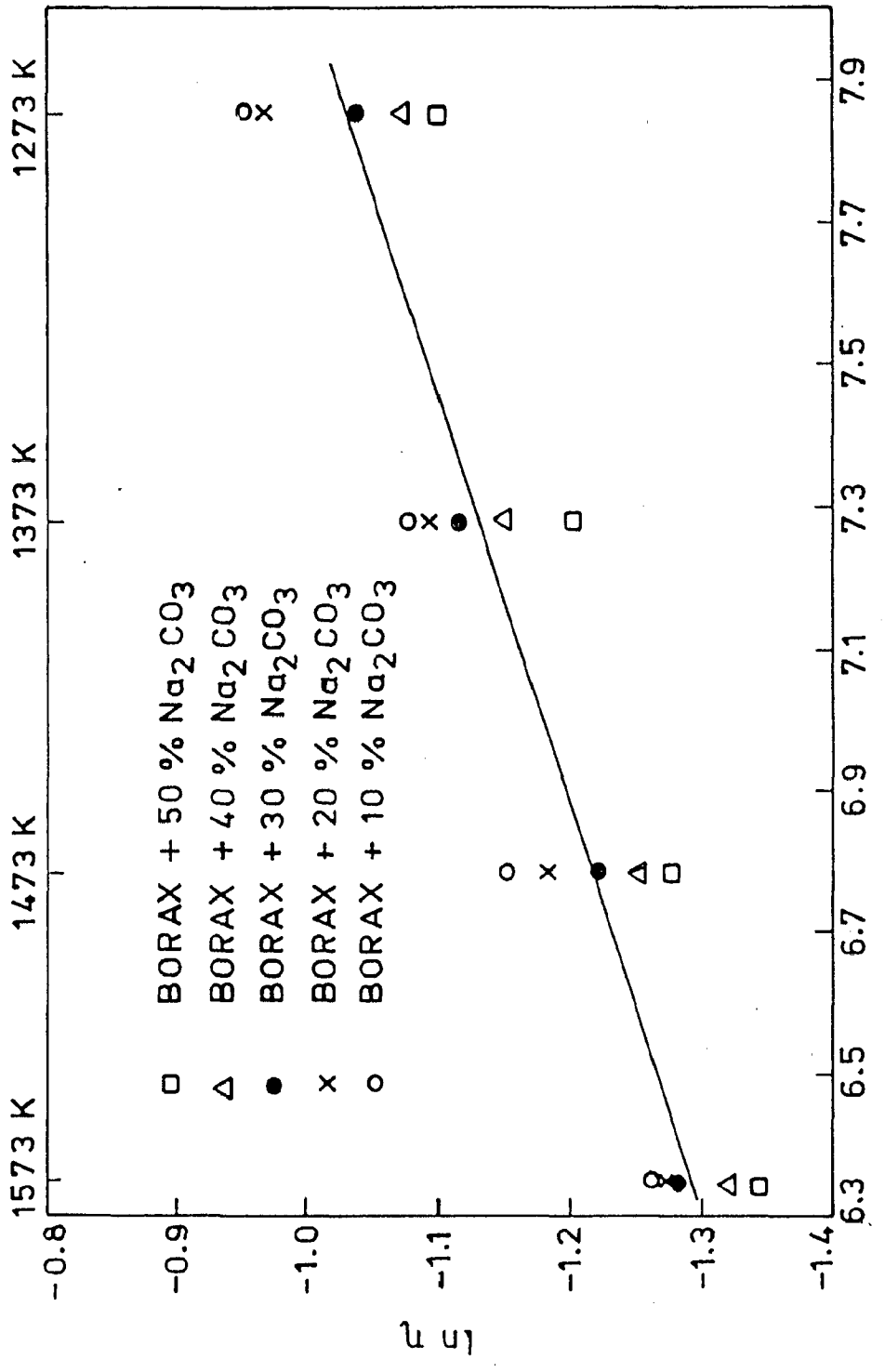

FIG. 3.4 ln η Vs. $\frac{1}{T}$ FOR $Na_2O - B_2O_3$ SLAGS.

energy has been found to be equal to 14.6 KJ/mole. Fig.3.5 shows a continuous decrease in viscosity with increase in Na_2O concentration in the composition range (37.3 to 49.4 mole %) for the present investigation.

The shape of the viscosity isotherms and their change with the concentration of alkali oxide i.e. Na_2O invite explanation. In alkali silicate glasses the classic concept of the function of the alkali oxide is to provide oxygens which enter the silicon-oxygen network to form singly bonded oxygens.

Since the singly bonded oxygen atoms do not connect two silicons together as do the oxygens in pure silica glass, their effect is to decrease the rigidity of the network i.e to decrease the viscosity of the glass. It may be postulated that the formation of singly bonded oxygen may also take place to some extent in boric oxide glass upon the introduction of alkali oxide such as Na_2O. In addition to the formation of singly bonded oxygens the boron atoms is able to utilise some of the oxygens supplied by alkali oxide to form BO_4 groups according to the concepts of Biscoe and Warren [140] and thus strengthens the network and eventually it will lead to higher viscosity. At any one temperature there are therefore two opposing tendencies caused by introduction of alkali oxide into boric oxide, namely (1) the weakening effect of forming singly bonded oxygens and

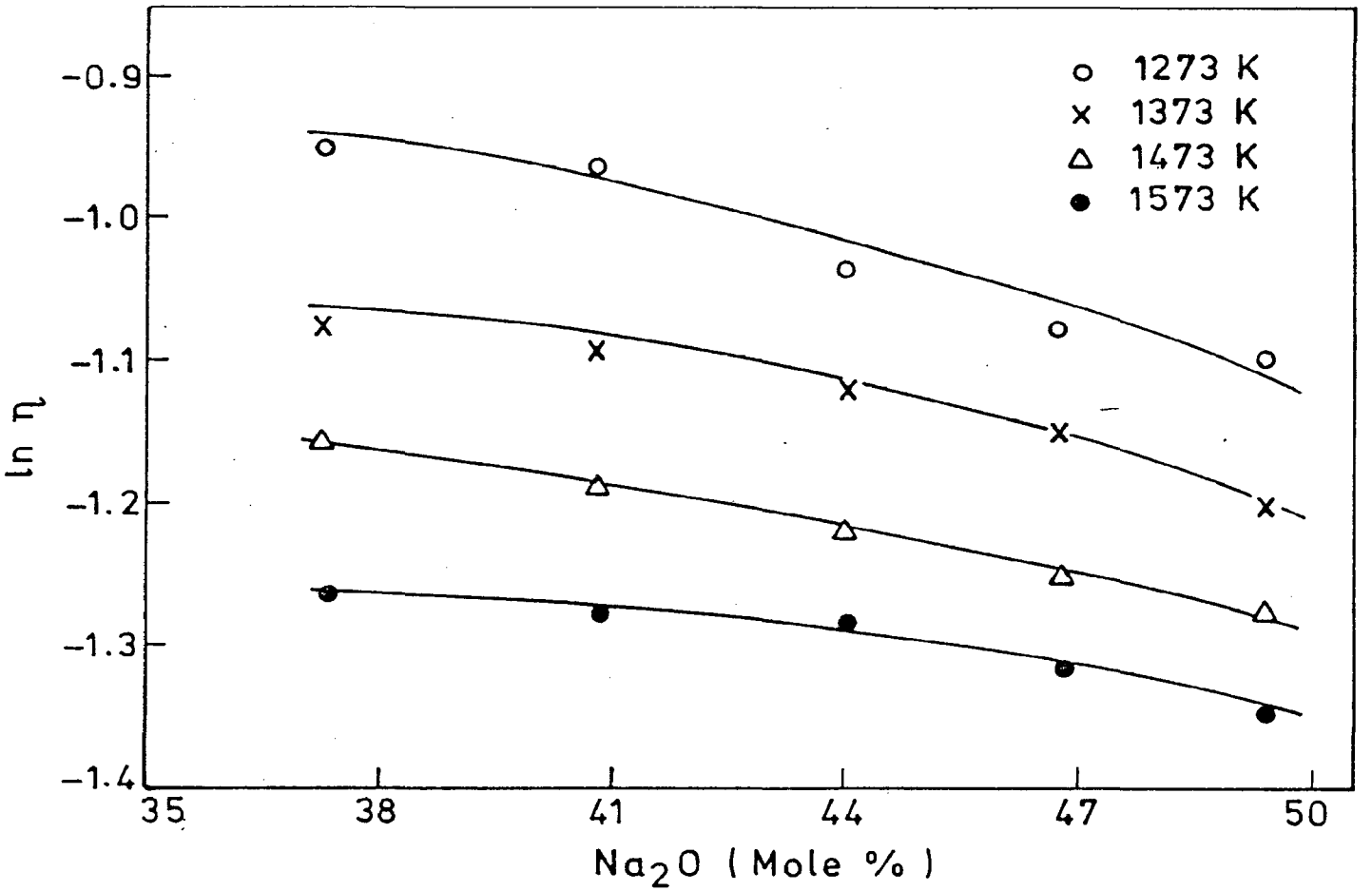

FIG. 3.5 EFFECT OF Na_2O CONTENT ON VISCOSITY OF Na_2O -B_2O_3 SLAGS.

(2)the strengthening effect of forming BO_4 groups.So at any given alkali oxide concentration it is then postulated that there is an equilibrium between the two proposed structures and this equilibrium is a function of temperature in the sense that increasing the temperature, tetrahedral oxygens decrease relative to that of the singly bonded oxygens. Thus a rational explanation for the observed viscosity behaviour may be given. The decrease in viscosity with increase in temperature and concentration of alkali oxide i.e. Na_2O can be attributed to the fact that as the temperature increases (from 1000^oC to 1300^oC) , the dominant action of oxygens introduced is to break B-O-B bonds and form B-O bonds although some of oxygens may also form groups which have an opposing effect on viscosity [141]. However, in the present research work, the alkali (Na_2O) concentration has been taken high enough (37.3 to 49.4 mole %) for which all the possible positions for an oxygen to go into tetrahedral coordination are filled and the formation of singly bonded oxygen is possible on further introduction of Na_2O, thereby reducing the viscosity. It may, therefore, be concluded that with the increase in temperature, very large concentration of alkali oxide i.e.Na_2O (>33 mole %) is required to offset the effect of BO_4 groups by formation of singly bonded oxygens and hence lowering the viscosity values. Due to non-availability of data on viscosity of sodium-borate

slag systems for the above mentioned temperature range and Na_2O concentrations, the results of the present investigation could not be compared with others.

The effect of addition of CaO to sodium borate slag (wt% Na_2O/wt% B_2O_3 = 0.86) on its viscosity has been studied by varying CaO proportion (ie. 10, 30,50, wt% CaO) in the Na_2O - B_2O_3 slag for diffrent temperatures (from 1273K to 1573K). It is noted from the data reported in Table 3.2 that the addition of (10 to 50 wt%) CaO to sodium borate slag increases its viscosity from 3.75 Pa-s to 5.23 Pa-s at 1273K temperature while at temperature 1573K, the value increases from 0.44 Pa-s to 0.60 Pa-s for the same increases in CaO amount (10 to 50 wt%) in the slag. The relation between ln (viscosity η) and reciprocal of absolute temperature as shown in Fig. 3.6 indicates that with increase in temperature, viscosity decreases and it follows an Arrhenius type relationship. The average value of activation energy has been found to be equal to 124.7K J/mole. The increase in viscosity value with addition of CaO to the slag can be attributed to the fact that CaO addition increases the liquidus temperature of the slag system there by decreasing the fluidity of the melt.

Similarly the effect of CaF_2 addition to the slag (30.9wt% Na_2O, 35.8wt% B_2O_3, 33.3wt% CaO) for which Se and Te distribution coefficients were noted to be maximum

TABLE - 3.2

VISCOSITY OF Na_2O-B_2O_3-CaO SLAGS AT DIFFERENT TEMPERATURES

Sl. No.	Slag Composition (by weight)	Temperature (K)	Viscosity η (Pa-s)	ln η
1.	(42.1% Na_2O + 48.8%	1273	3.747	1.321
2.	B_2O_3 + 9.1 % CaO)	1373	1.577	0.456
3.		1473	0.755	-0.281
4.		1573	0.437	-0.826
5.	(35.6% Na_2O + 41.3 %	1273	4.314	1.462
6.	B_2O_3 + 23.1 % CaO)	1373	2.005	0.696
7.		1473	0.903	-0.102
8.		1573	0.547	-0.602
9.	(30.9% Na_2O + 35.8 %	1273	5.227	1.654
10.	B_2O_3 + 33.3 % CaO)	1373	2.630	0.967
11.		1473	1.117	0.111
12.		1573	0.602	-0.507

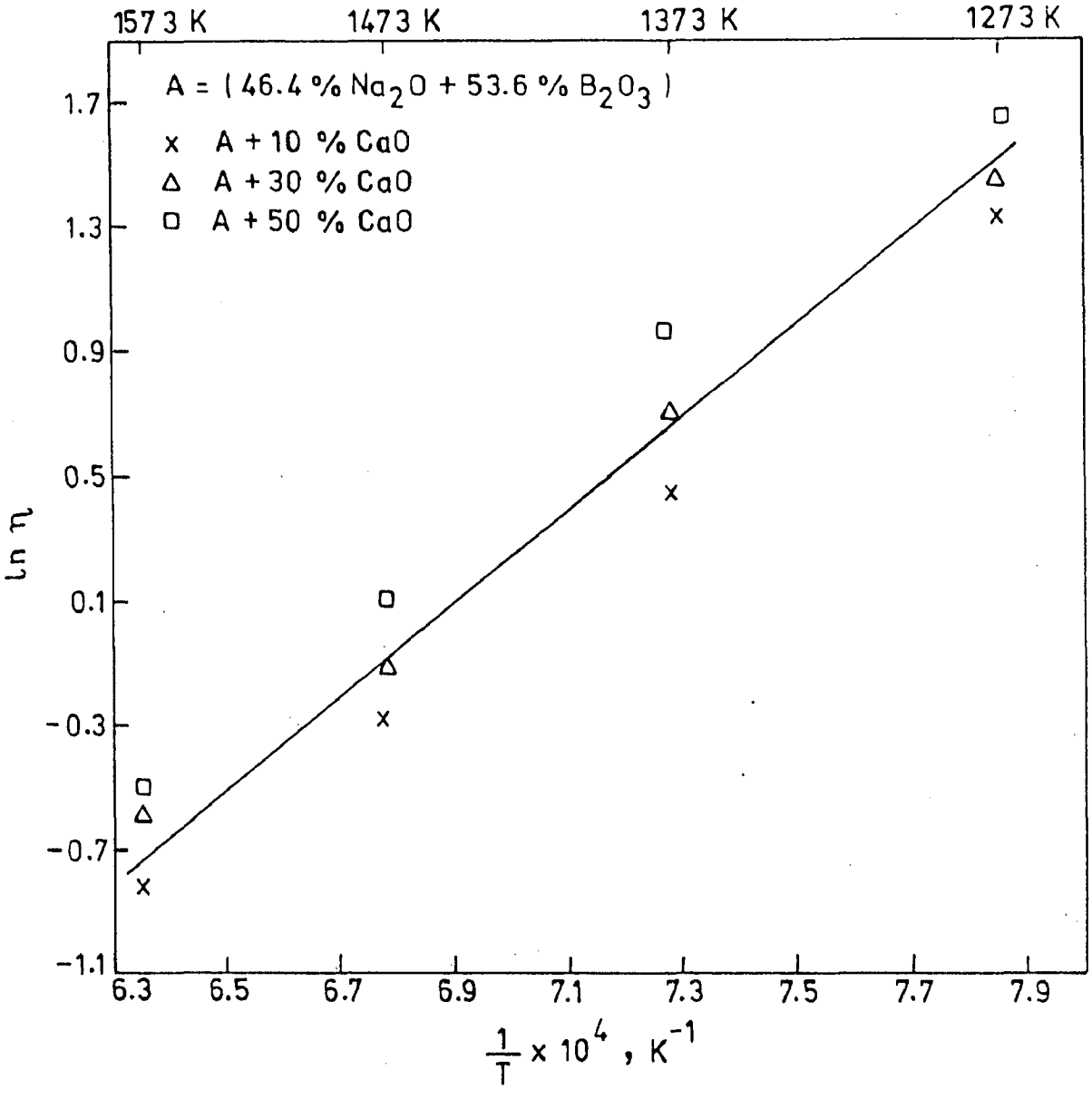

FIG. 3.6 EFFECT OF CaO ON VISCOSITY OF Na_2O -B_2O_3 SLAG FOR DIFFERENT TEMPERATURES.

(Section 2.4), viscosity measurements were taken by adding CaF_2 (5 to 20wt%) in the above slag at different temperatures as given in the Table 3.3. It is noted that there is a drastic decrease in slag viscosity.

From a value of 5.23 Pa-s for no CaF_2 addition in the slag (30.9wt% Na_2O, 35.8wt% B_2O_3, 33.3wt% CaO) to a value of 0.58 Pa-s for 20wt% CaF_2 addition in the above slag at 1273K. The plots of ln (viscosity,η) vs. 1/T follows an Arrhenius type relationship as shown in Fig. 3.7. The average value of activation energy has been found to be equal to 41.4 K J/ mole.The decrease in slag viscosity with CaF_2 additions can be attributed to the fact that single-charged fluoride ions breakdown the BO_4 tetrahedral network and facilitate the formation of BO_3 triangles (platelets) with singly bonded oxygens.

From the results and discussions , it is, therefore, inferred that in the composition and temperature ranges of the present study, the viscosity of slag decreases with increase in Na_2O content in Na_2O -B_2O_3 slags while addition of CaO in the above slag system increases its viscosity. The slag viscosity of Na_2O-B_2O_3-CaO decreases considerably on adding CaF_2. The fluidity of all slag compositions used show improvement on raising temperature.

TABLE - 3.3

VISCOSITY OF Na_2O-B_2O_3-CaO-CaF_2 SLAGS AT DIFFERENT TEMPERATURES

Sl. No.	Slag Composition (by weight)	Temperature (K)	Viscosity η (Pa-s)	ln η
1.	(29.4% Na_2O + 34.1% B_2O_3	1273	0.704	-0.351
2.	+ 31.7% CaO + 4.8 % CaF_2)	1373	0.565	-0.571
3.		1473	0.439	-0.823
4.		1573	0.381	-0.964
5.	(28.1% Na_2O + 32.5 % B_2O_3	1273	0.630	-0.462
6.	+ 30.3% CaO + 9.1 % CaF_2)	1373	0.561	-0.578
7.		1473	0.441	-0.818
8.		1573	0.360	-1.021
9.	(25.7% Na_2O + 29.8 % B_2O_3	1273	0.576	-0.551
10.	+ 27.8% CaO + 16.7 % CaF_2)	1373	0.476	-0.741
11.		1473	0.382	-0.963
12.		1573	0.319	-1.142

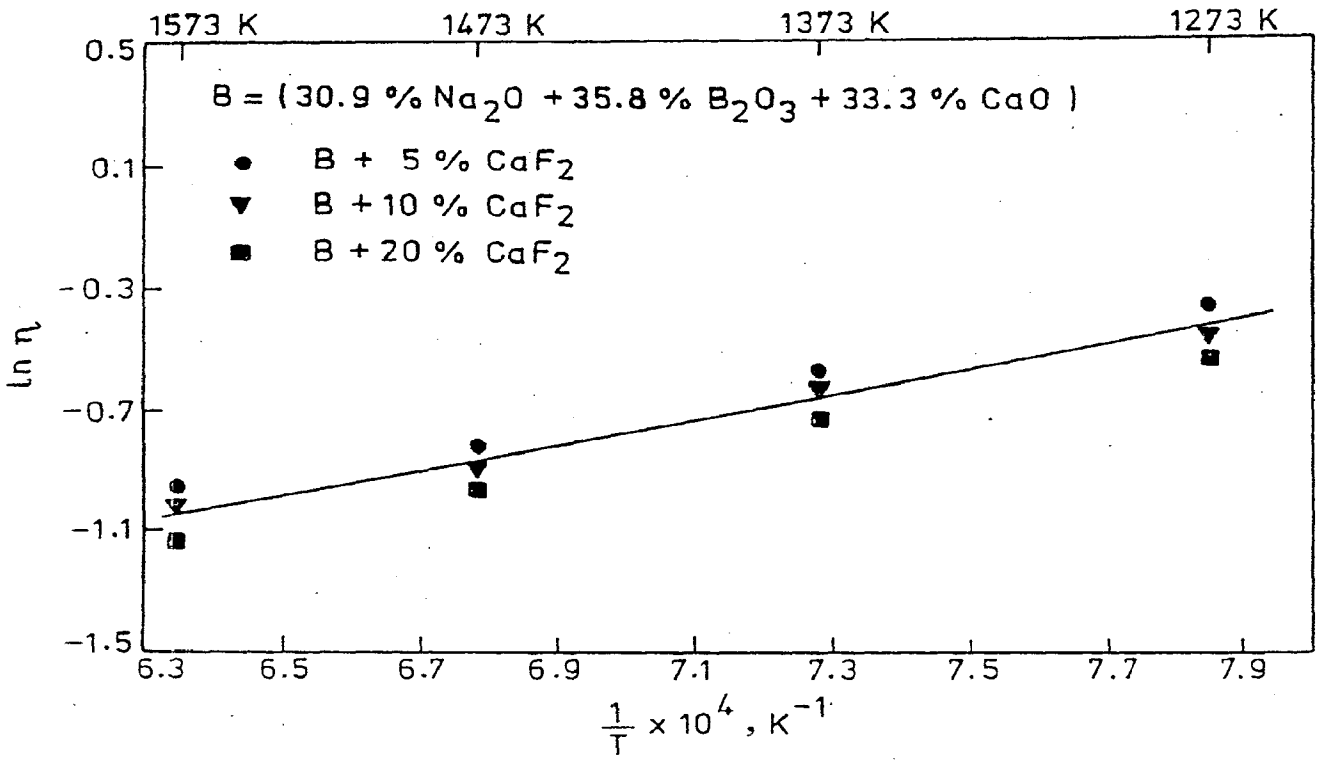

FIG. 3.7 EFFECT OF CaF_2 ON VISCOSITY OF Na_2O-B_2O_3-CaO SLAG FOR DIFFERENT TEMPERATURES.

CHAPTER - IV

KINETICS OF SLAG-METAL SYSTEM

4.1 THEORETICAL ANALYSIS

Since slag-metal reaction is heterogeneous in nature, the overall reaction involves following steps :

(i) Transport of reactants from bulk to slag-metal interface.

(ii) Interfacial chemical reaction between slag and metal.

(iii) Transport of products from interface to the bulk.

The overall rate of transfer of dissolved elements from metal to slag will be determined by the slowest of the above steps. The rate determining step may change according to the experimental conditions of the reactive system under study. At elevated temperatures, the chemical reactions are so fast that equilibrium is very closely approached at the interface throughout the course of the reaction. Under these conditions mass transport step controls the overall rate of reaction and it is possible to derive a simple relation between the flux across the phase boundary, the concentration differences and the mass-transfer coefficients. Assuming that one solute is moving from metal

to the slag phase and there is no build up of solute in the interfacial zone and that the mass-transfer coefficients are independent of concentration and of one another, the rate of solute element 'Me' transfer, J (gm/sec), from metal to slag across the interface under steady state conditions can be expressed by the relationship,

$$J = - k_M A ([C_b]_t - [C_i]_t)$$
$$= - k_S A ((C_i)_t - (C_b)_t) \qquad \ldots.(4.1)$$

where k_M and k_S are, respectively, the mass transfer coefficients (cm/sec) for element 'Me' in metal and slag phases, A is the interfacial area in cm^2, $[C_b]_t$ and $(C_b)_t$ are the concentrations (gm/cm^3) of 'Me' in bulk metal and slag phases respectively at time 't' and $[C_i]_t$, $(C_i)_t$ are the interfacial concentrations (gm/cm^3) of 'Me' on metal and slag side respectively at time 't'. Further since chemical equilibrium is assumed to prevail at the interface, one can write the following expression for the distribution coefficient, L,

$$L = \frac{(C_i)_t}{[C_i]_t} \qquad \ldots.(4.2)$$

It is to be noted that 'L' is a function of temperature and compositions of slag and metal phases. Assuming Henrian

behaviour of element 'Me' in metal and slag phases, the above expression can also be written as

$$L = \frac{\rho_S \ (wt\%\ Me_i)_t}{\rho_M \ [wt\%\ Me_i]_t} \qquad \ldots\ldots(4.3)$$

where ρ_M and ρ_S are the densities (gm/cm^3) of metal and slag phases respectively ; $(wt\%\ Me_i)_t$ and $[wt\%\ Me_i]_t$ are the interfacial 'Me'weight percent on slag and metal sides respectively. Also under steady state conditions,

$$J = \frac{d}{dt}\{V_M [C_b]_t\} = V_M \rho_M \frac{d\ [wt\%\ Me_b]_t}{dt} \qquad \ldots\ldots(4.4)$$

where V_M is volume of metal phase.

Using eq. (4.2) and eq.(4.4), eq.(4.1) may be written as

$$V_M \rho_M \frac{d\ [wt\%\ Me_b]_t}{dt} = - k_M A \{[C_b]_t - [C_i]_t\}$$

$$= - Lk_S A \{[C_i]_t - (C_b)_t/L\} \qquad \ldots\ldots(4.5)$$

Writing eq. (4.5) in two different ways

$$-\frac{V_M \rho_M}{A} \frac{d\ [wt\%\ Me_b]_t}{dt} \cdot \frac{1}{Lk_S} = [C_i]_t - (C_b)_t/L \qquad \ldots\ldots(4.6)$$

and $$-\frac{V_M \rho_M}{A} \frac{d\ [wt\%\ Me_b]_t}{dt} \cdot \frac{1}{k_M} = [C_b]_t - [C_i]_t \qquad \ldots\ldots(4.7)$$

Adding equations (4.6) and (4.7) , we get

$$\frac{V_M\,\rho_M}{A} \cdot \frac{d\,[wt\%\ Me_b]_t}{dt} = -\frac{\left([C_b]_t - (C_b)_t/L\right)}{\frac{1}{k_M} + \frac{1}{LK_S}} \quad \ldots.(4.8)$$

Further, from mass balance criterion,

$$V_M\,[C_b]_t + V_S(C_b)_t = V_M\,[C_b]_\infty + V_S\,(C_b)_\infty \quad \ldots.(4.9)$$

where $[C_b]_\infty$ and $(C_b)_\infty$ are the concentrations (gm/cm^3) of 'Me' in metal and slag phases respectively at infinite time. Equation (4.9) can be written as

$$\frac{V_M\,\rho_M}{V_S}\left\{[wt\%\ Me_b]_t - [wt\%\ Me_b]_\infty\right\} = (C_b)_\infty - (C_b)_t \ldots.(4.10)$$

Since at infinite time,

$$[C_i]_\infty = [C_b]_\infty\ ,\ (C_i)_\infty = (C_b)_\infty \text{ and}$$

As,

$$(C_i)_\infty = L\,[C_i]_\infty\ ,\ \text{we get}\ (C_b)_\infty = L\,[C_b]_\infty$$

Now equation (4.10) can be written as

$$\frac{V_M\,\rho_M}{L\,V_S}\left\{[wt\%\ Me_b]_t - [wt\%\ Me_b]_\infty\right\} = [C_b]_\infty - (C_b)_t/L \quad \ldots(4.11)$$

and

$$[C_b]_t - [C_b]_\infty = \rho_M \left\{ [wt\%\ Me_b]_t - [wt\%\ Me_b]_\infty \right\} \quad \ldots.(4.12)$$

adding equation (4.11) and (4.12), we get

$$\left\{ [wt\%\ Me_b]_t - [wt\%\ Me_b]_\infty \right\} \left\{ \rho_M + \frac{V_M \rho_M}{LV_S} \right\} = [C_b]_t - \frac{(C_b)_t}{L} \quad \ldots.(4.13)$$

Or

$$\frac{A}{V_M \rho_M} \left\{ [C_b]_t - (C_b)_t / L \right\} = \left\{ [wt\%\ Me_b]_t - [wt\%\ Me_b]_\infty \right\} \left\{ \frac{A}{V_M} + \frac{A}{LV_S} \right\}$$

$$= \left\{ [wt\%\ Me_b]_t - [wt\%\ Me_b]_\infty \right\} \left\{ \frac{1}{h_M} + \frac{1}{Lh_S} \right\}$$

$$\ldots.(4.14)$$

Hence, from equations (4.8) and (4.14), we get

$$\frac{d\,[wt\%\ Me_b]_t}{dt} = -\frac{\frac{1}{h_M} + \frac{1}{Lh_S}}{\frac{1}{K_M} + \frac{1}{Lk_S}} \left\{ [wt\%\ Me_b]_t - [wt\%\ Me_b]_\infty \right\} \ldots(4.15)$$

where 'h_M' and 'h_S' are the heights of metal and slag columns respectively in the reaction vessel. Integration of eq.(4.15) leads to the following expression,

$$\ln \frac{[wt\%\ Me_b]_t - [wt\%\ Me_b]_\infty}{[wt\%\ Me_b]_o - [wt\%\ Me_b]_\infty} = - \left(\frac{\frac{1}{h_M} + \frac{1}{Lh_S}}{\frac{1}{K_M} + \frac{1}{Lk_S}} \right) t \quad .....(4.16)$$

where $[wt\%Me_b]_o$ is the wt% Me in bulk metal at time t = o

Equation (4.16) can also be written as,

$$\ln \frac{[wt\%\ Me_b]_t - [wt\%\ Me_b]_\infty}{[wt\%\ Me_b]_o - [wt\%\ Me_b]_\infty} = -k \left(\frac{1}{h_M} + \frac{1}{Lh_S} \right) t \quad ...(4.17)$$

where, k, the overall mass transfer coefficient is defined by the expression,

$$\frac{1}{k} = \frac{1}{k_M} + \frac{1}{Lk_S} \quad ....(4.18)$$

Two specific cases arise from the above general relationship:

Case I : Assuming L to be large and therefore $Lk_S >> k_M$ and also $Lh_S >> h_M$, one gets,

$$\frac{1}{k_M} + \frac{1}{Lk_S} \simeq \frac{1}{k_M} \quad .....(4.19)$$

and therefore, eq.(4.16) takes the following form,

$$\ln \frac{[wt\%\ Me_b]_t - [wt\%\ Me_b]_\infty}{[wt\%\ Me_b]_o - [wt\%\ Me_b]_\infty} = - \frac{k_M}{h_M} t \quad ......(4.20)$$

In other words, for this case, the rate of overall chemical reaction will be controlled by the mass transfer in metal phase.

Case II : Assuming L to be very small and therefore

$Lk_S << k_M$ and $Lh_S << h_M$, one gets,

$$\frac{1}{k_M} + \frac{1}{Lk_S} \simeq \frac{1}{Lk_S} \qquad .....(4.21)$$

and therefore eq. (4.16) reduces to,

$$\ln \frac{[wt\%\ Me_b]_t - [wt\%\ Me_b]_\infty}{[wt\%\ Me_b]_o - [wt\%\ Me_b]_\infty} = - \frac{k_S}{h_S} t \qquad .....(4.22)$$

meaning thereby that in this case the reaction will be controlled by the mass transfer of the element 'Me' in slag phase.

In all other cases, the overall reaction rate will be controlled jointly by the mass transfer of element 'Me' in both slag-and metal-phase as indicated by eq.(4.16).

4.1.1 Models Proposed

Following theories have been proposed to explain the mass transfer across an interface in an agitated/stirred system.

(a) The Two-Film Theory:

In this theory [142], it is assumed that turbulence dies out at the interface and a laminar layer exists in each of the two fluids. Outside the laminar layer, turbulent eddies supplement the action caused by the random movement of the molecules, and the resistance to transfer becomes progressively smaller. For equimolecular counterdiffusion, the concentration gradient close to the interface is therefore linear and gradually becomes less at greater distance. The basis of the theory is the assumption that the zones in which the resistance to transfer lies can be replaced by two hypothetical layers, one on each side of the interface, in which the transfer is entirely by molecular diffusion. The concentration gradient is therefore linear in each of these layers and zero outside. Equilibrium is assumed to exist at the interface.

The mass transfer is treated as a steady state process ad therefore the theory can be applied only if the time taken for the concentration gradients to become established is very small compared with the time of transfer, or if the capacity of the film is negligible. The rate of transfer per unit area η_A, in terms of the two film theory for equimolecular counterdiffusion may be expressed for the first phase (phase-1) by following relationship,

$$\eta_A = \frac{D_1}{\delta_1} (C_{o1} - C_{i1}) = k_1 (C_{o1} - C_{i1}) \quad \ldots(4.23)$$

where D_1, is the diffusivity ; δ_1 the thickness of the film; C_{o1}, the molar concentration outside the film ; C_{i1} , the molar concentration at the interface ; and, k_1, the mass transfer coefficient, for this phase.

For the second phase (phase-2), using similar notations,

$$\eta_A = \frac{D_2}{\delta_2} (C_{i2} - C_{o2}) = k_2 (C_{i2} - C_{o2}) \quad \ldots.(4.24)$$

Because material does not accumulate at the interface, the two rates of transfer expressed by eqs. (4.23) and (4.24) must be identical. Therefore,

$$\frac{k_1}{k_2} = \frac{C_{i2} - C_{o2}}{C_{o1} - C_{i1}} \quad \ldots.(4.25)$$

The flow conditions are too complex for the film thickness to be evaluated. However, these are progressively decreased as the turbulence of the fluid is increased.

(b) The penetration theory :

This theory [143] assumes that the eddies in the

fluid bring an element of fluid to the interface where it is suddenly exposed to the second phase for a definite interval of time, for reaction to proceed, after which the surface element is mixed again with the bulk fluid. It is further assumed that equilibrium is immediately attained by the surface layers and that a process of unsteady state molecular diffusion then occurs and also that the element is remixed after a fixed interval of time. In the calculation, depth of the liquid element is assumed to be infinite and this is justifiable if the time of exposure is sufficiently short for penetration to be confined to the surface layers. Throughout, the existence of velocity gradients within the fluid is ignored and the fluid at all depths is assumed to be moving at the same rate as the interface.

With the boundary conditions,

$t = 0$	$0 < y < \infty$	$C_A = C_o$
$t > 0$	$y = 0$	$C_A = C_i$

and,

$t > 0$	$y = \infty$	$C_A = C_o$

where, C_o is the concentration in the body of the phase ; and, C_i, the equilibrium value at the interface. The rate of transference per unit area, η_A , across the phase may thus be given as,

$$\eta_A = (C_i - C_o) \left(\frac{D}{\pi t} \right)^{1/2} \quad \ldots.(4.26)$$

This equation gives the instantaneous transfer rate when the surface element under consideration has an age t. If the element is exposed for a time t_e , the average rate of transfer is given by,

$$\eta_A = 2 (C_i - C_o) \left(\frac{D}{\pi t_e} \right)^{1/2} \quad \ldots.(4.27)$$

Thus, the shorter the time of exposure, the greater is the rate of mass transfer. No precise value can be assigned to t_e in any practical equipment, but its value will clearly become less as the degree of agitation of the fluid is increased.

(c) The random surface renewal theory :

In this theory [144] it is considered that each element of surface would not be exposed for the same time, but a random distribution of ages would exist. It is assumed that the probability of any element of surface becoming destroyed and mixed with the bulk of the fluid was independent of the age of the element.

By supporting the rate of production of fresh

surface per unit total area of surface to be S, and that S is independent of the age of the element, the overall rate of transfer per unit area, when the surface is renewed in a random manner can be expressed as,

$$\eta_A = (C_i - C_o) \sqrt{D S} \qquad \ldots.(4.28)$$

The above equation might be expected to under-estimate the mass transfer rate because, in any practical equipment, there will be a finite upper limit to the age of any surface element. However, the proportion of the surface in the older age group is very small and the overall rate is largely unaffected. The numerical value of S is difficult to estimate, but will clearly increase as the fluid becomes more turbulent.

(d) The film-penetration theory :

This theory [145] incorporates some of the principles of both of the Two-Film Theory and the Penetration-Theory. The whole of the resistance to transfer is regarded as lying within a laminar film at the interface, as in the Two-Film Theory, but the mass transfer is regarded as an unsteady state process. It is assumed that fresh surface is formed at intervals from fluid which is brought

from the bulk of the fluid to the interface by the action of the eddy currents. Mass transfer then takes place as in the Penetration Theory, with the exception that the resistance is confined to the finite film, and the material which traverses the film is immediately completely mixed with the bulk of the fluid. For short times of exposure, when none of the diffusing material has reached the far side of the layer, the process is identical to that postulated in the Penetration Theory. For prolonged periods of exposure when a steady concentration gradient has developed, conditions are similar to those in the Two-Film Theory.

The boundary conditions are same as in the Penetration Theory, but the third boundary condition is applied at $y = \delta$, the film thickness, and not at $y = \infty$. With these boundary conditions the rate of mass transfer was given by,

$$\frac{\delta^2}{Dt} \geq \pi, \quad \eta_A = (C_i - C_o) \left[\frac{D}{\pi t}\right]^{1/2} \left\{ 1 + 2e^{-\delta^2/Dt} \right\} \qquad \ldots.(4.29)$$

$$\frac{\delta^2}{Dt} \leq \pi, \quad \eta_A = (C_i - C_o) \left[\frac{D}{\delta}\right] \left\{ 1 + 2e^{-\pi^2 Dt/\delta^2} \right\} \qquad \ldots.(4.30)$$

The mass transfer rates given by eqs. (4.29 and 4.30) are point values at surface elements of age t. The

mass transfer rates can be obtained, by assuming that all surface elements are exposed for the same time t_e, or by assuming a random age distribution. For very short time of exposure, eq. (4.29) reduces to eq. (4.26) for the Penetration Theory, and for long exposures, eq. (4.30) reduces to eq. (4.23) for the Two-film Theory. The difficulty in applying eqs. (4.29 and 4.30) are that they involve two quantities, the film thickness and the time of exposure, neither of which is readily known.

4.1.2 Role of stirring in liquid phase mass transfer

Improvement in the overall rate of reaction in a heterogeneous system as a result of stirring due to enhanced mass transport is well-known. Different methods used for stirring include mechanical stirring, pneumatic stirring electromagnetic stirring, gas bubbles stirring etc. [146-158].

4.1.3 Gas bubble-agitated liquid reactive systems

A reactive liquid system can be gas-bubble agitated due to, (i) evolution of dissolved gas resulting from decreased solubility, e.g., hydrogen and nitrogen evolution from molten steel on cooling, (ii) production of

gas due to chemical reaction within the liquid phase, e.g., CO evolution in molten steel resulting from deoxidation with carbon, and, (iii) flow of an inert gas through the liquid bath.

4.1.4 Characteristics of bubbles formed at an orifice in a gas-stirred liquid bath

At very low gas flow rates through an orifice, the bubble diameter and the frequency of bubble formation may be determined [159] by the balance between the buoyancy and the surface tension forces. Thus for $N_{Re,O} < 500$,

$$\frac{\pi}{6} d_b^3 g (\rho_l - \rho_g) = \pi d_o \sigma \qquad \ldots.(4.31)$$

where, d_b and d_o, are respectively the bubble and orifice diameters; ρ_l and ρ_g, respectively the liquid and gas densities; $N_{Re,O}$, the orifice Reynolds's number; and, σ ,the surface tension. As evident from the above expression,the bubble diameter is independent of flow rate of the gas. Under these conditions, frequency of bubble formation is proportional to the volumetric flow rate and the orifice diameter.

At intermediate gas flow rates ($500 < N_{Re,O} < 2100$), the bubble size depends upon the gas flow rate and nozzle

diameter. The frequency of bubbles from the orifice increases with an increase in the gas flow rate until a limiting value is reached. For the air-water system, Davidson and Emick [160] presented the following empirical relationships,

$$d_b = 0.54 \left[G.d_o^{0.5} \right]^{0.289} \quad \ldots.(4.32)$$

and,

$$F_{max} = 6.7\ G^{0.13}\ d_o^{0.43} \quad \ldots.(4.33)$$

where, G is the gas flow rate ; and, F_{max}, the maximum frequency of bubble formation which may range from 25 bubbles/sec for a 1.6 cm diameter orifice to 75 bubbles/sec for a 0.035 cm diameter orifice.

Variation of mean bubble diameter with gas flow rate and orifice diameter, expressed in terms of the orifice Reynold's number was also studied by Leibson et al.[161] for the air-water system. In laminar region($N_{Re,O}$<2100), they presented the following correlation,

$$d_b = 0.29\ d_o^{0.5}\ N_{Re,O}^{0.333} \quad \ldots.(4.34)$$

At high gas flow rates, small bubbles of varying sizes are formed at about 10 cm above the orifice by disintegration of large irregular bubbles formed at the

orifice. Leibson et al. [161] proposed the following equation for bubble diameter in the turbulent range,

$$d_{bvs} = 0.71\ N_{Re,0}^{-0.05} \qquad \ldots.(4.35)$$

where, d_{bvs} is the volume surface mean diameter of the bubble and $N_{Re,0}$>10000 in above equation.

The velocity at which bubble rises through a liquid is determined principally by the buoyancy force that drives the bubble upwards, and the viscosity resistance that tends to retard this motion. When these forces are equal, the bubble rises at a constant velocity. The principal parameters which characterise the motion of bubble include

i) bubble Reynold's number, $N_{Re,b} = \dfrac{d_{be}\,u.\rho_l}{\mu_l}$ ....(4.36)

ii) Weber number, $N_{We} = \dfrac{d_{be}.u^2\rho_l}{g_c.\sigma}$ ....(4.37)

and iii) Morton number, $N_{Mo} = \dfrac{g\,\mu_l^4}{\rho_l(g_c\sigma)^3}$ ....(4.38)

where, d_{be} is the diameter of a sphere of volume equal to the bubble under study; u, the rising velocity of the bubble; μ_l, viscosity of the liquid; and, g_c, the conversion constant. With the help of these parameters, behaviour of

bubbles inaccordance with [162] can be classified into four cateogories.

(a) Very small bubbles: small bubbles, for which $N_{Re,b}<2$, rise at a terminal velocity determined by Stokes' law,expressed as,

$$u_t = \frac{d_b^2}{18\mu} g\ (\rho_l - \rho_g) \qquad \ldots.(4.39)$$

these very small bubbles behave like rigid spheres, because the surface tension inhibits circulation of the gas.

(b) Intermediate size spherical bubbles : these bubbles with $2< N_{Re,b} < 400$, are still spherical and rise in a rectilinear path, but their rising velocity maybe as much as 50% greater than that predicted for very small bubbles.

(c) Spheroidal and ellipsoidal bubbles : the bubbles in this region with $400< N_{Re,b}< 5000$, may be spheroidal or ellipsoidal and rise in the fluid in a spiral path.

(d) Spherical cap bubbles :bubbles of diameter above 1 cm with $N_{Re,b} > 5000$ and $N_{We}> 18$, are of spherical-cap shape and rise at a terminal velocity which is independent of the properties of the liquid. The rising velocity of such bubbles may be expressed by the following expression derived by Davies and Taylor [163],

$$u_t = 1.02 \left[\frac{g.d_b}{2} \right]^{0.5} \qquad \ldots.(4.40)$$

Growth of bubbles takes place due to diffusion of gas from the liquid to the gas-phase and during their rise in the liquid, because its pressure decreases with decreasing liquid head. Since the velocity of rising bubble is related to its size, for calculating its residence time, the change in bubble size with distance above the orifice must be taken into account. In the spherical-cap bubbles, the terminal rising velocity can be related to the bubble volume by the following expression,

$$u_t = 0.8\ g^{1/2}\ V_b^{1/6} \qquad \ldots.(4.41)$$

where, the bubble volume $V_b = \pi\ d_b^3\ /6$

For g = 980 cm/sec^2 one gets,

$$u_t = 25\ V_b^{0.167} \qquad \ldots.(4.42)$$

By denoting the vertical distance of the bubble from the orifice, by x and assuming that the terminal velocity corresponding to a certain bubble size is attained very rapidly, one may write,

$$u_t = \frac{dx}{dt} = 25\ V_b^{0.167} \qquad \ldots.(4.43)$$

In order to integrate above equation it is

necessary to relate the bubble volume to the vertical co-ordinate x. For an isothermal system, the pressure-volume relationship in the bubble can be expressed by the ideal gas,

$$P_x V_x = P_o V_o \qquad \ldots.(4.44)$$

where, V_x and V_o are the bubble volumes respectively at a distance x from the orifice and at the orifice; and P_x and P_o, the corresponding pressures. The pressure at orifice can be calculated by adding the atmospheric pressure above the bath and the liquid head. Thus,

$$P_o = P_{atm} + \rho_l \, g \, H \qquad \ldots.(4.45)$$

where, H is the depth of orifice in the liquid (in cm). The pressure, P_x, on the bubble at a distance x from the orifice may be expressed as,

$$P_x = P_o - \rho_l \, g \, x \qquad \ldots(4.46)$$

By combining eqs. (4.42 - 4.44) with eq. (4.46), one gets,

$$\frac{dx}{dt} = 25 \left(\frac{P_o V_o}{P_o - \rho_l g x} \right)^{0.167} \qquad \ldots.(4.47)$$

and on subsequent integration of eq. (4.47) between the limits,

$$x = 0 \quad , \text{at} \quad t = 0$$

and $$x = H \quad , \text{at} \quad t = t_R$$

where, t_R is the residence time of the bubble in the liquid, one arrives at the following expression,

$$t_R = \frac{P_o^{1.167} - (P_o - \rho_l g H)^{1.167}}{29.2\, \rho_l g\, (P_o V_o)^{0.167}} \qquad \ldots.(4.48)$$

In derivation of eq. (4.48), it was assumed that the expanding bubble attains its new terminal velocity instantaneously, i.e., with a negligible time lag. This assumption is valid for practically all gas-liquid systems.

4.1.5 Analysis of gas-bubble characteristics

Hughes et al. [164] , Hayes et al. [165] and Sullivan et al. [166] studied the characteristics of the gas bubbles under laminar flow conditions at the orifice and observed that volume of the bubble formed was initially independent of the gas flow rate. However, as the gas flow

rate and hence the orifice Reynolds number was increased, the frequency of bubble formation increased in this region. With further increase in the gas flow rate, the frequency of bubble formation reached a maximum and the volume of the bubble formed at the orifice increased significantly. Haberman and Morton [167] , Hartunian and Sears [168], Garner and Hammerton [169], Peebles and Garber [170] , Davies and Taylor [163] also carried out extensive studies on the characteristics of gas bubbles in aqueous type liquids. Lanauze and Harris [171], Kumar et al. [172], Siemes and Haufmann [173], Siemes [174], Davidson and Schuler [175, 176] tried to model their experimental findings with various degrees of success. Papamantellos et al. [177] put forward a mathematical model which is adaptable to practical conditions to describe the purging of liquid steel with an inert gas. Sano and Mori [178] investigated the nitrogen mercury and nitrogen - silver systems at 25^{o}C and 1000^{o}C respectively and observed a transition from varying to constant bubble formation frequency in both systems. Bulk of their work was carried out under constant flow conditions. Under laminar flow conditions, Andreini et al. [179] studied the characteristics of gas bubbles injected into molten tin, lead, and, copper. They found that the bubble size generated for a particular orifice diameter was dependent upon the

magnitudes of the orifice, and the Frude and Weber numbers. Several other workers [180 - 186] reported theoretical and experimental studies on mass transfer into rising bubbles in metallurgical systems. Guthrie and Bradshaw [183] reported experimental data on the transfer of oxygen to molten silver during bubble rise. These studies followed earlier work [181 , 182] using CO_2 in aqueous solutions and were designed to test the applicability of general mass transfer theory to these types of systems. Baird and Davidson [187] developed a theoretical model for the mass transfer into spherical cap bubbles based on unsteady state diffusion. The model considers only transfer to or from the front surface. Following expression was arrived at for mass transfer coefficient, k,

$$k = 0.975\ d_{be}^{-1/4}\ D^{1/2}\ g^{1/4} \qquad \ldots.(4.49)$$

where, d_{be} , is the diameter of a spherical bubble with a volume equal to that of the spherical cap bubble (equivalent spherical bubble) ; D, the diffusivity in the metal; and g, the acceleration due to gravity. This equation was tested for solutes in water and alcohol [182 ,187] and for oxygen in liquid silver [181, 183] and it was found that the equation was valid within about 20%. Richardson [188,189] carried out the work on drops and bubbles in liquid metals

and represented the rate of transfer of gaseous solute between the liquid and the bubble in terms of an average mass transfer coefficient, k_M, in the metal by the following equation,

$$\dot{n} = k_M . A \left\{ [C_b] - [C_i] \right\} \qquad ....(4.50)$$

where, $\dot{n}$, is the total flux; A, the bubble area; and, $[C_b]$ and $[C_i]$, respectively the bulk and interfacial concentrations in the metal.

In liquid steel, bubbles smaller than 2 mm are spherical shaped, but with increasing volume they tend to become elliptical. With diameters greater than 8 mm, the bubble ascending in stagnant liquid layer are cap shaped [181,183,190,191], their ascending velocity is determined only by their size. Kraus [192] derived relationship for the ascending velocity for bubbles less than 8 mm diameter and Davies and Taylor [163] for ascending velocity for bubbles greater than 8 mm diameter. Guthrie and Bradshaw [181] , Richardson [193] and Johnson et al.[194] derived relationship for the mass transfer across the flat phase boundary area of the bubble cap.

Sano and Mori [195] presented a mathematical model to describe circulating flow in a molten metal bath with inert gas injection. The model is based principally on the

energy balance for the liquid phase. In the model, effects of gas hold-up in the bubble plume zone and energy dissipation due to bubble slip are taken into account. It has been shown by them that the 'liquid velocity' and the 'liquid circulating flow rate' are both directly proportional, and , 'mixing time', inversely proportional to one-third power of the gas flow rate or stirring power of gas. Asai et al.[196] also developed theoretically a correlation between mixing time and mixing power density for gas agitation from the view point of transport phenomenon and confirmed the theoretical results by the water model experiments. They concluded from their studies that same formulation can be employed both in 'gas agitation 'and 'mechanical agitation' as far as the relationship between fluid velocity and mixing power density is concerned.

4.2 EXPERIMENTAL

Inert gas bubble agitation method has been adopted for improving the contact between sodium-borate slag and molten copper for the present investigation. The rate of mass transfer from metal to slag was studied with the change in gas flow rate. Brief account of design and fabrication of experimental set-up and experimental runs is presented below.

4.2.1 Experimental set-up

Fig.4.1 shows the schematic block-diagram of experimental set-up used in the present investigation. The essential components of this set-up, designed and fabricated locally, include: a gas purification train and a gas bubble-agitated slag-metal contacting unit for kinetic studies of element transfer from metal to slag. Details of different units are briefly presented below.

4.2.1.1 Gas purification train

High purity nitrogen gas procured from M/s Modi Gas and Chemicals Ltd., Modi Nagar, was further purified by removal of associated moisture vapour and oxygen using a simple purification train shown schematically in Fig. 4.2. Nitrogen gas from the cyclinder was first bubbled through alkaline pyrogallol solution and conc. sulphuric acid and then passed over phosphorous pentaoxide powder. Ten pyrex-glass bubblers were connected in series with the first, fourth, seventh and tenth bubblers kept empty to avoid mixing of different reagents used. The second and third bubblers containing alkaline pyrogallol solution remove oxygen while bubblers containing conc. sulphuric acid and powdered phosphorous pentaoxide remove moisture

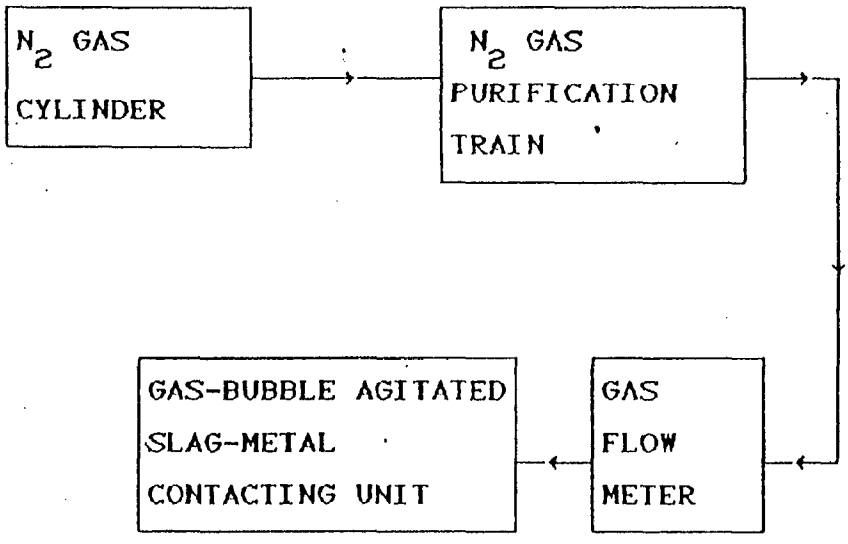

FIG. 4.1 SCHEMATIC BLOCK-DIAGRAM OF EXPERIMENTAL SET-UP FOR KINETIC STUDIES.

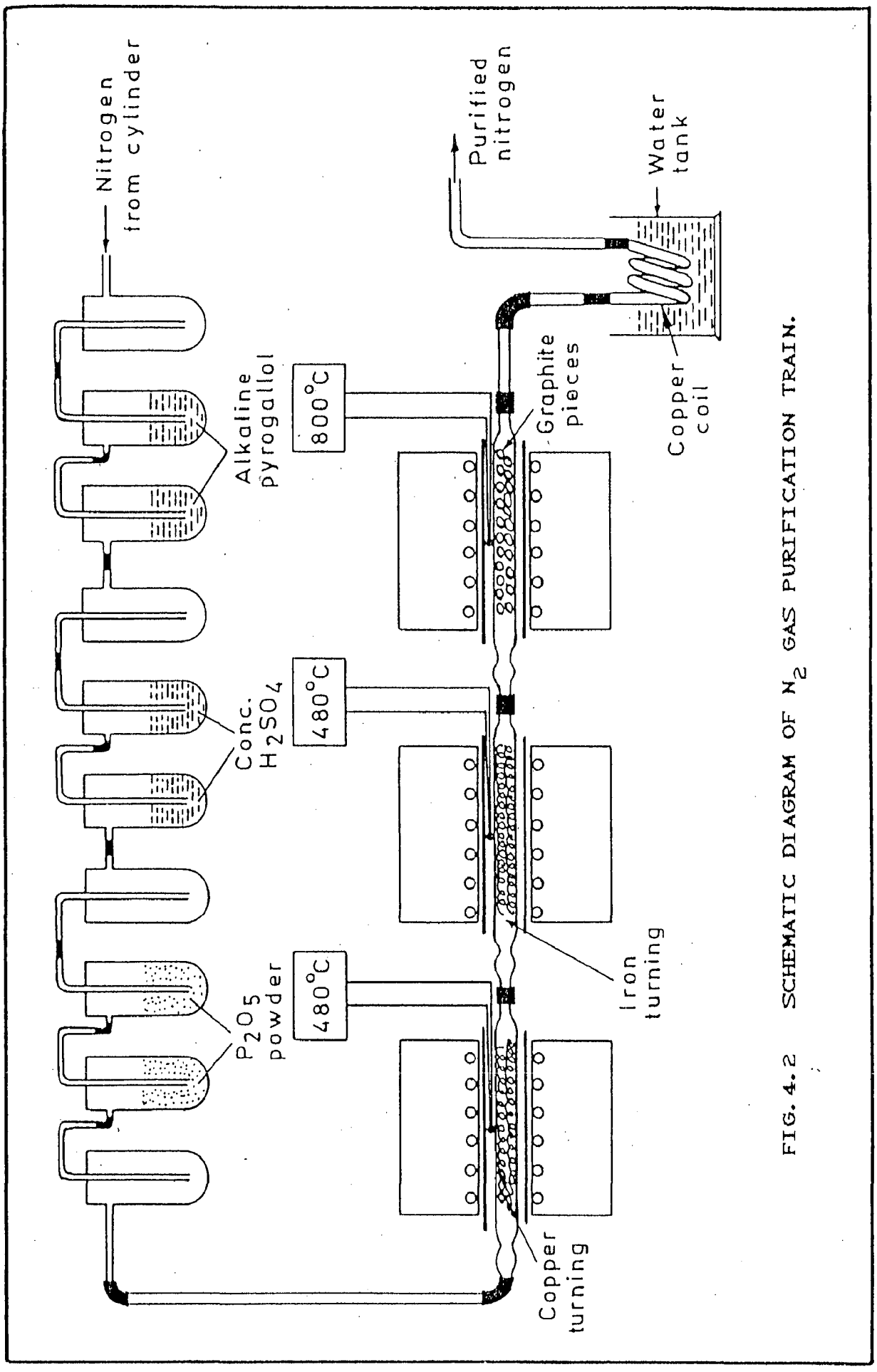

FIG. 4.2 SCHEMATIC DIAGRAM OF N_2 GAS PURIFICATION TRAIN.

from nitrogen gas. The bubbled gas was then passed over copper turnings, iron turnings, and graphite pieces of 1-2 mm size, kept in three different tubular furnaces maintained respectively at 480,480 and 800^{o}C to ensure oxygen and moisture removal. Finally, the purified gas was passed through a copper coil increased in a water tank, for cooling before entering the gas bubble into agitated slag-metal contacting unit.

4.2.1.2 Gas-bubble agitated slag-metal contacting unit

Fig.4.3 shows the essential components of the experimental unit. It includes ,

(a) Furnace assembly : A vertical globar furnace with both ends open and employing silicon carbide rods as heating element to develop a temperature upto 1400^{o}C , was used for melting the charge. High alumina tube of 65 mm OD and 55 mm ID was vertically placed between the four silicon carbide rods. Temperature of the furnace was controlled within $\pm$ 2^{o}C . Pt/Pt- 13% Rh thermocouple was used to measure the temperature.

(b) Graphite reaction crucible : Graphite crucibles of 35 mm OD, 25 mm ID and 140 mm height fabricated from spent graphite electrodes obtained

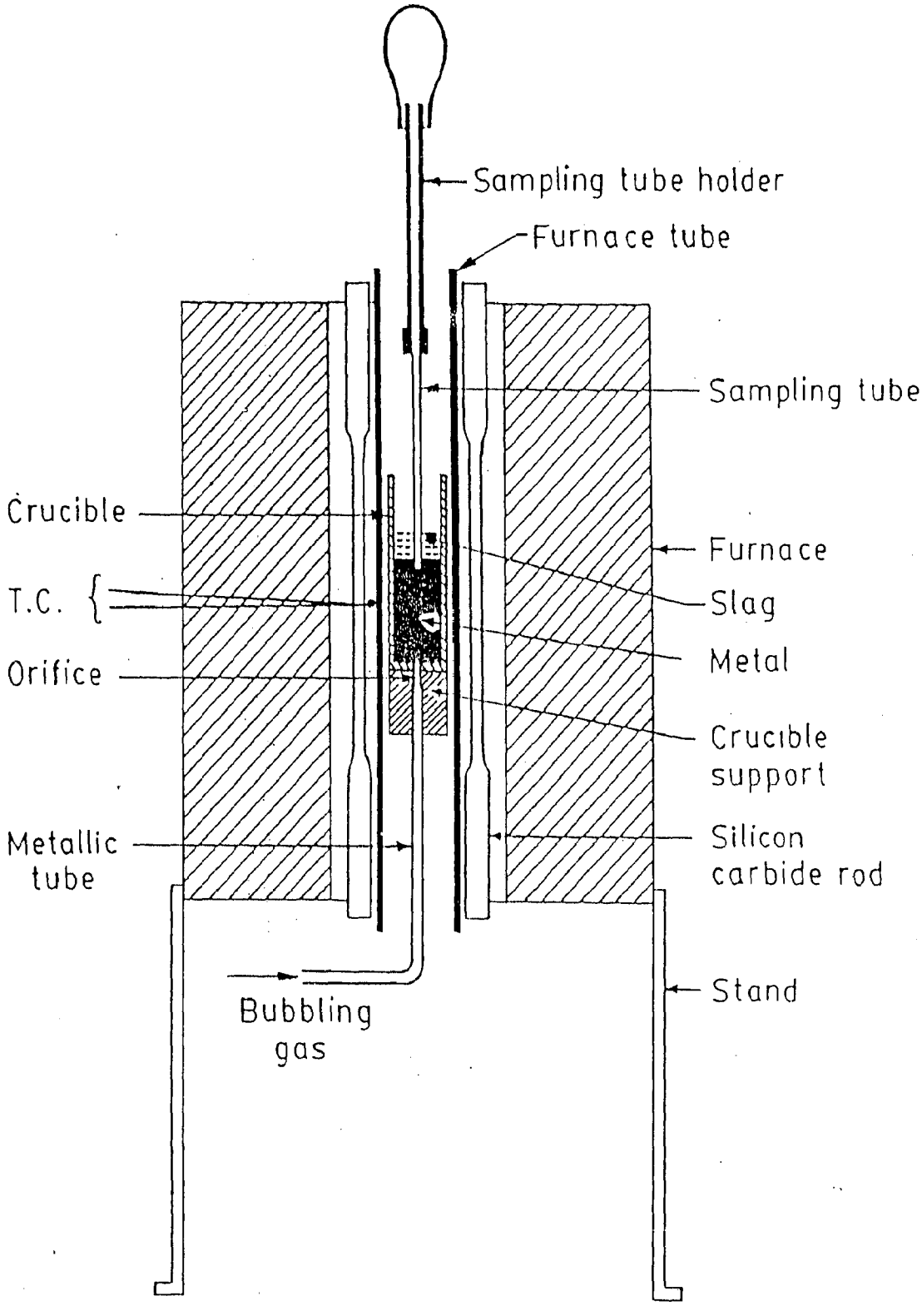

FIG. 4.3 GAS-BUBBLE AGITATED SLAG-METAL CONTACTING UNIT.

from mini-steel plant, were used for melting the charge. This was placed centrally inside alumina tube in the furnace assembly for experimental runs.

(c) Sampling device : High alumina tubes of 2-4 mm ID were used for withdrawing the metal and slag samples from the crucible during contacting of slag and metal at regular time intervals to study the progress of element transfer from copper.

4.2.1.3 Gas flow meter

The purified and dried nitrogen gas was passed through the gas flow meter to measure its flow rate in cc/sec .before entering into the gas-bubble agitated slag-metal contacting unit.

4.2.2 Preparation of Slag

Initially sodium-borate slag (wt% Na_2O /wt % B_2O_3 = 0.86) was prepared by mixing sodium carbonate and borax both of anal.r.grade in desired proportion and calcining the mixtures in the furnace for long time (3-4 days) at 1023K. This was followed by crushing , grinding,thorough mixing, and recalcination of the mixtures for two days at the same

temperature. Now for preparation of Na_2O -B_2O_3 - CaO - CaF_2 slag of desired composition , calculated amounts of CaO and CaF_2 (both of anal.r.grade) were thoroughly mixed with the sodium-borate slag and metal at 1173K and kept for long time (35-40 hrs) at this tempeerature. The different mixtures were once again crushed and put in the furnace at 1200K for 10-12 hours to ensure proper mixing.

4.2.3 Preparation of Copper Alloys

For selenium transfer studies, Cu-0.228 wt % Se alloy was obtained from Cu-12.9 wt % Se master alloy using copper (99.99 wt % pure) and selenium (99.99 wt % pure). Similarly for tellurium transfer studies, Cu-0.143 wt % Te alloy was obtained from Cu-4.0 wt % Te master alloy using 99.99 wt % pure tellurium and copper. The copper alloys were melted in graphite boats under purified N_2 atmosphere and the compositions were determined by Inductively Coupled Plasma Spectrophtometry. (I.C.P.S.)

4.2.4 Procedure

For experimental runs, optimum weight of slag (22 gms) and metal (150 gms) were placed in the graphite crucible especially designed and fabricated for the purpose,

which was then heated to melt the charge under purified nitrogen atmosphere. Nitrogen gas was passed at slow controlled rate during initial heating and melting period but once the desired temperature was attained , its flow rate was adjusted to result in the desired degree of agitation in bubble-stirred slag-metal reacting system. Samples of metal and slag were withdrawn using high alumina sampling tubes, at regular intervals of 4 minutes and analysed for their Se and Te contents.

4.3 RESULTS AND DISCUSSIONS

Improvement in the overall rate of reaction in a heterogeneous system as a result of gas phase stirring due to enhanced mass transport is well known [197]. In the present work, effect of different flow rates (5.0 to 17.0 cm^3/sec) of nitrogen gas through the liquid bath on selenium and tellurium transfer rate from liquid copper to the slag phase has been studied at temperature 1473K.

Results of different experimental runs are given in Tables (4.1-4.8) and Figs. (4.4-4.7) represent the variation of selenium and tellurium concentrations in copper as well as in slag as a function of time. It is evident from the Figs.(4.4, 4.6) that the concentration of both selenium and tellurium in copper initially decreased rapidly

TABLE -4.1

SELENIUM TRANSFER FOR GAS FLOW RATE G=5.0 cm^3/sec at 1473K

Sl No.	Time, t (min)	$[\%Se_b]_t$	$(\%Se_b)_t$	$\ln \frac{[\%Se_b]_t-[\%Se_b]_\infty}{[\%Se_b]_o-[\%Se_b]_\infty}$
		(% Values by weight)		
1.	0	0.2282	0	0
2.	4	0.2089	0.1288	-0.248
3.	8	0.1871	0.2792	-0.635
4.	12	0.1718	0.3805	-1.038
5.	16	0.1622	0.4424	-1.412
6.	20	0.1589	0.4689	-1.576
7.	24	0.1531	0.5092	-1.973
8.	28	0.1509	0.5215	-2.173
9.	32	0.1471	0.5498	-2.675
10.	36	0.1451	0.5604	-3.081
11.	48	0.1429	0.5782	-3.879
12.	60	0.1411	0.5892	-

TABLE - 4.2

SELENIUM TRANSFER FOR GAS FLOW RATE G=9.0 cm^3/sec at 1473K

Sl No.	Time, t (min)	$[\%Se_b]_t$	$(\%Se_b)_t$	$\ln \frac{[\%Se_b]_t-[\%Se_b]_\infty}{[\%Se_b]_o-[\%Se_b]_\infty}$
		(% Values by weight)		
1.	0	0.2282	0	0
2.	4	0.2011	0.1804	-0.372
3.	8	0.1799	0.3242	-0.809
4.	12	0.1672	0.4114	-1.205
5.	16	0.1605	0.4570	-1.502
6.	20	0.1541	0.5007	-1.902
7.	24	0.1492	0.5341	-2.375
8.	28	0.1479	0.5429	-2.550
9.	32	0.1453	0.5606	-3.032
10.	36	0.1442	0.5681	-3.336
11.	48	0.1418	0.5844	-4.698
12.	60	0.1411	0.5892	-

TABLE - 4.3

SELENIUM TRANSFER FOR GAS FLOW RATE G=12.5 cm^3/sec at 1473K

Sl No.	Time, t (min)	$[\%Se_b]_t$	$(\%Se_b)_t$	$\ln \frac{[\%Se_b]_t - [\%Se_b]_\infty}{[\%Se_b]_o - [\%Se_b]_\infty}$
		(% Values in weight)		
1.	0	0.2282	0	0
2.	4	0.1982	0.2001	-0.422
3.	8	0.1749	0.3591	-0.946
4.	12	0.1653	0.4242	-1.281
5.	16	0.1588	0.4688	-1.593
6.	20	0.1512	0.5204	-2.155
7.	24	0.1481	0.5414	-2.521
8.	28	0.1452	0.5612	-3.056
9.	32	0.1439	0.5702	-3.437
10.	36	0.1431	0.5754	-3.774
11.	48	0.1416	0.5861	-4.859
12.	60	0.1411	0.5892	-

TABLE - 4.4

SELENIUM TRANSFER FOR GAS FLOW RATE G=17.0 cm^3/sec at 1473K

Sl No.	Time, t (min)	$[\%Se_b]_t$	$(\%Se_b)_t$	$\ln \frac{[\%Se_b]_t-[\%Se_b]_\infty}{[\%Se_b]_o-[\%Se_b]_\infty}$
		(% Values by weight)		
1.	0	0.2282	0	0
2.	4	0.1932	0.2339	-0.514
3.	8	0.1729	0.3732	-1.008
4.	12	0.1611	0.4528	-1.471
5.	16	0.1532	0.5072	-1.974
6.	20	0.1481	0.5415	-2.521
7.	24	0.1462	0.5542	-2.838
8.	28	0.1439	0.5702	-3.437
9.	32	0.1429	0.5771	-3.879
10.	36	0.1419	0.5838	-4.571
11.	48	0.1411	0.5892	-
12.	60	0.1411	0.5892	-

TABLE - 4.5

TELLURIUM TRANSFER FOR GAS FLOW RATE G=5.0 cm^3/sec at 1473K

Sl No.	Time, t (min)	$[\%Te_b]_t$	$(\%Te_b)_t$	$\ln \frac{[\%Te_b]_t-[\%Te_b]_\infty}{[\%Te_b]_o-[\%Te_b]_\infty}$
		(% Values by weight)		
1.	0	0.1433	0	0
2.	4	0.1182	0.1669	-0.309
3.	8	0.1021	0.2762	-0.576
4.	12	0.0829	0.4071	-1.027
5.	16	0.0732	0.4738	-1.366
6.	20	0.0691	0.5012	-1.554
7.	24	0.0628	0.5442	-1.934
8.	28	0.0592	0.5691	-2.242
9.	32	0.0559	0.5912	-2.627
10.	36	0.0535	0.6078	-3.086
11.	48	0.0516	0.6206	-3.669
12.	60	0.0492	0.6382	-

TABLE - 4.6

TELLURIUM TRANSFER FOR GAS FLOW RATE G=9.0 cm^3/sec at 1473K

Sl No.	Time, t (min)	$[\%Te_b]_t$	$(\%Te_b)_t$	$\ln \frac{[\%Te_b]_t-[\%Te_b]_\infty}{[\%Te_b]_o-[\%Te_b]_\infty}$
		(% Values by weight)		
1.	0	0.1433	0	0
2.	4	0.1129	0.2028	-0.390
3.	8	0.0951	0.3241	-0.718
4.	12	0.0789	0.4345	-1.153
5.	16	0.0711	0.4881	-1.458
6.	20	0.0652	0.5279	-1.772
7.	24	0.0583	0.5739	-2.336
8.	28	0.0571	0.5830	-2.477
9.	32	0.0542	0.6029	-2.935
10.	36	0.0521	0.6169	-3.479
11.	48	0.0505	0.6282	-4.282
12.	60	0.0492	0.6382	-

TABLE - 4.7

TELLURIUM TRANSFER FOR GAS FLOW RATE G=12.5 cm^3/sec at 1473K

Sl No.	Time, t (min)	$[\%Te_b]_t$	$(\%Te_b)_t$	$\ln \frac{[\%Te_b]_t-[\%Te_b]_\infty}{[\%Te_b]_o-[\%Te_b]_\infty}$
		(% Values by weight)		
1.	0	0.1433	0	0
2.	4	0.1091	0.2284	-0.452
3.	8	0.0909	0.3527	-0.814
4.	12	0.0742	0.4664	-1.325
5.	16	0.0682	0.5073	-1.599
6.	20	0.0599	0.5639	-2.174
7.	24	0.0575	0.5804	-2.428
8.	28	0.0539	0.6049	-2.996
9.	32	0.0531	0.6104	-3.183
10.	36	0.0511	0.6241	-3.903
11.	48	0.0500	0.6314	-4.768
12.	60	0.0492	0.6382	-

TABLE - 4.8

TELLURIUM TRANSFER FOR GAS FLOW RATE G=17.0 cm^3/sec at 1473K

Sl No.	Time, t (min)	$[\%Te_b]_t$	$(\%Te_b)_t$	$\ln \frac{[\%Te_b]_t-[\%Te_b]_\infty}{[\%Te_b]_o-[\%Te_b]_\infty}$
		(% Values by weight)		
1.	0	0.1433	0	0
2.	4	0.1021	0.2762	-0.576
3.	8	0.0849	0.3936	-0.969
4.	12	0.0718	0.4829	-1.426
5.	16	0.0641	0.5353	-1.843
6.	20	0.0582	0.5756	-2.347
7.	24	0.0544	0.6013	-2.896
8.	28	0.0527	0.6131	-3.292
9.	32	0.0510	0.6247	-3.956
10.	36	0.0502	0.6302	-4.544
11.	48	0.0492	0.6382	-
12.	60	0.0492	0.6382	-

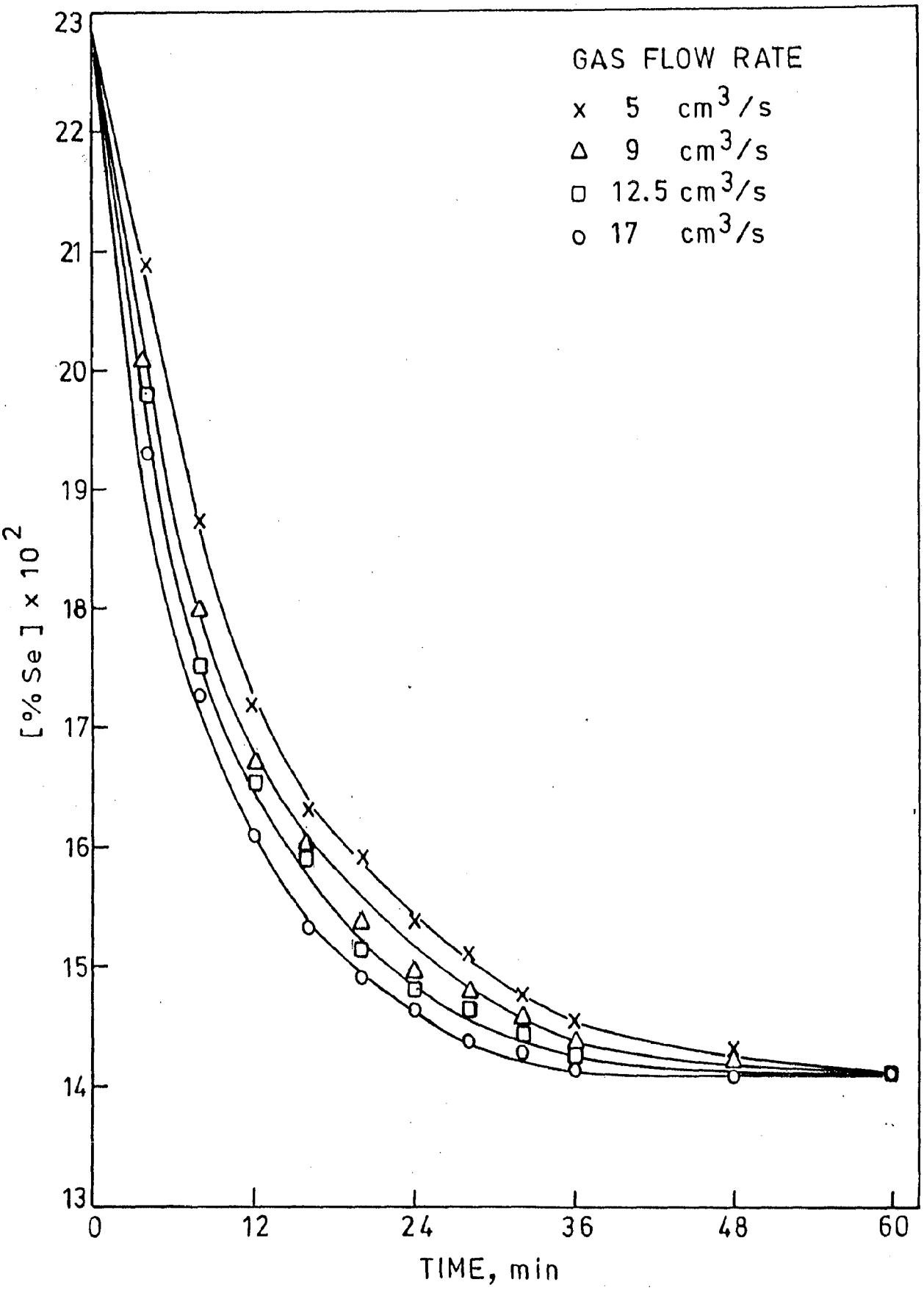

FIG. 4.4 EFFECT OF GAS FLOW RATE ON SELENIUM CONTENT IN MOLTEN COPPER WITH TIME.

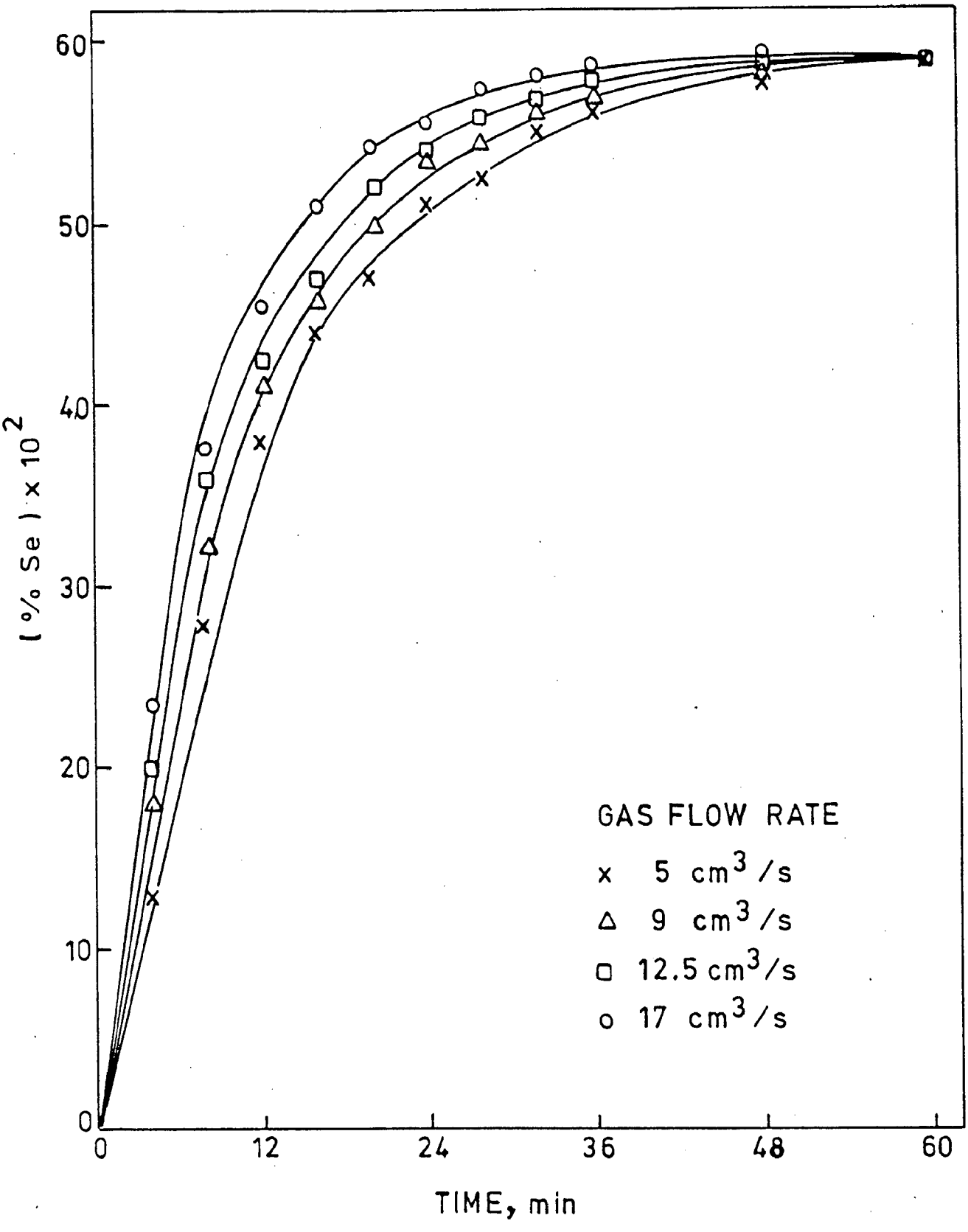

FIG. 4.5 EFFECT OF GAS FLOW RATE ON SELENIUM CONTENT IN SLAG WITH TIME.

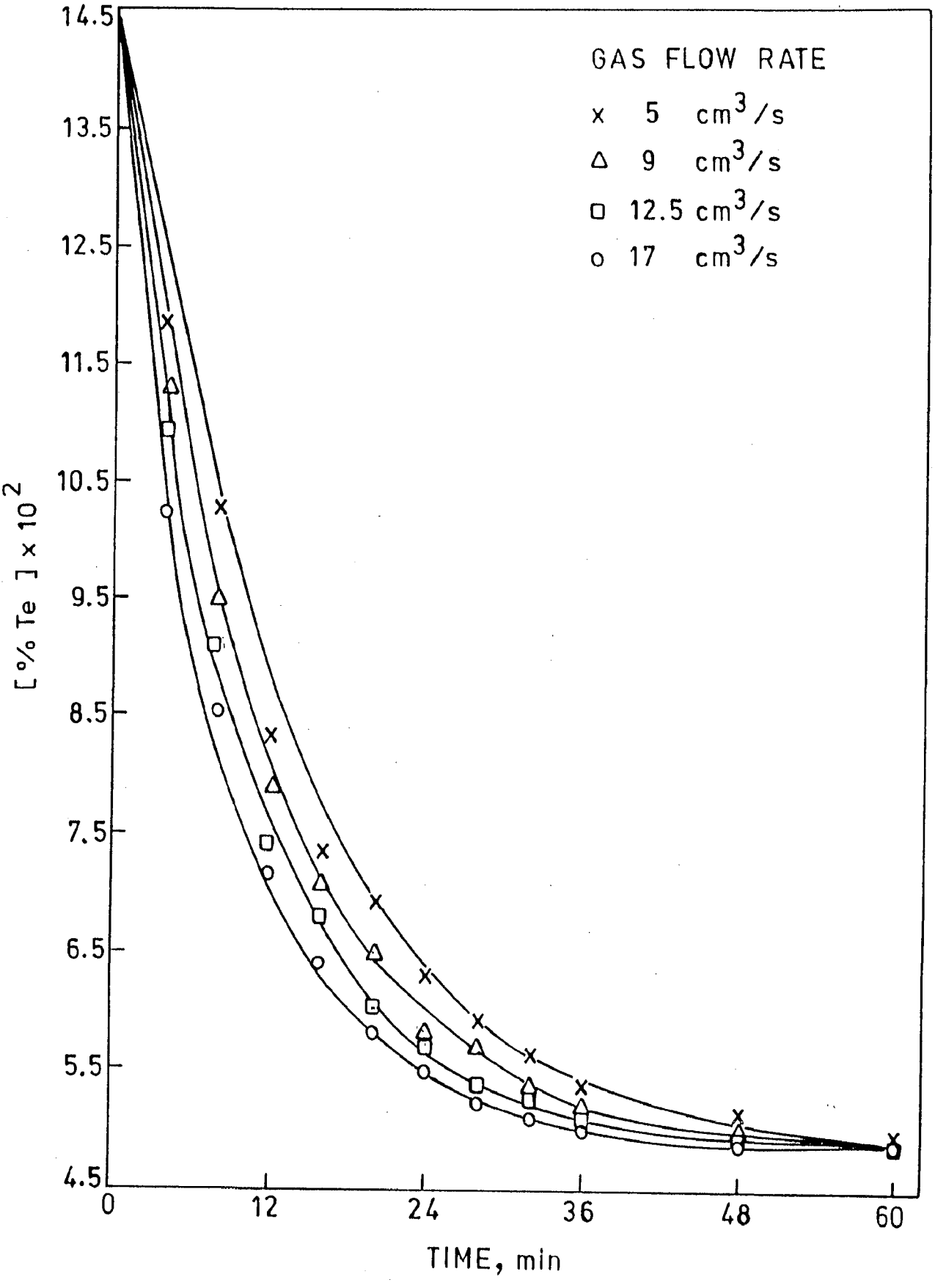

FIG. 4.6 EFFECT OF GAS FLOW RATE ON TELLURIUM CONTENT IN MOLTEN COPPER WITH TIME.

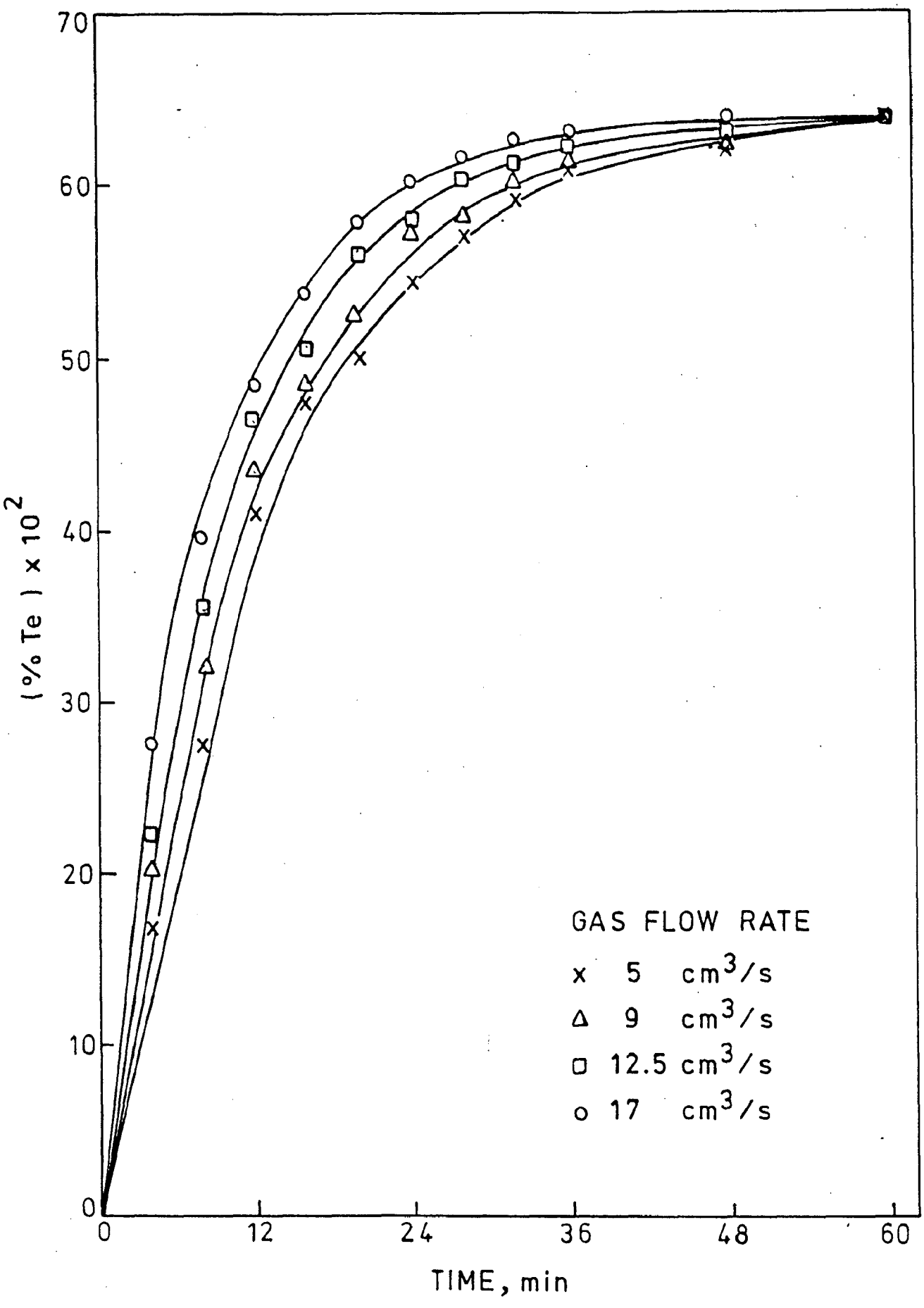

FIG. 4.7 EFFECT OF GAS FLOW RATE ON TELLURIUM CONTENT IN SLAG WITH TIME.

and then slowly and finally attained a constant value as the element transfer progressed. The last values given in the Tables (4.1-4.8) for selenium and tellurium contents both in metal and slag did not change even after a long time of experimentation and thus refer to the ultimate or equilibrium values of the element 'Me' representing selenium and tellurium in the respective phases i.e. $[wt\%\ Me]_{\infty}$ and $(wt\%\ Me)_{\infty}$ as the weight percent 'Me' in bulk metal and slag phases respectively at infinite time. These equilibrium values were used to calculate the distribution coefficient, L, of 'Me' between molten copper and slag using the relation,

$$L = \frac{\rho_S\ (wt\%\ Me)}{\rho_M\ [wt\%\ Me]} \qquad \ldots.(4.3)$$

The value 'L' so calculated for selenium and tellurium are 1.25 and 3.88 respectively using slag composition (25.7 wt% Na_2O, 29.8 wt% B_2O_3, 27.8 wt% CaO, 16.7 wt% CaF_2) for Cu - 0.23 wt% Se and Cu - 0.14 wt% Te alloys at 1473K.

Figs. (4.8-4.9) show the plots of values on LHS of equation (4.17) against time for different gas flow rates.

The equation (4.17) is expressed as

$$\ln \frac{[wt\%\ Me_b]_t - [wt\%\ Me_b]_{\infty}}{[wt\%\ Me_b]_o - [wt\%\ Me_b]_{\infty}} = -\ k \left(\frac{1}{h_M} + \frac{1}{Lh_S}\right) t \qquad \ldots.(4.17)$$

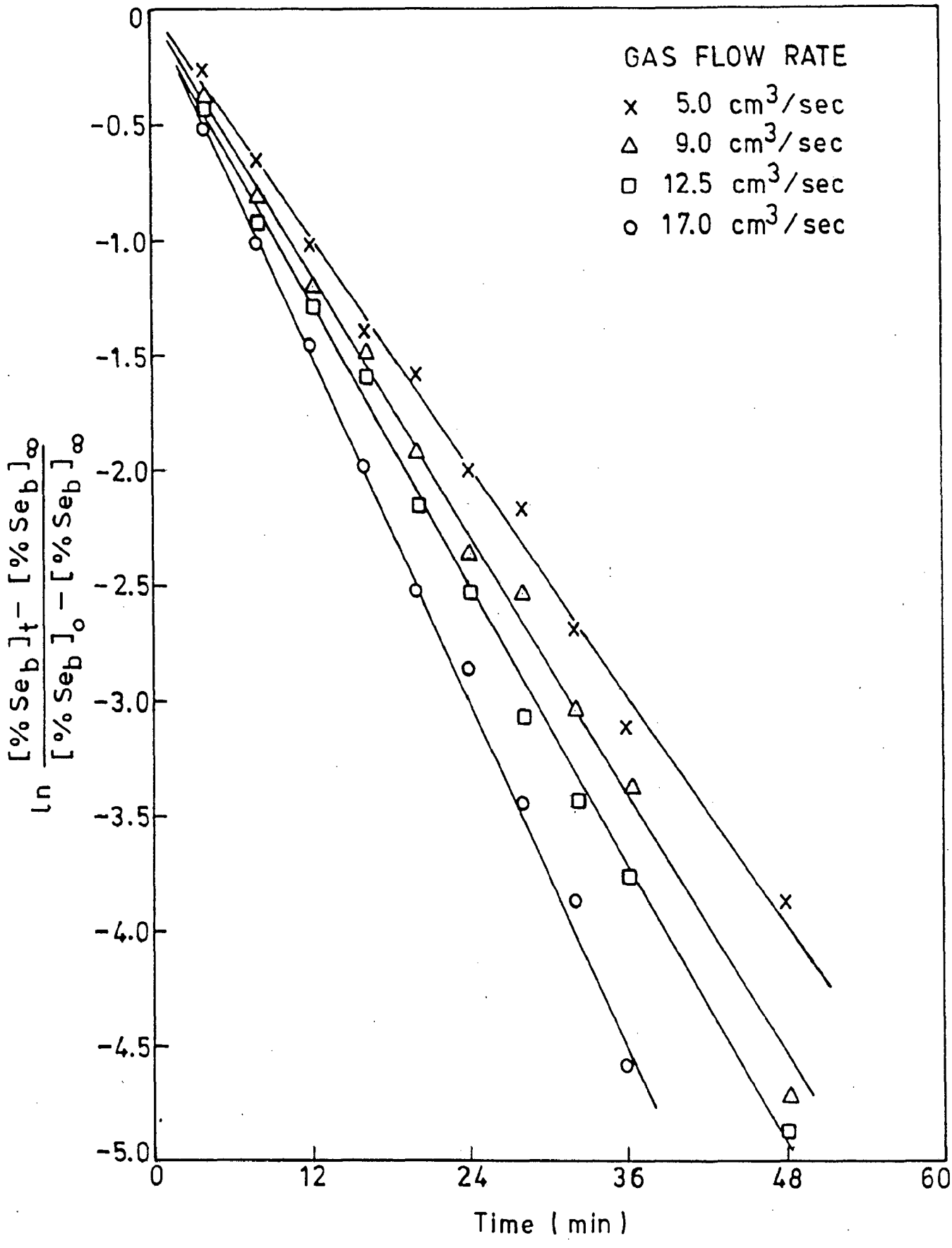

FIG. 4.8 SELENIUM TRANSFER RATE FOR DIFFERENT GAS FLOW RATE AT 1473K.

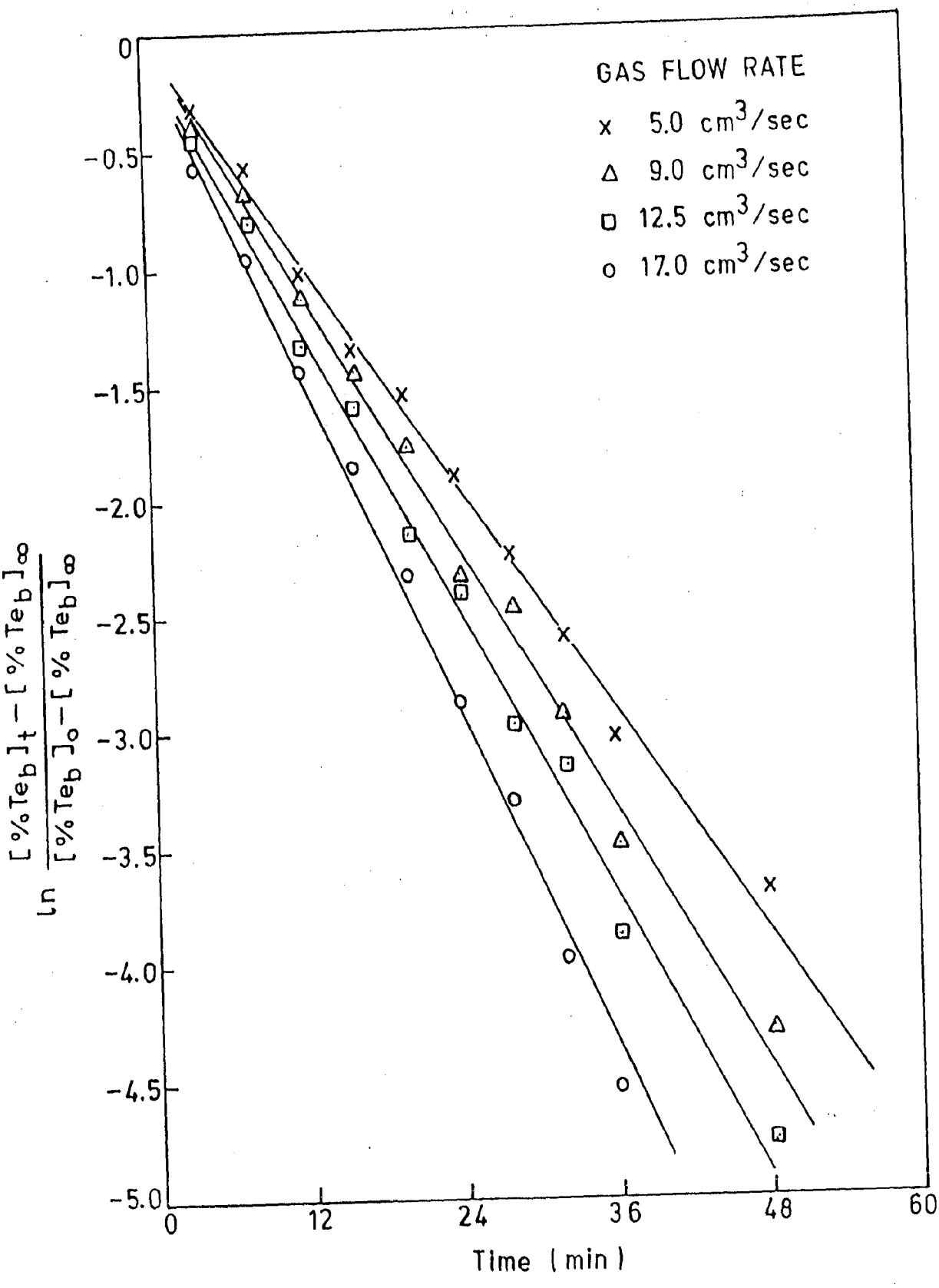

FIG. 4.9 TELLURIUM TRANSFER RATE FOR DIFFERENT GAS FLOW RATE AT 1473K.

(where k, the overall mass transfer coefficient, h_M and h_S are the heights of metal and slag baths respectively and Me_b represents Se_b and Te_b).

From the slopes of these plots, values of overall mass transfer coefficient, k (cm/sec),for selenium and tellurium, are calculated and given in the Table 4.9.

As described in section 4.1, a slag-metal reaction can be controlled basically either by (a) transport process and/or (b) chemical reaction. As at elevated temperature, the chemical reaction at the interface is known to be much faster than the mass transfer rates, it can be assumed that for all practical purposes chemical equilibrium prevails at the interface. Therefore, under steady state conditions, the rates of element 'Me' transferred from metal to slag phase can be defined by equation 4.17 in the present investigation.

Effect of gas flow rate

The size of gas bubbles was calculated for different gas flow rates, using the relation [198],

$$d_b = \left(\frac{6G}{\pi F}\right)^{1/3} \qquad (4.51)$$

TABLE- 4.9

OVERALL MASS TRANSFER COEFFICIENT FOR SELENIUM AND TELLURIUM AT DIFFERENT GAS FLOW RATES.

Sl. No.	Gas Flow rate (cm^3/sec)	$k_{overall}$ for Cu-0.23 wt%Se alloy (cm /sec)	$k_{overall}$ for Cu-0.14wt%Te alloy (cm /sec)
1.	5.0	2.042×10^{-3}	3.41×10^{-3}
2.	9.0	2.297×10^{-3}	3.848×10^{-3}
3.	12.5	2.47×10^{-3}	4.216×10^{-3}
4.	17.0	3.064×10^{-3}	5.02×10^{-3}

Where d_b is bubble diameter (cm), G, gas flow rate (cm^3/sec) and F, frequency of bubbles formation (sec^{-1}) calculated from the relation $F = 6.7\ G^{0.13}\ d_o^{0.43}$ [160] where d_o is orifice diameter (cm).

The values so calculated are gvien in table 4.10. Bubbles of these sizes (exceeding 1 cm dia.) are reported to adopt the spherical cap or mushroom shape [189]. The geometry of fully developed spherical cap bubbles is found to be independent of their sizes and their shapes and velocities are virtually independent of the liquid through which they rise whether it is mercury, steel, water or slag [181, 182, 188]. Such bubbles rise with velocities proportional to the square root of their diameter [163] and they carry behind them wakes as shown in Fig. 4.10. In a bath of metal they cause mixing by carrying up liquid in this wake and exchanging it relatively slowly with the surrounding liquid as vortices are shed. The bubbles also provide mixing by cleaving the liquid through which they pass. In swarms such bubbles tend both to break up due to turbulance and to join together because large bubbles sweep up smaller bubbles which they overtake and are drawn into their wakes. Because of this mixing caused by the bubbles, transport distances are cut down and, therefore, mass transfer coefficient in metal phase is increased . As this mixing effect increases with increase in gas flow rate,

TABLE- 4.10

BUBBLE FREQUENCY AND DIAMETER AT DIFFERENT GAS FLOW RATES.
CRUCIBLE ORIFICE DIAMETER d_o = 0.10 cm

Sl. No.	Gas flow rate (cm^3/sec)	Frequency of bubble formation $F=6.7\ G^{0.13}.d_o^{0.43}$ (sec^{-1})	Bubble diameter $d_b=\left(\frac{6G}{\pi F}\right)^{1/3}$ (cm)
1.	5.0	3.06(~ 3)	1.46
2.	9.0	3.29(~ 3)	1.73
3.	12.5	3.44(~ 3)	1.91
4.	17.0	3.58(~ 4)	2.08

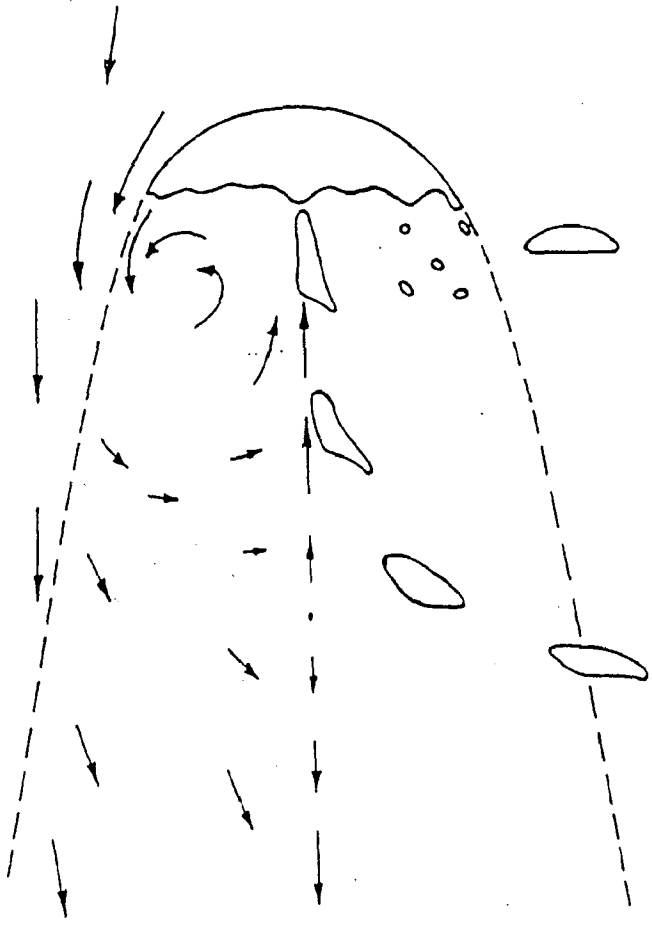

SPHERICAL CAP BUBBLE SHOWING WAKE, AND BY ARROWS DIRECTIONS OF FLOW RELATIVE TO THE BUBBLE.

FIG. 4.10 SPHERICAL CAP BUBBLE SHOWING WAKE.

therefore, with increase in gas flow rate mass transfer coefficient increases.

Large bubbles help mass transfer across the interface between the metal and slag. The bubble first pushes a large dome of metal into the upper liquid,it then carries through into the upper slag phase a skin of liquid metal which drains away at the base.

The effect of gas flow rate on mass transfer coefficient is depicted quantitatively in Fig. 4.11. which shows that the log k Vs. log G plots are straight lines for both Se and Te and follow the quantitative relationships:

$$k_{ov,Se} = 1.4791 \times 10^{-3} G^{0.20} \quad \ldots(4.52)$$

$$k_{ov,Te} = 2.3415 \times 10^{-3} G^{0.23} \quad \ldots(4.53)$$

where 'G' represents the gas flow rate (cm^3/sec).

From the results and discussions, it is, therefore, inferred that in the gas flow rate range and temperature of the present study, the overall mass transfer coefficients of selenium and tellurium increase with increase in gas flow rate for particular copper alloys and slag composition used.

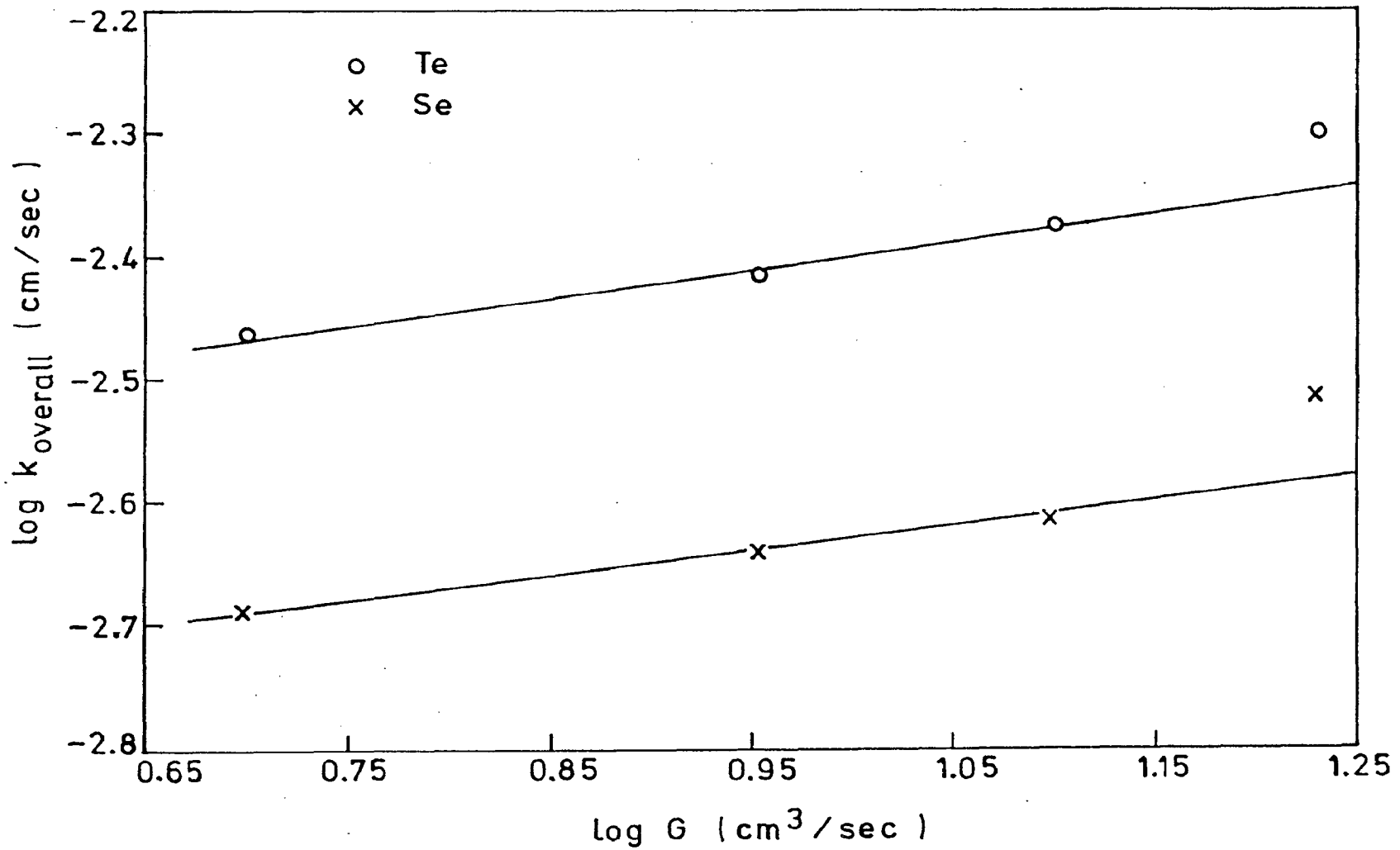

FIG. 4.11 EFFECT OF GAS FLOW RATE ON OVERALL MASS TRANSFER COEFFICIENT AT 1473K.

CHAPTER - V

CONCLUSIONS

The present work leads to the following conclusions :

5.1 THERMODYNAMIC STUDIES

1. With increase in Na_2O - B_2O_3 slag basicity (wt% Na_2O/wt% B_2O_3 = 0.53 to 0.86), Se distribution coefficient increases from 0.4 to 2.9 for Cu - 0.446 wt% Se alloy and Te distribution coefficient increases from 2.9 to 11.9 for Cu - 3.923 wt % Te alloy.
2. On adding CaO (10 to 50 wt %) to the Na_2O - B_2O_3 slag (wt % Na_2O/wt % B_2O_3 = 0.86), the distribution coefficients, for both Se and Te, increases. Data for 50 wt% CaO addition to Na_2O -B_2O_3 slag show that Se distribution coefficient increases by about 100% for Cu - 0.446 wt% Se alloy while Te distribution coefficient increases by about 140% for Cu - 3.923 wt % Te alloy.
3. On CaF_2 addition (5 to 20 wt%) to the slag composition (30.9 wt% Na_2O, 35.8 wt% B_2O_3, 33.3 wt% CaO),the distribution coefficents for both Se and Te increase further and for 20 wt % CaF_2 in slag, the values obtained are around (100-120%) more than the values of

distribution coefficient obtained for slag with no CaF_2 for same Cu - 0.446 wt% Se and Cu - 3.923 wt% Te alloys.

4. Also with increase in initial concentrations of Se and Te in Copper, the distribution coefficients of both Se and Te increase for all slag compositions in general.

5.2 VISCOSITY MEASUREMENTS

1. Viscosity measurements of sodium - borate slags at high Na_2O concentrations (37.3 to 49.4 mole%) and high temperatures (1273 to 1573K) show that variation of viscosity with temperature follows Arrhenius type relationship. This relationship is also observed for sodium-borate slags (wt % Na_2O/ wt% B_2O_3 = 0.86) containing CaO and CaF_2.The viscosity of all slag compositions, used in the present study, decreases with increase in temperature.
2. Viscosity of Na_2O - B_2O_3 slag decreases with increase in slag basicity (i.e. wt% Na_2O/wt% B_2O_3) from 0.53 to 0.86 in the temperature range 1273K- 1573K .
3. There is considerable increase in viscosity of slags on addition of CaO (10 to 50 wt%) to the slag (46.4 wt% Na_2O,53.6 wt% B_2O_3).
4. Addition of CaF_2 (5 to 20 wt%) to the slag (30.9 wt% Na_2O,35.8 wt% B_2O_3, 33.3 wt% CaO) decreases the viscosity of the slag.

5. The average activation energies of $Na_2O - B_2O_3$, $Na_2O - B_2O_3 - CaO$ and $Na_2O - B_2O_3 - CaO - CaF_2$ slag systems are 14.6, 124.7, and 41.4 KJ/mole respectively for the given composition ranges and 1273K - 1573K temperature range.

5.3 KINETIC STUDIES

1. With increase in gas flow rate from 5.0 cm^3/sec to 17.0 cm^3/sec, the overall mass transfer coefficient of Se increases from 2.04 x 10^{-3} cm/sec to 3.06 x 10^{-3} cm/sec for Cu-0.228 wt % Se alloy and the overall mass transfer coefficient of Te increases from 3.41 x 10^{-3} cm/sec to 5.02 x 10^{-3} cm/sec for Cu-0.143 wt % Te alloy using slag composition (25.7 wt% Na_2O, 29.8 wt% B_2O_3, 27.8 wt% CaO, 16.7 wt% CaF_2) in both the cases at 1473K.
2. The overall mass transfer coefficients for Se and Te can be represented quantitatively as

$$k_{ov,Se} = 1.4791 \times 10^{-3}\ G^{0.20}$$

and

$$k_{ov,Te} = 2.3415 \times 10^{-3}\ G^{0.23}$$

where G represents the gas flow rate (cm^3/sec).

SCOPE FOR FUTURE WORK

1. Suitable process can be developed to recover selenide and telluride from slag phase in a marketable form.
2. Sodium - borate slags of suitable compositions can be developed for removal of impurities such as As, Sb and Bi from molten copper and studies can be conducted on thermodynamic and kinetic aspects of slag - metal reactions.

REFERENCES

1. A.Butts: Copper, The Science and Technology of the Metals, its Alloys and Compounds, Reinhold Publishing Corporation, (1954),p.411-413.
2. A.K.Biswas and W.G.Davenport : Extractive Metallurgy of Copper, Pergamon Press, Second Ed.,(1980), p.97-192.
3. W.Domalski, K.Fabian, and D.Nolle: Eisen.,Vol.88(17), 1968,p.906.
4. R.Inoue, and H.Suito : Trans. ISIJ, Vol.22, 1982,p.514.
5. H.Schenck, M.G.Frohberg, and T.El.Gammal: Arch. Eisenhuttenwesen, Vol.31, 1969, p.11; Vol.32, 1961, p.63.
6. V.Giedroye, A.N.McPhail, and J.G.Mitchell: JISI, Vol.202, 1964, p.11.
7. W.Oelsen,H.G.Schubert, and U.K.Klein: Arch. Eisenhuttenwesen, Vol.38, 1967, p.675.
8. F.Korber, and W.Oelsen : Stahl Eisen, Vol.58,1938, p.905; Vol.58, 1938, p.943.
9. W.Oelsen : Ibid, Vol.58, 1938, p.1212.
10. N.J.Grant, and J.Chipman : Ibid, Vol.167, 1946, p.134.
11. B.Platz : Stahl Eisen, Vol.12, 1892,p.2.
12. L.Blum : Ibid, Vol.19, 1901, p.1024.
13. L .S.Darken and B.M.Larsen : Trans. AIME, Vol.150,1942,p.87.
14. T.B.Winkler, and J.Chipman : Ibid, Vol.167, 1946,p.111.

15. G.G.Hatch and J.Chipman : Ibid, Vol.185,1949, p.274.

16. M.R.Kalyanram, T.G.Macfarlane, and H.B.Bell: JISI, Vol.195, 1960,p.58.

17. H.Suito, A.Ishizaka, R.Inoue, and Y.Takahashi : Ibid, Vol.21,1981,p.156.

18. J.D.Shim, and S.Banya: Tetsu-to-Hagane, Vol.68(2), 1982, p.251.

19. G.A.Toporishchev, A.S.Churkin, V.N.Voronenkov,and O.A.Esin: Izvest. Akad. Nauk SSSR, Metally, 1969(4), p.3.

20. T.Takenouchi, K.Suzuki, and S.Hara: Trans. ISIJ, Vol.19, 1979, p.758.

21. V.Parma, J.Bazan, and Z.Adolf:Hutn. Listy, 1981(6), p.402.

22. D.Y.Cho, J.K.Yoon, and J.D.Shim : J.Korean Inst. Met., Vol.20(5), 1982,p.437.

23. N.Theisen : Stahl Eisen., Vol.58, 1938,p.773.

24. D.A.Neudorf,and J.F.Elliott: Met.Trans.B, Vol.11B(4), 1980, p.607.

25. X.F.Zhang, and J.M.Toguri: Can Metall. Quart., Vol.26(2), 1987, p.117.

26 T.Tsao,and H.G.Katayama:Trans. ISIJ,Vol.26(9), 1986, p.717.

27. A.H.Chan, and R.J.Fruehen: Met. Trans. B, Vol.17(3), 1986, p.491.

28. W.Chen, R.Zhou, Z.Lin, and S.Chin: Hsult. Pao., Vol.23(6), 1987, p.290.

29. F.Tsukihashi, A.Werme, A.Kasahara, M.Okada, and N.Sano : Tetsu To Hagane, Vol.71(7), 1985,p.831.

30. R.Inone, X.P.Zhang, H.Li, and H.Sinto : Trans.ISIJ, Vol.27(12), 1987, p.946.

31. S.R.Simeonov,and N.Sano: Trans. ISIJ, Vol. 25 (11), 1985, p.1116.

32. N.Shinozaki, S.Sakamoto, K.Mori, and Y.Kawai : Tetsu To Hagane, Vol.73(9), 1987,p.1109.

33. J.J.Pak, and R.J.Fruehen : Met. Trans. B., Vol.17(4), 1986,p.797.

34. K.Kunisada, and H.Iwai:Trans ISIJ,Vol.27(4),1987,p.263

35. M.Hirasawa,K.Mori,M.Sano, Y.Shimatani, and Y.Okazaki : Trans.ISIJ, Vol.27(4), 1987,p.283.

36. K.Kunisada, and H.Iwai:Trans. ISIJ, Vol.26(12), 1986, p.364.

37. R.Magabayashi, M.Hino, and S.Banya : Trans.ISIJ, Vol.26(3), 1986, p.90.

38. T.Ting, H.G.Katayama, and A.Tanaka : Tetsu To Hagane, Vol.72(2), 1986, p.225.

39. T.K.Rytkoner, and A.I.Klarin : Scand. J.Metall, Vol.16(5),1987, p.210.

40 J.M.Cigan, T.S.Mackey, and J.O.O'Keefe: Lead-Zinc-Tin'80,(TMS -AIME, New York), 1979, p.491

41. M.Nagamori, P.J.Mackey, and P.Tarasoff : Met. Trans.B, Vol.6(1),1975,p.197; Met. Trans.B, Vol.6(2),1975,p.295.

42. B.P. Burylev, L.Sh. Tsemekhman, and N.N.Fedorova : Zh. Fiz.khim., Vol.49(12),1975, p.3112.

43. L. Komorova : Hutnicke Leslig, Vol.28(8),1973, p.577.

44. J.Bode, J.Gerlach, and F.Pawlek : Erzmetall., Vol.24(10),1971, p.480. (German).

45. J.Czernecki,S.Brateck,T.Cioseck, and L.Adamkieoicz : Rudy Met, Niezelaz., Vol.27(2),1982, p.63-67.(Polish).

46. A.Roine, and H.Jalkanen : Met. Trans.B, Vol.16(2),1985, p. 129-141.

47. I.V.Kajo, P.A.Taskinen, and K.R.Lilius : IInd Int.Symp.on Met. slags and fluxes [Proc. Conf.], Nevada, USA,11-14 Nov,1984, The Met.Soc./AIME, 420 commonwealth Dr.Warrendale, PA15086, USA, p. 723-737.

48. A.Boichev, A.Kirov, D.Denev, and E.Neikova : Godish.naNauchn.Inst.Tsvet. Metallurg., 10, 1972,p. 19-25. (Bulgarian).

49. G.Riveros, Y.J.Park, Y.Takeda, and A.Yazawa : Trans. Japan Inst. of Metals, Vol.28(9),1987, p.749-756.

50. H.Jalkanen, A.Roine, and E.Koski : Lammi. Nene. Hintte., Vol.27(12), 1982, p.446-449. (German).

51. V.S.Sibanda, and E.H.Baker : Trans. Inst. Min. Metal. C., Vol.88, 1979, p.c129-c130.

52. E.J.Canning, Jr. and Western Electric : Off.Gaz., 9 March 1982, Patent no, us 4318737 (USA), 20 Oct. 1980.

53. T.Sakai, T.Nakamura,F. Noguchi, and Y. Ueda : Noppon kogyo kaishi, Vol 103(1195), 1987, p.587-592. (Jpn).

54. I.V. Kojo,P. A. Taskinen,H. O. Rannikko,H. M. Takala, and K. R. Lilius : Erzmetall., Vol.40(3), 1987, p.138-144.

55. T. Sakai, T. Nakamura, F. Noguchi, and Y. Ueda : Nippon kogyo kaishi, Vol.103(1193), 1987, p.455-460.

56. T. Nakamura, F. Naguchi, and Y. Ueda : Metall. Rev. MMIJ, Vol. 3(2), 1986, p.102-116.

57. Y.Takeda, S. Ishiwata and A. Yazawa : Nippon kogyo kaishi, Vol 100(1152), 1984, p.103-108.

58. Y.Takeda, S. Ishiwata, and A.Yazawa : Nippon kogyo kaishi, Vol. 100(1153), 1984, p. 259-264.

59. Y.Takeda, and A.Yazawa : Nippon kogyo kaishi, Vol.102(1179), 1986, p.311-316.

60. H.Eerola,K.Jylha, and P.Taskinen:Trans Inst. Min. Metall., Sect.C, Vol.93, 1984, p.193-199.

61. P.Taskinen:Scand. J.Metall., Vol.11(3), 1982, p.150-154.

62. D.C.Lynch and K.W.Schwartz :Can. Metall. Q., Vol.20(3), 1981, p.269-278.

63. S.Goto, O.Ogawa and I.Jimbo : Symp.Ser Austrlas Inst. Min. Metall. Aust, Jul.16-18,1980. Publ. by the Australas Inst of Min. and Metall. Victoria, Aust.,1980, p.127.

64. I.V.Kojo, P.Taskinen, and K.Lilius : Erzmetall., Vol.37(1), 1984, p.21-26.

65. C.Yamauchi, K.Ohtsuki, Toshiharu, and H.Sakao : Trans. JIM, vol.29(9), 1988, p.727-734.

66. I.V.Kajo : Acta. Polytech. Scand. Cheum. Tech. Metall. Ser, Vol.161, 1985, p.48.

67. M.Nagamori and P.J.Mackey : Metall. Trans. B, Vol 8(3), 1977, p.39-46.

68. I.V.Kojo, P.A.Taskinen and K.R.Lilius : Metall. Trans. B, Vol 16B, March 1985, p.171-172.

69. P.Patel, M.G.Frohberg, and K. Biswas : Kinetics of Metallurgical Processes in steel making, 1975, p.180.

70. N.El-Kaddah and J.Szekely : Iron making and steel making, Vol. 8(6), 1981, p.269.

71. R.G.Ward and K.A.Salmon : JISI, Vol.196,1960, p393.

72. K.Marukawa, Y.Shirota, S.Anezaki and H.Hirahara : Tetsu-to-Hagane, Vol 67(2), 1981. p.323

73. S.Yamamoto, H.Kajioka and Y.Nakamura : Australia/Japan Extractive Metallurgy Symposium [Proc.Conf.], Sydney, Australia, 16-18 July 1980, Australasian Inst. of Min. and Metall., 191 Royal Parade, Parkville, Victoria, Australia 3052, 1980, p.363.

74. S.Yamamoto,M.Yoshii,H.Kajioka,Y.Nakamura,and T.Matsuo: Nippon Steel Technical Report No.15,June,1980,p.94.

75. R.Inoue and H.Suito : Trans. ISIJ, Vol.21,1981, p.545.

76. L.A.Smirnov, Y.A.Deryabin,and L.V.Dovgolyuk : Steel in the USSR, Vol. 10,1981, p.564.

77. T.Moriya and M.Fujii : Trans. ISIJ, Vol.21,1981,p.732.

78. P.Silva, E.Acciarito, A.Segreto, L.E.P. Lillis, and C.A chaves : Metal ABM ,Vol. 35(258),1979,p. 349.

79. I.Honjo : International Magnesium Assoc., 33rd Annual Meeting, 1976, p.73.

80. P.Hausen, and K.D.Schulz : Hoesch Worke AG off. Gaz., 25 March 1980, Patent No. us4194903 (U.S.A).

81. S.Yamaguchi, T.Uemura, H.Nashiwa, and H.Sugita : Ironmaking steelmaking, Vol.4(5),1977,p.276.

82. H.Sandberge : Ironmaking and steelmaking, Vol.4(5), 1977, p.280.

83. H.P.Schutz : Stahl Eisen., Vol.89(6), 1969, p.249.

84. B.Bahout, Y.Bienvenu and G.Denier : Iron making and steelmaking,Vol. 5(4), 1978, p.162.

85. R.J.Fruchan : Met.Technol.,March1980,Vol.7(3),p.95.

86. Anonymous : Development in Basic Oxygen Steel making , Conf. Preprints, Redear, England, 1969

87. V.A.Surin, D.I.Borodin, S.J.Bystrov, and V.I.Stepanov : Izv. V.U.Z., Chernaya Metall., Vol.5, 1979, p.34.

88. K.Nakanishi et al. : Trans. Iron Steel Inst. Japan, Vol.19(4), p.212.

89. K.Koch, T.Kootz and H.D.Pflipsen : Arch. Eisenhuttenw., Vol,52(3), March 1981, p.103.

90. J.Ishida et al. : Denbi-Seiko (Electr. Furn. Steel), Vol.52(1), 1981, p.2.

91. L.M.Soifer, N.N.Makarova, S.P.Sustavov, V.M.Pobegailo, andV.P.Savanin:Russ.Metall.Met.,no.5,1985,p.203.

92. T.Nakamura, Y.Ueda, F,Noguchi,and J.M.Toguri : Can Metall. Q., Vol.23(4), 1984, p.413-419.

93. M.Hirasawa, K.Mori and M.Sano : Trans. Iron Steel Inst. Japan., Vol, 28(2), 1988, p.B 49.

94. M.Hirasawa, K.Mori, M.Sano, Y.Shimatani, and Y.Okazaki: Trans.Iron Steel Inst.Japan.,Vol.27(4),1987, p.283-290.

95. M.Hirasawa, K.Mori, M,Sano, A.Hatanaka, Y.Shimatani, and Y.Okazaki : Trans. Iron Steel Inst. Japan, Vol.27(4)1987, p.277-282.

96. M.Hirasawa, M.Matsu-ura, and K.Mori:Trans. Japan Inst. Met., Vol.28(6), 1987,p.507-516.

97. M.Hirasawa, M.Matsu-ura, and K.Mori : Nippon Kinzoku Gakaishi. Vol.50(9), 1986,p.796-803.

98. K.Mori, M.Hirasawa, M.Shinkai, and A.Hatanaka : Tetsu To Hagane, Vol.71(9), July 1985, p,1110-1116.

99. M. Hirasawa,K. Mori,M. Sano,A. Hatanaka,Y. Shimatani, and Y.Okazaki : Tetsu To Hagane, Vol.73(10), August 1987,p.1343-1349 (Japnese).

100. S. T. Tadeusz and N. J. Themelis : Met. Trans.B, Vol.21, Dec. 1990, p. 967-975.

101. M. Kato, andS. Minowa : Trans. Iron. Steel Inst. Japan, Vol.9 (1), 1969, p. 31-38.

102. S. Tokumoto,andK. Chekyu : Technol. Rep. Osaka Univ., Oct. 1968, 18, (823/825), p. 345-352.

103. A. A. Gimmelfarb : Russ. Met., 1968, Vol.2, p.43-47.

104. I. P. Semik, V. I. Varava and S. V. Nesterenko : Sbornik Trudo Donets. Nauchno- Issled. Inst. Chem-Met. (Met.A.7003-440045).

105. V. G. Korpachev,S. I. PopelandV. I. Sokolov : Trudy. Ural. Nauchno-Issled. Chem. Met. Vol. 8, 1968, p.157-164.

106. M. W. Davies and F. A. Wright : Chem. and Ind., Vol.11, March 1970, p.359-363.

107. A. V. Vanyukov,V. Ya. Zaitser,V. V. Mecher,V. D. Romanov and S. A. Glushkov : Izvest. V. U. Z. Tsvetnaya Met.Vol. 1, 1971, p.31-35.

108. G. A. Klemeshov,V. I. Dorokhov,V. I. Glazov,B. G. Ryabinin, and V. D. Roztorguer: Izvest. Akad. Nauk. SSR Metally.,Vol.3, May-June 1971, p.41-47.

109. G. Handfield andG. G. Charette:Can. Metall. Q.,Vol.10(3), 1971,p. 235-243.

110. V. A. Efimov et al. : Izvest V. U. Z.C hernaya Met, Vol.8, 1971, p.67-70.

111. S. Tokumoto, M. Sakamoto, H. Yamaji, and K. Yoskikawa : Technol. Rep. Oska. Univ., Vol. 22 (1027-1052), Feb. 1972, p. 103-111.

112. J. M. Toguri et al.: Ext Met. of Copper, Vol. I, Pyrometallurgy and Electrolytic Refining, 1976, p. 259-273.

113. B.Sikova: Hutnik (Katowice), Vol.44 (1), 1977,p.10-15.

114. B. Dobovisek: Rud-Metal. Zb., Vol. 2(3), 1978, p.227-237.

115. L.Bodnar et al.: Hutn.Listy.,Vol. 33(7), July 1978, p. 497-501.

116. A. S. Pomelnikova et al. : Izv. V. U. Z. Chernaya Metally., Vol.10, 1978, p.32-35.

117. Y. Shiraishi et al. : Trans. Japan Inst. Met., Vol.19(5) May 1978, p. 264-274.

118. J. Nowakowski, and W. Ptak : Arch. Hutn., Vol.30(4), 1985, p. 435-442.

119. A. A. Akberdin, G. M. Kireeva, and I. A. Medvedovskaya :Russ. Metall. Met.,Vol.3, 1986, p. 54-56.

120. K. Seki, and F. Oeters : Trans. Iron Steel Inst. Jpn., Vol.24(6), 1984, p. 445-454.

121. P. Williams, M. Sunderland, and G. Briggs : Trans. Inst. Min. Metall., Vol.92, June 1983, p. c105-109.

122. N. Kuzuhiro, O. Katsumi, Y. Hisao, and S. G. Kazuhiro : Met. Trans. B, Vol. 18B, Sept. 1987, p. 549-555.

123. M. P. Volarovich, and D. M. Tolstoi: Bull. acad. sci.U. R. S. S., classe sci. physics-math., 1930, p. 897-906.

124. L. Shartsis, W. Capps, and S. Spinner : J. Am. Ceram. Soc., Vol.36(10), 1953, p. 319-326.

125. Data from J. C. Bailar : Comprehensive Inorganic Chemistery, Pergamon Press, Vol.2, 1973. p. 955.

126. K. C. Mills: Thermodynamic Data for Inorgamic Sulphieds, Selenide and Tellurides, Butterworths, London, 1974, p.46.

127. O. Kubaschewski and E. LL. Evans : Metallurgical Thermochemistery, Pergamon Press, 1958, p.338.

128. W. A. Weyl and E. C. Marboe : The Constitution of Glasses-A Dyamic Interpretation, "Fundamental of the structure of Inorganic liquids and Solids." Vol.1, Interscience Publishers, 1964.

129. R. Hultgren, R. L. Orr, P. D. Anderson and K. K. Kelley : Selected Values of Thermodynamic Properties of Binary Alloys, ASM, (1963).

130. C. B. Alcock : Principles of Pyrometallurgy, Academic Press, London, 1976. p. 113.

131. F. D. Richardson : Physical Chemistry of Melts in Metallurgy, Vol.1, Academic Press, London, 1974.

132. R.A.Rapp. Ed.,' Techniques in Metals Research', Vol.IV, Pt.2., Chapter on 'Viscometry and Densitometry' by Layton J.Wittenberg, Interscience,1970.

133. J.OM.Bockris, J.C.White and J.D.Mackenzie : Ed., 'Physicochemical Techniques at high temperatures'., chapter on 'The measurement of viscosity', Butterworths,1959.

134. J.R.Vanwazer, J.W.Lyons, K.Y.Kim and K.E.Colwell : 'Viscosity and flow Measurements', Interscience N.Y.1963, p.47,68.

135. J.D.Mackenzie : J.Chem.Phys., Vol.29,1958,p.605.

136. J.Stanworth : Soc.Glass.Tech., Vol.36, 1957, p.217.

137. Bockris, Mackenzie and Kitchener : Trans. Faraday Soc., Vol.51, 1955,p.1734.

138. Data from Instru. Mannual : 'Rotovisco RV 20', Measuring System M, Haake Mess-Technik, GmbH U.Co. Duselstrabe 4.D-7500,Karlsruhe 41, Germany.

139. K.Seki and F.Oeters : Trans. Iron Steel Inst.Jpn., Vol.24(6),1984, p.445-454.

140. J.Biscoe and B.E.Warren : J.Am.Ceram, Soc., Vol.21(8), 1938, p.287-293.

141. L.Sharsis, W.Capps, and S.Spinner :J.Am.Ceram. Soc., Vol.36(10), 1953, p.319-326.

142. W.G.Whitman : Chem and Met.Eng., Vol.29,1923, p.147.

143. R.Higbie: Trans. Am. Inst. Chem.Eng.,Vol.31,1935,p.365.

144. P.V.Danckwerts: Ind.Eng.Chem.,Vol.43,1951, p.1460.

145. H.L.Toor, and J.M.Marchello : A.I.Ch.E.J., Vol.4,1958,p.97.

146. G.Carlsson : Intern. Symp. on Modern Developments in steelmaking, Vol.1 (Proc.Conf.) National Metallurgical laboratory, Jamshedpur, India, 16-18 Feb., 1981,p.7:3:1.

147. U.Kalla : Iron steel (China), Vol.1, 1980,p.9.

148. V.S.Zhivchenko, N.F.Parakhin, E.A.Demidovich, Yu.V.Drobtsev, and I.I.Bornatskii : Steel USSR, Vol.11(4), 1981, p.220.

149. Anon : Development in Metallurgical Control in Basic Oxygen Steelmaking (Proc.Preprints),Redear,England 1979.

150. M.Cavallini, and G.Signorelli : Fonderia Ital., Vol.24(10), 1975, p.317.

151. P.Ritakallio : SCANINJECT, 1977,p.13:1.

152. Bo.Ohman, and T.Lehner: SCANINJECT, 1977,p.2:1

153. B.Pelucha,and J.Lovecky: Slevarenstvi, Vol.28 (11), Nov. 1980, p. 457.

154. J.Ishida et al. : Denki-Seiko (Electr. Furn. Steel), Vol.52(1),1981, p.2.

155. C.Zhipeng, M.Enxiang,Y.Jianging, and Q.Zhanmin :Iron Steel (China), Vol.16(5), 1981,p.21.

156. K.Suzuki, K.Kitamura, T.Takenouchi, M.Funazaki, and Y.Iwanami : Iron Steelmaker, Vol.9(7),1982,p.33.

157. A.Ukai et al. : Deoxidation Practice - With and Without Ladle Metallurgy [Proc. Conf.], Pitsburgh, Pa., 20-21 Apr. 1982, American Iron and Steel Institute, 1000 16th St.N.W., Washington,D.C.20036, 1982, p.70.

158. G.Zaino, and N.Brousseau : Electric Furnace Conference, 40th [Prof. Conf.] , Kansas City, Mo., U.S.A., 7-10 Dec.1982, Iron and Steel Socieity/AIME,Electric Furnace Div., P.O.Box 411, Warrendale, Pa. 15086,U.S.A., 1983, p.295.

159. D.W.Van Krevelen, and P.J.Hoftijzer : Chem.Eng. Progr., Vol.46, 1950, p.29.

160. L.Davidson, and E.H.Emick : A.I.Ch.E.J., Vol.2,1956,p.337.

161. I.Leibson, E.g.Holcomb, A.G.Cacoso, and J.J.Jasmic A.I.Ch.E.J., Vol.2, 1956, p.296.

162. J.Szekely, and N.J.Themelis : 'Rate Phenomena in Process Metallurgy', John Wiley and Sons, Inc.Publication, 1971, p.684.

163. R.M.Davies, and G.I.Taylor : Proc.Roy. Soc. (London), Vol. A 200, 1950, p.375.

164. R.R.Hughes,et al.:Chem.Engg.Prog.,Vol.51,1955,p.557.

165. W.B.Hayes,et al.: Advanc.Chem.Eng.,Vol.2,1956,p.296.

166. S.L.Sullivan, et al. : ibid., Vol.10, 1964, p.848.

167. W.L.Haberman, and R.K.Morton : David Taylor Model Basin Rep.,U.S.Department of Naval Reseach, No.802,1953.

168. R.A.Hartunian and W.R.Sears : J.Fluid Mech., Vol.3, 1957, p.27.

169. F.H.Garner and D.Hammerton : Chem. Eng. Sci., Vol.3,1954, p.1

170. F.N.Peebles,and H.J.Garber : Chem. Eng. Prog., Vol.39, 1953, p.88.

171. R.D.Lanauze, and I.J.Harris : Chem. Eng.Sci,, Vol.29,1974,p.1663.

172. A.Satyanarayan, R.Kumar and N.R.Kuloor : ibid, Vol.24, 1969, p.749.

173. W.Siemes, and J.F.Haufmann : ibid, Vol.5, 1956,p.127

174. W.Siemes : Chem. Eng.Tech., Vol.26, 1954, p.479.

175. J.F.Davidson, and B.O.G.Schuler : Trans. Inst.Chem. Eng., Vol.38, 1960, p.144.

176. J.F.Davidson, and B.O.G.Schuler : ibid,Vol.38, 1960,p. 335.

177. D.Papamantellos, K.W.Lange,K.Okohira, and H.Schenck : Met. Trans., Vol.2, 1971, p.3135.

178. M.Sano, and K.Mori : Tetsu-to-Hagane, Vol.60, 1974, p.348.

179. R.J.Andreini, J.S.Foster, and R.W.Callen : Met. Trans. B., Vol.8B, 1977, p.625.

180. T.Kraus : Trans. Vacuum Metallurgical Conference 1963, Boston, Mass. 1964,p.50.

181. W.G.Davenport, A.V.Bradshaw, and F.D.Richardson : JISI, Vol.205, 1967, p.1034.

182. W.G.Davenport, F.D.Richardson, and A.V.Bradshaw : Chem. Eng. Sci., Vol.22, 1967, p.1221.

183. R.I.L.Guthrie, and A.V.Bradshaw : Trans. Met. Soc.AIME,Vol.245, 1969, p.2285.

184. J.Szekely, and G.P.Martins: ibid, Vol.245, 1969, p.629.

185. K.W.Lange, M.Ohji, D.Papamantellos, and H.Schenck :Arch. Eisenhuttenwes, Vol.40,1969, p.99.

186. M.Ohji, D.Papamantellos, K.W.Lange, and H.Schenck : ibid, Vol.41, 1970,p.321.

187. M.H.I.Baird, and J.F.Davidson : Chem. Eng. Sci.,Vol.17, 1962, p.87.

188. F.D.Richardson : Met. Trans., Vol.2, 1971, p.2747.

189. F.D.Richardson : Trans.ISIJ, Vol.13, 1973,p.369.

190. M.Paneni, and W.G.Davenport : Trans. Met. Soc.,AIME, Vol.245, 1969, p.735.

191. K.W.Lange, M.Ohji, D.Papamantellos, and H.Schenck : Arch. Eisenhuttenwes, Vol.41, 1970, p.321.

192. T.Kraus :Schweiz. Arch. Angew. Wiss. Techn., Vol.28, 1962, p.452.

193. F.D.Richardson : Trans. Met. Soc.-AIME,Vol.230, 1964, p.1221.

194. A.J.Johnson, F.Besik, and A.E.Hamiliec : Can.J.Chem. Eng., Vol.47, 1969, p.559.

195. M.Sano, and K.Mori : Trans. ISIJ, Vol.23, 1983 p,169.

196. S.Asai, T.Okamoto,J.He, and I.Muchi : ibid,Vol.23,1983, p.43.

197. S.K.Gupta : Ph.D. Thesis, Deptt. of Met. Engg., University of Roorkee, Roorkee, India, 1985, p.31.

198. K.K.Mishra, and M.L.Kapoor : Hydrometallurgy, Vol.3, 1978, p.75.